University of Bergen

Master Thesis in Petroleum Chemistry

Biosurfactants as Anti-Agglomerants for Gas Hydrates

Author:
Gudny Øyre Flatabø

Supervisor:
Professor Tanja Barth

Faculty of Mathematics and Natural Sciences

Department of Chemistry

August 2013

UNIVERSITY OF BERGEN

Abstract

Faculty of Mathematics and Natural Sciences
Department of Chemistry

Master of Science

by

Gas hydrate blockages in petroleum pipelines are considered a major hazard in the petroleum industry, and with increasing water content and decreasing temperatures, a solution is sought upon that is both environmentally friendly and less costly than the current strategy. The application of biosurfactants at low concentrations in order to avoid agglomeration of hydrates in a cold flow, would significantly decrease environmental impact, in comparison to traditional thermodynamic inhibition methods.

In this thesis, the hydrate anti-agglomerating effects at 500 ppm of commercial naphthenic acids, *ARN*-acids, and the glycosides octyl glucoside and lauryl maltoside were assessed through wetting index, interfacial tension and contact angle measurements on stainless steel. Out of these, lauryl maltoside was found to be the most promising at this concentration, showing a major decrease in adhesion energy on stainless steel in addition to an increase in the wetting index, a quantification of gas hydrate plugging risk, from negative (high plugging risk) to positive (low plugging risk).

In addition, the sulfate reducing bacteria *Desulfotignum toluenicum* was cultivated for 7 and 10 months using toluene and crude oil as substrates. It was hypothesized that the bacteria would create water soluble biosurfactants that would change wettability characteristics of the cultivation medium. Adhesion energy was found to be reduced by bacteria present the media, to a larger degree for the medium where crude oil was used as a substrate rather than the medium where toluene was used as a substrate.

The wetting index did not show any significant difference when the media were tested against a model oil. The small degree of influence of wetting properties was attributed to being an effect of low concentration. When tested against a crude oil rather than a model oil, the anaerobic biodegradation was found to have some effect on the wetting index, interpreted as slightly decreased risk of plugging. The bacteria was found to grow as a biofilm in the water/hydrocarbon interface, reducing the concentration of bacteria and organic matter present in the samples of the media that were used for testing.

Acknowledgements

I am very thankful for all the guidance, advice and encouragement given by my supervisor, Professor Tanja Barth. I would like to express my gratitude to Dr. Anna E. Borgund for showing me several of the methods applied in this work, and to PhD candidate Ina Hvidsten for thorough instruction and guidance in the world of biosurfactants. Dr. Edin Alagic is appreciated for his encouragement and for good discussions and guidance regarding physical methods.

Professor Terje Torsvik at UniCIPR and Institute for Microbiology is highly appreciated for showing continued interest in my work, and patiently answering questions and teaching me about the field of microbiology. The guidance from the engineers at the oil microbiology lab is greatly appreciated.

I would like to thank my family for their support and advice in every decision. My mother for bringing me down to earth whenever I convince myself that I can fly, my sister for always caring and believing in me, and my friends for always accepting me for who I am. Especially Anja and Anna for always being there, Mari for always being interested and positive and my housemates for making everyday life an enjoyment.

Finally, I would like to thank the Bergen office of SINTEF and all the employees, for accepting me into their office, giving me an office space and laboratory access. Thanks for all the pleasant lunch breaks and interesting discussions at coffee break, and I look forward to continuing it in the future.

Contents

List of Figures

List of Tables

Chapter 1

Introduction

1.1 Background and purpose

Plugging by natural gas hydrates in subsea pipelines remains a flow assurance challenge in the petroleum industry - and the need for a more environmentally friendly and cost saving solution is highly present.[1]

Between 2005-2008, the HYPERION (HYdrates in PEtroleum productION - Assessment of Plug Risk) was funded by the Research Council of Norway and StatoilHydro ASA. Three PhD theses from the Department of Chemistry at the University of Bergen were submitted on the topic of natural inhibiting components found in crude oil, and its influence on gas hydrate plug risk.[2–4]

Through these theses, an hypothesis on biodegradation as a means of creating natural inhibiting compounds was launched. In the PhD thesis of Kristin Erstad,[2] an anaerobic and an aerobic bacterium previously isolated from a model oil reservoir column at the Centre for Integrated Petroleum Research, [5, 6] were used to degrade a crude oil.

Subsequent to biodegration, the acids from both oils were extracted, and controlled concentrations of each acid fraction were added to a non-biodegraded oil. The non-modified and modified oils were tested in a high-pressure sapphire cell, and the tendency of the different systems to form either gas hydrate plugs or dissociated gas hydrate crystals when natural gas and water was presented, was compared. Both acid fractions were found to have an impact on the system, but the largest impact was found from the anaerobically degraded oil. Even though gas hydrates continued to be formed, these were generally formed as many small, separate crystals, and the time needed before plugs were observed greatly increased.[7]

In this work, the same anaerobic bacterium, *Desulfotignum toluenicum*, was chosen to degrade pure toluene and a crude oil. The crude oil was chosen due to its low wetting index, associated with high risk of gas hydrate plugging (explained in section 1.5.2), when tested prior to degradation.

The purpose of the degradation was to see whether the bacteria would produce water soluble biosurfactants which could influence the plugging tendency and the interfacial characteristics of the model oil systems. Rather than using the high-pressure sapphire cell, a different method for assessing plugging tendency, the assessment of the *wetting index*-method or *emulsion method* has been applied.

In addition to the microbial degradation of toluene and crude oil, tests were done using selected additives to a model system; two biosurfactants and petroleum acids were tested, in order to compare results against each other and the laboratory biodegraded system.

1.2 Multiphase flow

In order to cost-efficiently extract oil from remote and difficult fields, especially off shore, and to avoid having to build a platform for each oil field, an interest in a multiphase flow technology appeared in the 70s and 80s. In petroleum production, multiphase flow refers to a mixture of phases transported together. This would typically be a gas phase consisting of natural gas, light hydrocarbons, steam and other gases, an oil phase of crude oil or condensate, an aqueous phase of produced or condensed water, and solid phases like sand, wax and hydrates.[8]

In contrast to single fluids, multiphase fluids cannot be conveniently quantified by knowledge of pressure, fluid viscosity, density, compressibility and geometry of a measurement device. Multiphase fluids flow at different velocities, may or may not dissolve/disperse and create emulsions, mixtures have unpredictable physical properties like viscosity and density, and precipitation and separation can easily occur.[8]

An understanding and possibility of measuring multiphase flows became apparent, leading to Esso in 1982 investing in a large two-phase flow loop at Tiller outside of Trondheim. From 1983, this large scale flow loop was operated by SINTEF. The data gathered from the multiphase experiments lead to the development of OLGA, a flow simulator that could predict multiphase behaviours. This simulator has been continuously developed and flow simulation is considered a prerequisite for the development of many fields using multiphase flow technology, examples being Ormen Lange, Troll and Snøhvit.[9–11]

When reservoir production tapers off, an increasing proportion of water is produced. Injection of water has also been used to enhance oil recovery of some reservoirs, introducing another phase to the hydrocarbon flow. Multiphase transport pipelines are usually laid along the sea bottom, which cools the flow to the temperature of the surrounding environment. In such a high pressure, low temperature environment, mixtures of gas and water can form hydrates that can agglomerate and potentially block the pipeline, a cause of great concern for petroleum producers.[1]

1.3 Gas hydrates

Clathrate hydrates are crystal structures with a hydrogen bonded cavity of water molecules trapping a guest molecule. Gas hydrates are characterized by a gas molecule encapsuled by water molecules.[1, 12] Gas hydrates look similar to snow or ice, but are formed at different temperature and pressure conditions.

1.3.1 Molecular structure

Gas hydrates can form as different structures, depending on the gas being the guest molecule. In petroleum pipelines, the most common gas is methane. Methane will always form type I hydrates,[13] illustrated in figure 1.1, but natural gas in petroleum production usually contain other, larger molecules as well, for example ethane and propane.

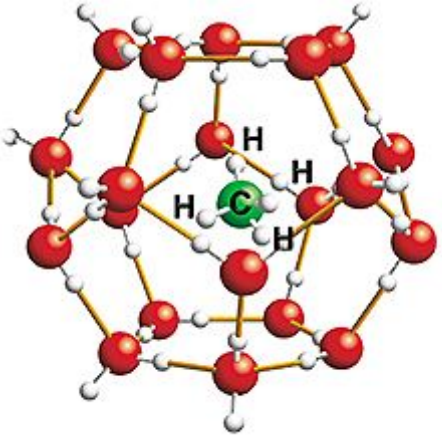

FIGURE 1.1: A simplified structure I representation of a methane hydrate, adapted from Schlumberger.[14]

As a consequence of this mix, mainly structure II hydrates form in oil and gas production.[1] For example methane and ethane present simultaneously will form structure II hydrates, and propane forms a structure II hydrate due to this having a more suitable cavity

size.[12] Figure 1.2 shows the most common possible clathrate structures for different components of natural gas.

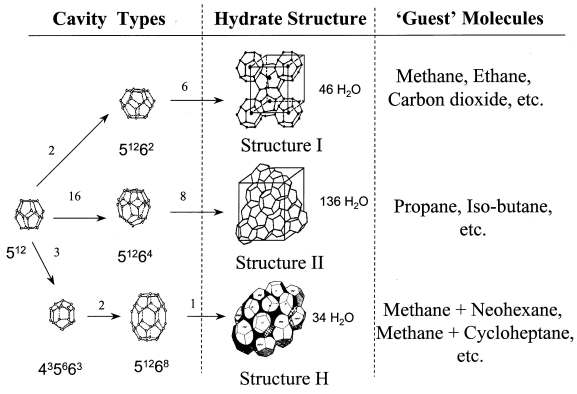

FIGURE 1.2: Three common hydrate structures made from different components of natural gas. $5^{12}6^4$ indicates that the water cage is composed of 12 pentagonal and 4 hexagonal faces. The number of molecules in the cages are indicated along the lines. Example: Structure II is composed of 16 5^{12} cages, 8 $5^{12}6^4$ cages and 136 water molecules. From Sloan (2000).[15]

1.3.2 Inhibition

Due to the health and safety risks and high costs associated with gas hydrate plugging in petroleum production, measures have to be put into place in order to minimize the risk of plugging. There are several strategies possible to attain this. Figure 1.3 shows the temperature and pressure conditions necessary for hydrate formation to occur.

In order to prevent hydrate formation, the pipeline in risk of plugging needs to either be heated to a temperature above the hydrate forming region for its pressure, or the pressure must be relieved to a pressure below the hydrate forming region for its temperature.

In practice, physically heating or relieving pressure in subsea pipelines is currently not economically viable and could cause large impacts on the marine environment. A different strategy is to add chemicals that shift the hydrate forming temperature out of the region of hydrate formation. This is called thermodynamic inhibition.

Another strategy to prevent hydrates from forming in pipelines is to delay hydrate formation by decreasing the rate of hydrate formation and growth. With a sufficient delay time, fluids can be transported to its end point without hydrates occuring. Chemicals causing this effect are called kinetic hydrate inhibitors (KHIs).[1]

A third strategy to minimize hydrate plug risk is by preventing hydrates to agglomerate. Using this strategy, hydrates are allowed to form, but will not stick together to form aggregates that eventually can cause plugging of pipelines. This effect is seen

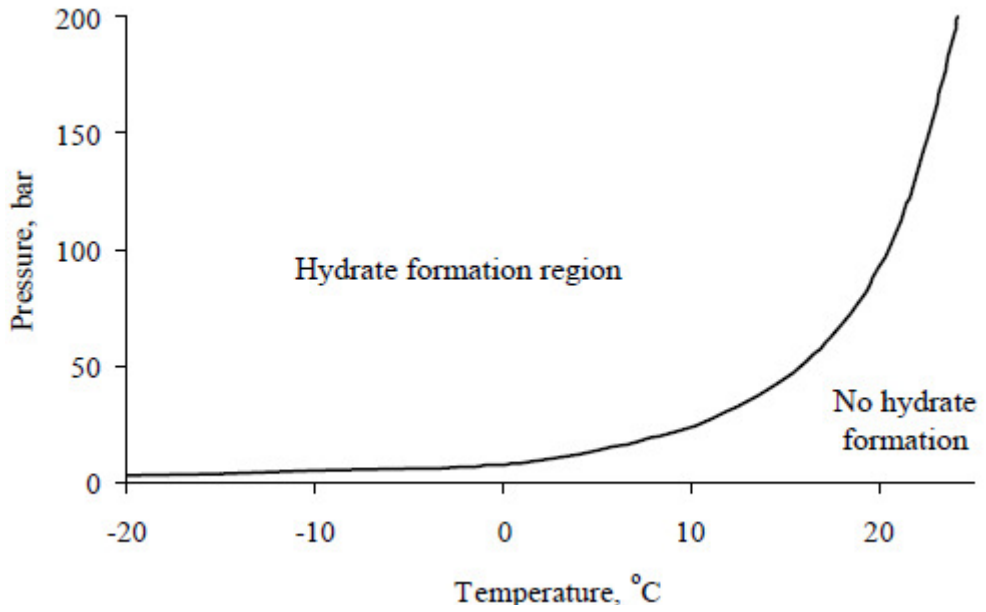

FIGURE 1.3: Pressure-temperature phase diagram for hydrate formation of natural gas (90.4 % methane, 5.2 % ethane, 2.1 % propane and trace amounts of N_2, CO_2, iso-butane, n-butane, iso-pentane, n-pentane and C_6) with water. The line separates the hydrate forming region to the left, from the non-hydrate forming region to the right. At 5 °C and 25 bar, hydrates will form, but increasing the temperature to 15 °C at 25 bar, the temperature is outside the hydrate forming area of that pressure, and hydrates will not form. From Borgund (2007).[3]

to naturally occur in some oils,[16–18] or can be attained by adding chemicals (anti-agglomerants).[19] The formed hydrates will flow in a multiphase slurry without causing plugs.[1, 12]

Thermodynamic inhibitors

The effect on the phase diagram of natural gas-water from some additives at 20 % is shown in figure 1.4. The most common thermodynamic inhibitors in use is methanol (MeOH) and monoethylene glycol (MEG). There are different advantages/disadvantages associated with these; methanol is more efficient than MEG and has a low viscosity, but a lot of it is lost in the gaseous phase and not recoverable, or it is dissolved in the oil phase, reducing the value of the oil. MEG is more viscous, but is more recoverable and thus better for the environment and more often applied. Inorganic electrolytes can also alter the phase diagram, but a high salt concentration can cause corrosion.[1]

The main disadvantage of thermodynamic inhibitors is the high concentration necessary to completely avoid hydrate formation, making it costly and not environmentally friendly. An extreme example to illustrate this is the Ormen Lange gas field. The flow line from the field carries wet gas at temperatures below zero, and the transport pipeline

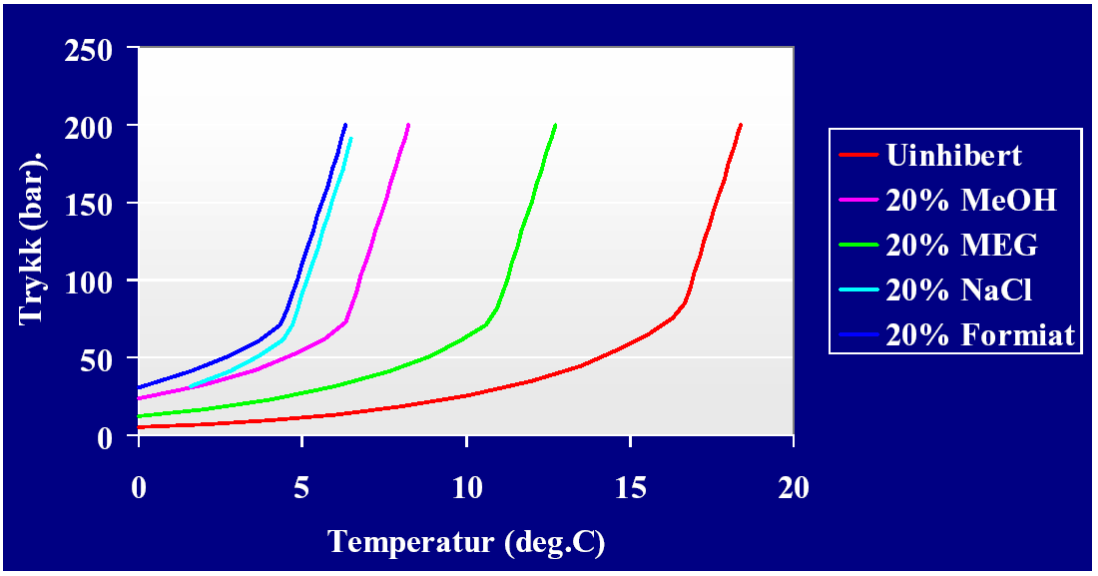

FIGURE 1.4: The effect of the temperature-pressure phase diagram from different thermodynamic inhibitors at 20 %. The hydrate forming region for the different additives is to the left of each line (high pressure, low temperature). The red line shows the phase diagram of hydrate formation for natural gas and water. The green line shows the phase shift with addition of 20 % MEG. The pink line shows the phase shift with the addition of 20 % MeOH. The two blue lines shows the phase shift with the addition of 20 % of the electrolytes NaCl and formiate, respectively. The figure is reproduced from UiB internal presentations, courtesy of S. Hiland.

must be saturated using 60 % MEG to avoid hydrate formation and another 10 % to avoid ice formation. Seperate pipelines are built to accomodate the supply of MEG.[1] Typical concentrations of thermodynamic inhibitors are 10-50 %.[20]

Low dosage hydrate inhibitors

Kinetic inhibitors (KHI) and anti-agglomerants are often called low dosage hydrate inhibitors (LDHI), due to their efficiency at low doses compared to thermodynamic inhibitors. A typical concentration of an LDHI is 0.1-3 %wt of the aqueous phase.[2, 20]

KHIs are generally water-soluble polymers, and act as anti-nucleators that increase the induction time of hydrate formation. Most KHIs also slow hydrate crystal growth by adsorbing to the hydrate/water interface. This delays the growth rate of small hydrate crystals into growing into larger hydrate crystals.[20]

Anti-agglomerants (AAs) are generally surface active compounds (see section 1.5.1) that are thought to work by a polar head group interacting with the water molecules in the hydrate lattice, while a hydrophobic tail group interacts with the bulk hydrocarbon phase, making the hydrate particles "oil-wet". Oil-wet particles have been found to stabilize water-in-oil emulsions.[16, 19] Dispersed hydrate particles are transported in

the fluid as a slurry, making the maximum water cut when applying AAs approximately 50 % due to the increase in viscosity.

The efficiency of LDHIs can be compared in their performance during subcooling. Subcooling is the difference between the hydrate equilibrium temperature and the operating temperature at a given pressure. Efficient AAs perform at higher subcoolings than KHIs.[20]

LDHIs are good alternatives to thermodynamic hydrate inhibitors, but are restricted on the Norwegian continental shelf due to their low biodegradability.[20]

Natural inhibiton

In some multiphase systems transporting crude oil, plugging is never observed even in the hydrate stable P-T area for natural gas present in the system. Some crude oils have been identified to exhibit these properties,[16–18, 21, 22] and are believed to naturally contain surfactants, *natural inhibiting compounds* (NICs), providing anti-agglomerating properties in a multiphase system.

Such crude oils have been found to generate oil-wet hydrate surfaces, thus preventing agglomeration of hydrates and avoiding plugging in multiphase systems in the hydrate forming P-T area. NICs are believed to occur in the polar fractions of the crude oil, such as asphaltenes and resins.[21, 22] NICs have been especially associated with the acid fraction of the crude oils.[2, 3, 23]

1.3.3 Hydrates as a resource

Gas hydrates has received a lot of attention as a potential energy resource, especially due to the large amount and widespread occurrence of naturally formed methane hydrates. Table 1.1 shows the estimated worldwide amounts of different carbon sources. The natural occurrence of gas hydrates is conservatively estimated to the double of the total amounts of estimated reserves of oil, gas and coal added together.[24]

Methane in naturally occuring gas hydrates are dominantly formed from the anaerobic microbiological decay of organic matter, but can also occur from thermogenic origin. With enough gas present, hydrates generally form at two types of geologic settings: beneath the permafrost in arctic areas and at water depths deeper than 500 m, beneath the ocean floor. The high pressure and low temperatures here can lead to several hundred meter thick hydrate deposits.

TABLE 1.1: Worldwide sources of organic carbon and estimates of their amounts. Carbon from gas hydrates are estimated to total twice the amount of carbon to be found in all known fossil fuels on Earth. Adapted from Demirbas 2010.[24]

Source of organic carbon	**Amount (Gigaton)**
Gas hydrates (onshore and offshore)	10 000 - 11 000
Recoverable and non-recoverable fossil fuels (oil, coal, gas)	5000
Soil	1400
Dissolved organic matter	980
Land biota	880
Peat	500
Others	70

There are still many production problems to overcome with respect to extraction of methane from naturally occuring hydrates. The geology underneath the ocean floor is a balanced system, and removing several meter of hydrate layer may destabilize an entire system with unknown consequences.[24]

1.4 Crude oil

Crude oil is generally a mixture of hydrocarbons with minor amounts of compounds containing nitrogen, sulphur and oxygen. Trace amounts of inorganic constituents such as nickel, vanadium, copper and iron is also present.

Due to the large amounts of compounds present in a crude oil, fractional separation is common rather than separation into single compounds. Several separation procedures are used with accompanying fractional descriptions. The most common procedures are based on boiling point, separating crude oil into light and heavier fractions with different applications.

A different procedure is the separation based on solubility. An example of that is the characterization of a crude oil based on its content of saturated, aromatic, resin and asphaltene compounds (SARA-fractionation). The resins and asphaltenes are considered the polar fractions, containing the nitrogen, sulfur and oxygen (NSO) compounds.[25]

1.4.1 Biodegraded crude oil

Biodegraded crude oils are crude oils altered by living organisms. Figure 1.5 shows the GC profiles of a typical non-biodegraded oil and a typical moderately biodegraded oil.

Crude oils with a higher biodegradation classification have been found to have a higher content of acids,[26] and have also been correlated with having a lower tendency to form

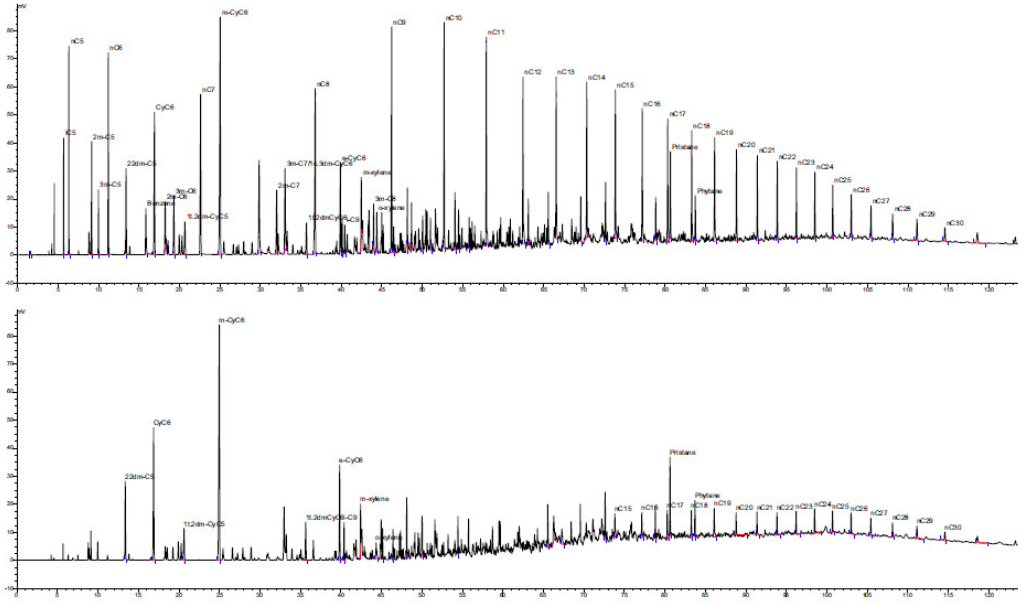

FIGURE 1.5: Examples of changes in the composition of a crude oil due to biodegradation, illustrated by a gas chromatogram. n-alkanes are given as nCx, where x is the corresponding carbon number. Upper: a typical non-biodegraded crude oil. Lower: a crude oil that has undergone moderate biodegradation (crude oils spectra obtained from the HYPERION project, University of Bergen 2007).[2]

gas hydrate plugs in multiphase systems.[2, 3] It has been hypothesized that the process of biodegradation create NICs, surface active compounds that work as anti-agglomerants in the multiphase crude oil/water/gas system.[2, 7]

1.5 Wettability

Wettability can be defined as the degree of spreading (*wetting*) a liquid has on a solid surface, and is determined by a balance of the adhesive and cohesive forces. A quantification of the wetting of a solid can be attained through the contact angle θ, measured through the heavy phase in the three-phase contact point of a liquid drop in thermal equilibrium with a horizontal surface.[4]

The contact angle is related to the interfacial tension through Young's equation[27]:

$$\cos\theta = \frac{\sigma_{so} - \sigma_{sw}}{\sigma_{wo}} \tag{1.1}$$

The interfacial tension is represented by σ. In this work, the relevant interfaces have been solid-oil, solid-water and water-oil. The light phase (oil in this case) is more commonly represented by a gas phase (air). The contact angle value of a solid/water/oil-system characterizes the wetting of the surface as water-wet for contact angles lower than 75°

and oil wet for contact angles larger than 115°. The intermediate angles represents no particular wetting characteristic of neither oil-wet or water-wet.

1.5.1 Surfactants

Surfactants or surface active compounds are characterized by a molecular structure containing a hydrophibic and a hydrophilic part. The hydrophilic part is often referred to as the head group, while the hydrophobic part is called the tail.

Surfactants reduces the surface tension against air or a solid, or the interfacial tension between liquid/liquid. Surfactants have a wide application as detergents, emulsifiers, dispersants and are often used for enhanced oil recovery.

At a certain concentration in water, surfactants will form aggregates, micelles. This concentration is called critical micelle concentration (cmc). The cmc is different between different surfactants and also depend on other additives to the aqueous phase, for example inorganic electrolytes.[28]

1.5.2 Wetting index

The wetting index or emulsion method was established by Høiland et.al. [16] as a simple method of assessing and comparing the potential of crude oils for creating gas hydrate plugs under gas hydrate-forming conditions.

The surface energy of hydrates in petroleum is thought to be a key parameter in the plugging tendency of crude oils. Because wettability of the hydrates is governed by the surface energy, and is similarly influenced by the properties of the fluids in which they grow,[19] this characteristic is a practical way to compare plugging tendencies.

Hydrates in an oil/water emulsion can be seen as either oil wet or water wet particles. Additives can adsorb to the surface of the hydrates so that wettability is changed. Oil wet particles (contact angles >90°) tend to stabilise water-in-oil emulsions, while water wet particles (contact angles <90°) tend to stabilise oil-in-water emulsions.[19] Figure 1.6 shows a schematic of a solid particle and its wettability in the oil/water interface.

It has been demonstrated by several authors, for example Binks and Lumsdon,[29, 30] that by altering the volume ratio of the two liquid phases, the inversion of emulsions stabilised by solid particles, in effect the shift from water-continuous to oil-continuous emulsions or vice versa, can be induced. The point of phase inversion is dependent on the wettability of the hydrate particles.

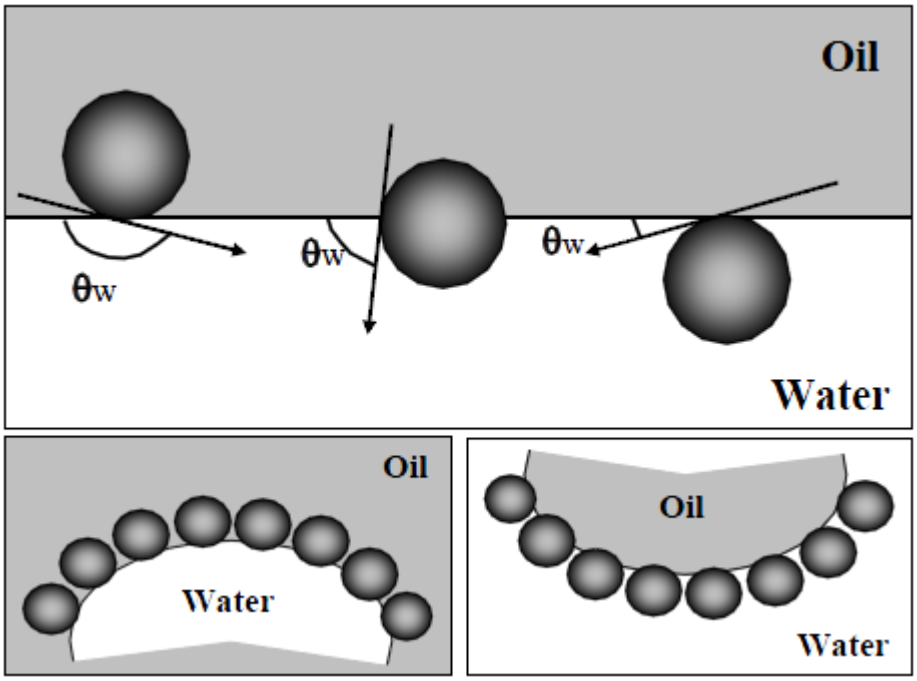

FIGURE 1.6: Schematic of wetting of spherical particles at a planar oil/water interface. Left: Contact angle >90° indicates an oil-wet particle, residing mainly in the oil phase. The tend to stabilize water-in-oil emulsions. Right: Contact angle <90°, indicating a water-wet particle residing mainly in the aqueous phase. These particles tend to stabilize oil-in-water emulsions. Figure from Høiland et.al.[19]

In the studies by Høiland and Borgund et.al.,[16, 18] hydrate wettabilities obtained from observing emulsion phase transition were compared to natural gas hydrate plugging tendencies at realistic conditions. The results revealed that crude oils generating oil wet hydrates form hydrate dispersions, whereas crude oils generating intermediate wet or water wet hydrates form hydrate plugs. This indicates that agglomeration could be prevented by the presence of chemical additives that form oil wet hydrates.

Trichlorofluoromethane, Freon R11, form structure II hydrates below 8.5°C at 1 bar.[31] It has been shown that the addition of Freon to different oil/brine systems below 8.5°C changes the point of phase inversion compared to oil/brine systems without Freon at the same temperature. This observation could not be replicated at 12°C, a temperature outside the hydrate forming area.[16] This is assumed to be an indication that Freon hydrates acts as particles that changes the emulsion behaviour of an oil/brine system.

1.6 Biodegradation

Biodegradation is a process where microorganisms break down organic compounds, either through transformation into less complex metabolites or through mineralization

into inorganic minerals, H_2O, CO_2 and CH_4. Other gases such as H_2, H_2S and N_2 are also possible byproducts. The degree and rate of biodegradation depend on many factors including oxygen access, pH, temperature, microbial population, degree of acclimation, accessibility of nutrients, chemical structure of the compound, cellular transport properties, and chemical partitioning in growth medium. The presence or absence of oxygen promotes aerobic or anaerobic biodegradation. Aerobic degradation is the most common pathway, where oxygen is an electron acceptor. In order for anaerobic biodegradation systems to function, terminal electron acceptors such as iron (III), manganese oxide, nitrate or sulfate must be present.[32]

1.6.1 Anaerobic sulfate reduction

According to Jørgensen (1982),[33] oxidation of organic compounds coupled to sulfate reduction into H_2S may account for more than 50% of the mineralization of carbon in marine sediments. In oil fields where saline water with high content of sulfate are present, the activity of sulfate reducing bacteria may be detrimental. The production of hydrogen sulfide gas through sulfate reduction is a large cause of corrosion, decreases the quality of oil and gas by increasing sulfur content and leads to precipitation of insoluble ferrous sulfide, potentially causing plugs and stabilizing oil-in-water emulsions.[34]

When sulfate is reduced rather than oxygen or nitrate, the energy obtained from the reaction is significantly lower. Equation 1.2 shows the stoichiometric equation of anaerobic oxidation of toluene using sulfate reduction, and the energy obtained. Equation 1.3 shows the stoichiometric equation of anaerobic oxidation of toluene using nitrate reduction, and the energy obtained.[35]

$$C_7H_8 + 4.5\,SO_4^{2-} + 3\,H_2O \longrightarrow 7\,HCO_3^- + 2.5\,H^+ + 4.5\,HS^- \;\delta G'^{\circ} = -205\,kJ\;(mol\;toluene)^{-1} \tag{1.2}$$

$$C_7H_8 + 7.2\,NO_3^- + 0.2\,H^+ \longrightarrow 7\,HCO_3^- + 3.6\,N_2 + 0.6\,H_2O \delta G'^{\circ} = -3554\,kJ\;(mol\;toluene)^{-1} \tag{1.3}$$

1.6.2 Biosurfactants

Biosurfactants are surface active compounds synthesized by microorganisms. Structures are diverse, and their ability to reduce surface- and interfacial tensions in both aqueous solutions and hydrocarbons give them wide application possibilities. Among other applications, these compounds are good candidates for enhancing oil recovery and for deemulsification purposes. The main advantages over synthetic surfactants are the possibility to extract from renewable feedstocks, the lower toxicity, higher biodegradability and specific activity at extreme temperatures, pH and salinities.[36] A review of some structural classes, their properties and application potential is given by Lang (2002).[37]

Many biosurfactant classes include acidic functionalities, and is thought to be one source of acidic compounds found in petroleum.[2] A biosurfactant is produced when a bacteria existing in the aqueous phase needs to reduce the interfacial tension between the oil and water in order to access the oil as a carbon source.[38]

1.7 Approach

In order to measure changes done from using different additives, a model system had to be established. As a model oil, Marcol 52, a non-reactive white oil was selected. Using a white oil makes wetting properties easier to measure with a standard pendant drop instrument, and thus results can be compared to wetting index and quantification measurements.

The bacteria *Desulfotignum toluenicum* was used to degrade pure toluene and crude oil as a follow-up to the work of Dr. Kristin Erstad.[2] This bacterium was found to decrease plugging tendency in a crude oil biodegraded for 10 months. According to the PhD thesis of Hege Ommedal,[5] this bacterium grows faster on toluene than on crude oil, so a system of pure toluene to promote growth was chosen in addition to the crude oil system.

The hypothesis was to see whether these bacteria produced any biosurfactants in the aqueous phase of the system. Using toluene was hypothesized to have a similar effect on the aqueous medium as when using crude oil. The suitable crude oil was chosen based on having a negative plugging index, in effect a high tendency for plugging. Several crudes were tested, chosen based on results from previous years, but the general tendency was for crudes that had been kept for extended amounts of time, some for several years, to have a positive plug index, in effect a low tendency for hydrate plugging. The crude oil chosen, Statfjord A, was supplied by Professor Terje Torsvik at UniCIPR, Institute for Microbiology, considered fresh and stored on a dark bottle with a nitrogen atmosphere.

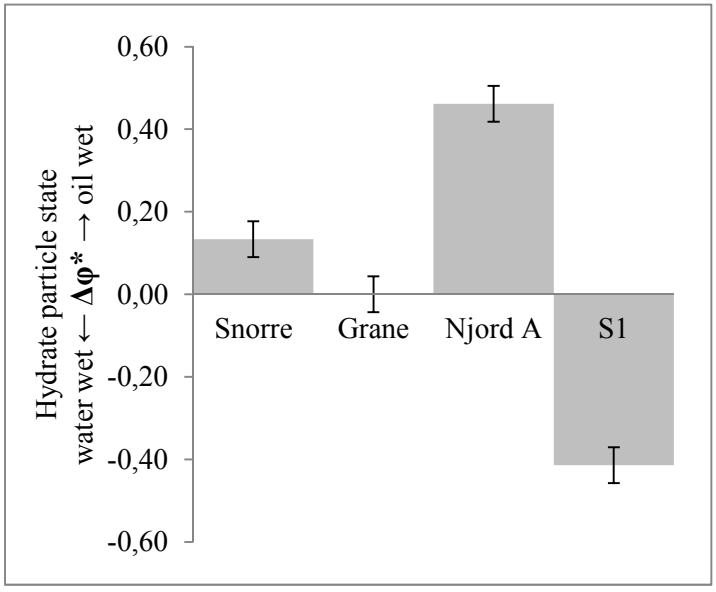

FIGURE 1.7: Wetting index of different crude oils analysed prior to microbial degradation.

Chapter 2

Methods

2.1 Materials

Table 2.1: Additives to model system applied, and labels used in figures subsequently. Additives are added in a concentration of 500 ppm by mass.

Labelled	**Name**	**Supplier**
BL0	Marcol^{TM} 52 (blank)	ExxonMobil
NAC	Naphthenic acids, commercial	Sigma Aldrich
NA	Naphthenic acids, extracted	Naphthenate deposit obtained from Hege Kummernes, Statoil.
LM	Lauryl maltoside (n-dodecyl-β-D-maltopyranoside)	Avanti polar lipids, Inc.
OG	Octyl glucoside (n-octyl-β-D-glucopyranoside)	Avanti polar lipids, Inc.
S1	Crude oil, Statfjord A	Prof. Terje Torsvik, UniCIPR

All chemicals used are HPLC grade and used without purification if not otherwise mentioned. All water used is ultra pure, unless otherwise mentioned. All equipment is properly rinsed and dried prior to use. Table 2.1 shows the model oils, additives and labels used throughout this thesis. Figure 2.1 shows an overview of the additives and tests on the model system.

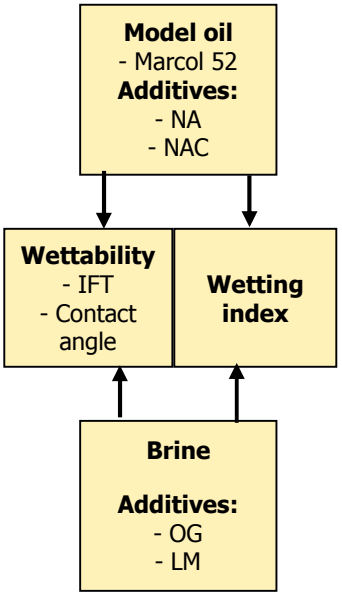

FIGURE 2.1: Flow chart of additives to model system and tests done.

2.2 Physical properties

2.2.1 Wetting index

This method for evaluating hydrate wettability from phase inversion in crude oil/brine emulsions is described in Høiland et al.[16] The basic principle of the method is to determine the *catastrophic point of phase inversion*, φ_w^{inv}. This is done by stepwise increasing the brine to oil ratio (v/v) from 10 %vol brine to 90 %vol brine (steps of 5 %vol), and determining the volume of brine at which phase transition from an oil continuous to a water continuous emulsion can be observed. The point of phase inversion can be detected by an abrupt change in emulsion behaviour, for example the behaviour of the emulsion when added to pure water. A sample picture is shown in figure 2.2.

The points of phase inversion is determined for oil/brine emulsions both with hydrates (φ_w^{inv}) and without hydrates (φ_w^0) in order to elucidate the effect of the hydrates. The difference between the two inversion points is given as

$$\Delta\varphi_w^{inv} = \varphi_w^{inv} - \varphi_w^0 \tag{2.1}$$

The value of $\Delta\varphi_w^{inv}$ is correlated to the wettability of the hydrates present in each system, based on the assumption that water wet particles will decrease the stability of the water-in-oil (w/o) emulsion, whereas oil wet particles could increase the stability of water-in-oil (w/o) emulsions.[19] The standard error of the point of phase inversion

FIGURE 2.2: Example pictures of emulsion states taken during laboratory experiments by the author. Left: water-in-oil emulsion, right: oil-in-water emulsion.

is ±0.025 due to the stepwise increase of 0.05 v/v ratio of brine in the method. A significant value of $\Delta\varphi_w^{inv}$ is typically ±0.1. A positive value indicates the presence of oil wet hydrate particles, whereas a negative value indicates the presence of water wet particles. In between -0.1 and 0.1, the hydrate particles are considered weakly water wet, intermediate wet and weakly oil wet.

The value of φ_w^0, is the initial inversion point for systems without hydrates, and affects the maximum possible alteration of φ_w^{inv} (either decrease or increase) that the presence of hydrates may impose in either direction. In order to account for the influence of φ_w^0, the values of $\Delta\varphi_w^{inv}$ are normalised according to Equation 2.2

$$\Delta\varphi* = \frac{\Delta\varphi_w^{inv}}{\Delta\varphi_{max}} \quad for \quad \begin{aligned} &\Delta\varphi_w^{inv} \geq 0 \Rightarrow \Delta\varphi_{max} = 1 - \Delta\varphi_w^0 \\ &\Delta\varphi_w^{inv} \leq 0 \Rightarrow \Delta\varphi_{max} = \Delta\varphi_w^0 \end{aligned} \tag{2.2}$$

As a model hydrate former, CCl_3F, Freon (R11) is used. This molecule forms structure II hydrates below 8.5° C at 1 bar,[31] making it easy to work with at atmospheric pressure and relevant to natural gas hydrates in petroleum production. All wetting index tests were performed at -2 to 0°C, in order for the conditions to be below the hydrate forming temperature of Freon.

2.2.2 Density

The density of a material is defined as the mass of the material per unit volume and is dependent on the temperature applied. Density was measured by the use of a density

meter.

The instrument used was an Anton Paar Density meter DMA 4500M with an attached Xsample 52 sample handling unit. Density was measured at room temperature (22°C) in parallels of two by leaving the injector tube in the liquid to be measured. The sample tube was rinsed using toluene and acetone and dried between each measurement.

2.2.3 Interfacial tension

The interfacial tension (IFT) is measured as the force acting at a boundary between two immiscible liquids and defined as the force per unit length or energy per unit area. When measured liquid/solid- or liquid/gas-interfaces, the value is called surface tension. There are several techniques to measure IFT, the method used in this work is the pendant drop method. The pendant drop method is a geometric method, based on the shape of the drop. The interfacial tension is found based on a rewriting of the Young-Laplace equation, equation 2.3.[39]

$$\sigma = \frac{\Delta\rho g R^2}{\beta} \tag{2.3}$$

$\Delta\rho$ is the difference in density of the two phases, g is the gravitational constant, R is the the radius of the curvature at the apex of the pendant drop. β is the form factor constant, a function of the drop shape observed.

Interfacial tension was measured at room temperature (22°C) using a Teclis Tracker H Pendant drop instrument connected to a computer, which is an automated intrument for carrying a needle and accurately dispensing a drop, equipped with a light source and a CCD camera that automatically obtain images to the software. The tip of a calibrated needle carrying the heavy phase was immersed in a cuvetted filled with the light phase. Each system was optically calibrated using a calibration ball in the cuvette containing the light phase.

A drop of 10 μL was dispensed from the needle, and the image of the drop was analysed using the Windrop software. The interfacial tension was measured as a function of time, and the average of the stable tension was used. For some systems with lower interfacial tension, a lower drop volume had to be applied. For the system with the lowest interfacial tension, the available needles could only support 0.1 μL, so the value of the IFT for this system is not reliable. No effort was made to measure this more accurately using other methods, as the value is still considered to serve the purpose of this thesis.

2.2.4 Contact angle measurement

Contact angle measurements were carried out through drop shape analysis, applying the same method as described by Aspenes et.al.[40]

Contact angles were measured at room temperature (22°C) using a Teclis Tracker H instrument connected to a computer, in sessile drop mode. Each system was optically calibrated using a calibration ball in a cuvette containing the light phase. The tip of a calibrated needle carrying the heavy phase was immersed in the cuvetted filled with the light phase and a pre-aged stainless steel plate. A pre-set volume of heavy phase was dispensed from the needle, and left on the stainless steel plate to settle. The contact angle was calculated from the obtained image using the Windrop software.

The stainless steel plates used were described by Aspenes et.al.[40] to contain approximately 68 % iron, 18 % chromium, 12 % nickel, 2 % molydenum, with traces of carbon and silica. The composition of the surface area is dependent on chemical composition, pH and temperature of the aqueous solution the steel plate is in contact with. In air and at pH values <6, the plates will form a corrosion resistant protective layer consisting of mainly insoluble chromium oxides (Cr_2O_3 / $Cr(OH)_3$) with traces of iron oxide (Fe_2O_3). The surface free energy of the plates were found to be 64 ±5 mJ/m^2.[40]

The plates were cleaned using Sodosil detergent, rinsed with distilled water and dried after each measurement. The dried plates were flushed with iso-propanol, dried using N_2-gas and submerged in the light phase for minimum 24 hours, for aging purposes prior to contact angle measurement.

2.2.5 Viscosity

The viscosity, η, is defined as the slope of the function when shear stress, τ, is plotted against shear rate, γ. When this function is linear, meaning that the viscosity does not change with increasing shear, the fluid is called a Newtonian fluid.

The shear stress is defined as the shear force F, divided by the area of contact between a liquid and a plate, A (equation 2.4).

$$\tau = \frac{F}{A} \tag{2.4}$$

The shear rate is the difference in velocity between the different layers, and can be calculated using the velocity, v, of the top plate with an immovable bottom plate and the distance between the plates, h, as in equation 2.5.[41]

$$\gamma = \frac{v}{h} \tag{2.5}$$

Viscosity was measured with increasing shear rate using an Anton Paar Modular Compact Rheometer, MCR 102. The samples were measured in parallel plate mode with a gap of 0.8 mm, and results were analysed using Rheoplus software.

2.3 Characterisation of Crude Oil

2.3.1 Fourier Transform Infrared Spectroscopy

Infrared spectroscopy is mainly applied for information on functional groups present in a sample. The sample is irradiated by infrared light, wavelengths typically from 2500 to 20 000 nm, which is absorbed by bonds of some functional groups. When IR radiation is absorbed, this leads to a change in vibrational energy state, which only occurs with a change in the dipole moment of a bond. Different vibrational modes of different bonds requires different wavelengths, and this can be related to the absorption bands observed in the IR spectrum. In fourier transform infrared spectroscopy, the transmitted light is registered and transformed by a mathematical operation, fourier transformation, into a plot against the wavelengths absorbed, given as reciprocal cm by convention.

With the attachment of an attenuated total reflectance measuring cell, the infrared light is sent into a diamond crystal which is in contact with the sample to be analysed. The radiation is reflected in the crystal, sending a wave into the sample, and the signal is attenuated in the spectral region where the sample has absorbed energy. The difference in the transmitted radiation is detected as the basis of the obtained spectra. Usually, many spectra are acquired for the same sample and automatically averaged for a final spectrum.[42]

The FT-IR instrument used was of the type Thermo/Nicolet 380 FTIR, with an attenuated total reflectance crystal attached. The IR spectra were obtained by placing the liquid samples directly on the attached attenuated total reflectance crystal. The spectrum was measured subsequent to evaporation of any solvent.

2.3.2 Whole Oil Gas Chromatography

Gas Chromatography is based on the principle of separating organic compounds on a column by heating the column and flowing through an inert carrier gas, the mobile

phase. The column, in GC normally a capillary column, can be covered with different stationary phases, typically a heavy liquid polymer.

The compounds to be analyzed are separated mainly based on their boiling points, and to some extent their different affinity for the stationary phase. The samples are detected based on the retention time on the column, and the separation between signals can be optimized by applying temperature programming to include a wider range of boiling points in a shorter amount of time.

The most common detector in GC for analysis of organic compounds is the flame ionisation detector (FID), which works by burning the sample in a flame, counting the ions produced by relating it to the electrical conductivity, and relating this to the concentration in the sample.[43]

The whole oil gas chromatography in this thesis was kindly performed by master student Stian Fonnes.

An undiluted oil sample was directly injected into a ThermoFinnigan Trace GC equipped with a flame ionization detector (FID). The column was J&W Scientific ($30m \times 0.25mm \times 0.25\mu m$) with a DB-5 5%-Phenyl-methylpolysiloxane stationary phase and Helium gas as mobile phase.

The temperature program applied is described by Erstad 2009,[7] initial temperature 30 °C held for 15 minutes, then increased to 60 °C with a ramp rate of 1.5 °C/min and finally 4 °C/min to the final temperature of 320 °C, where it was kept for 15 minutes. The injector temperature was 300 °C and detector temperature was 350 °C. The resulting chromatograms were compared to chromatograms of Norwegian Standard Oil (NSO-1) from NIGOGA,[44] in order to identify the largest peaks.

2.3.3 SARA – Saturates, Aromatics, Resins and Asphaltenes

The saturates, aromatics and resins were separated using solid phase extraction (SPE), method described by Moen, L. K.[45] The SPE columns were conditioned using three portions of 1 mL hexane. 100 mg of oil was diluted with 1 mL hexane and the diluted oil was added to the column. The saturated fraction was eluted by 2x1 mL hexane, the aromatic fraction was eluted by 2x1 mL DCM:hexane (10:90) and the resin fraction was eluted by 2x1 mL DMC:MeOH (50:50). The asphaltenes were assumed irreversibly adsorbed to the column. Each fraction was collected in a separate pre-weighed vial, and the total mass of the solution was determined.

The relative content of saturates, aromatics and resins in the different oils were quantified by weighing 10 μL of each solution. The solvent was evaporated after 20 minutes and

the stable weight of the remaining organic material was recorded. Each weighing was done twice in order to ensure the results were within 10% of each other. The total volume in each vial was calculated using the density of the solvent divided by the total mass of the solution.

The asphaltene content of the crude oils was determined by the method described by NIGOGA.[44] 0.5 g crude oil was weighed directly into pre-weighed centrifuge tubes, and added 300 μL 93:7 (v/v) DCM:MeOH in order to dissolve potentially pentane soluble compounds encapsuled in large aggregates. 13.89 g of pentane was added to each tube, and they were put in an ultrasonic bath for 10 minutes before being stored in a dark, cool place for 24 hours. For simplification, and in order to make sure that an excess of pentane, 40 volumes of pentane by volume of oil, was added, the density of the oil samples were assumed to be 0.9 g/mL.

After 24 hours, the tubes were centrifuged for 5 mins at 3000 rpm, excess liquid was removed and the precipitated asphaltenes were washed with 5 mL pentane, centrifuged again, excess liquid was removed and the washing procedure was repeated until the excess pentane was colourless. The remaining precipitate was dried until stable weight, approximately 1 day.

The asphaltene content of each oil was quantified by dissolving the dried precipitate in DCM:MeOH (93:7) and transferring it analytically into pre-weighed vials. The stable weight was recorded after solvent evaporation. The asphaltene content was determined from the average of two parallels.

2.3.4 TAN – Total Acid Number

Total Acid Number (TAN) is a non-aqueous potentiometric titration procedure that has been standardised by the American Society for Testing and Materials (ASTM664-89). The procedure is commonly used by the petroleum industry, in order to keep track of acidity. Oils high in TAN is considered lower quality due to corrosion and refinery problems.[46] TAN is defined as the mass in mg of base (potassium hydroxide) necessary to titrate 1 g of sample to an inflection point on a titration curve.

1 g of oil was dissolved in 40 mL of the solvent in a beaker for the automatic titrator. The solution was stirred for two minutes prior to addition of titrant. The equivalence point (EQP, mL KOH added) on each titration curve was determined, and the total acid number was calculated using equation 2.6. C_{KOH} is the concentration of the titrant in mol/L, B is the blank value of the solvent in mmol, Mm_{KOH} is the molar mass of KOH in g/mol and m_{oil} is the mass of oil in g.

$$TAN = \frac{(C_{KOH} \times EQP - B) \times Mm_{KOH}}{m_{oil}} \tag{2.6}$$

The electrode on the automatic titrator was calibrated using buffers of pH 4.00, 7.00 and 11.00. The titrant used was 0.05 M KOH in iso-propanol (prima quality), and was standardised using potassium hydrogen phthalate. The solvent used was 50:49.5:0.5 (v/v) toluene:iso-propanol:water. Each sample was tested in parallels of two. A blank value was determined for each new batch of solvent prepared. The titration curve was found as mL titrant against signal from electrode in mV.

2.3.5 Acid extraction

A naphthenate deposit was obtained from Hege Kummernes at Statoil ASA. This was extracted using 1.0 M hydrochloric acid and toluene (Sigma-Aldrich, used without further purification). Acids were extracted from this using ion-exchange chromatography, described by Mediaas et al.[47] and Borgund et al.[48] QAE Sephadex A-25 was used as the solid-phase material for the ion exchange of the naphthenic acids.

The oil to be extracted was weighed into a jar, and put on stirring with a magnetic stirrer. At least 0.5 g of ion exchange resin (IER) was weighed out (calculated based on TAN and mass of oil weighed out, see Mediaas et.al.[47]), added to a Whatman GF/C filter and washed with 75 mL carbonate buffer per g IER. pH was adjusted to neutral with rinsing the IER with distilled water, and then the IER was saturated with methanol, approximately 25 mL methanol per g IER.

The IER was added to the oil and put on stirring at 150 rpm for 16 hours. After 16 hours, the non-acidic compounds were removed from the resin by filtering the oil through a Whatman GF/C filter and washing using 10 mL toluene and 10 mL of 2:1 toluene:methanol. The washing procedure was repeated twice by filtering the filtrate through two separate Whatman GF/F filters. This filtrate was evaporated on a rotating evaporator, dissolved in 93:7 DCM:MeOH transferred to a pre-weighed jar.

The IER was added to a bottle with 50 mL 1:1 toluene:methanol per g IER and 3.5 mL 1M formic acid per g IER, and stirred at 250 rpm for 3 hours and 150 rpm for 30 minutes.

The acids were recovered by applying the same washing procedure using 2:1 toluene:methanol. The IER was was then added to a bottle with 50 mL 1:1 toluene:methanol per g IER and 0.5 mL 1M formic acid per g IER, and stirred at 200 rpm for 3 hours and 30 minutes. The same washing procedure was repeated and the filtrates were evaporated on a rotational evaporator, dissolved in 93:7 DCM:MeOH transferred to a pre-weighed jar.

The relative content of extracted acids from the oil was quantified by weighing 10 μL of the solution on a Mettler Toledo XP2U microweight. The solvent was left for 20 minutes to evaporate, and the weight of the remaining organic material was recorded. Each weighing was done twice in order to ensure the results were within 10 % of each other.

2.4 Microbial degradation

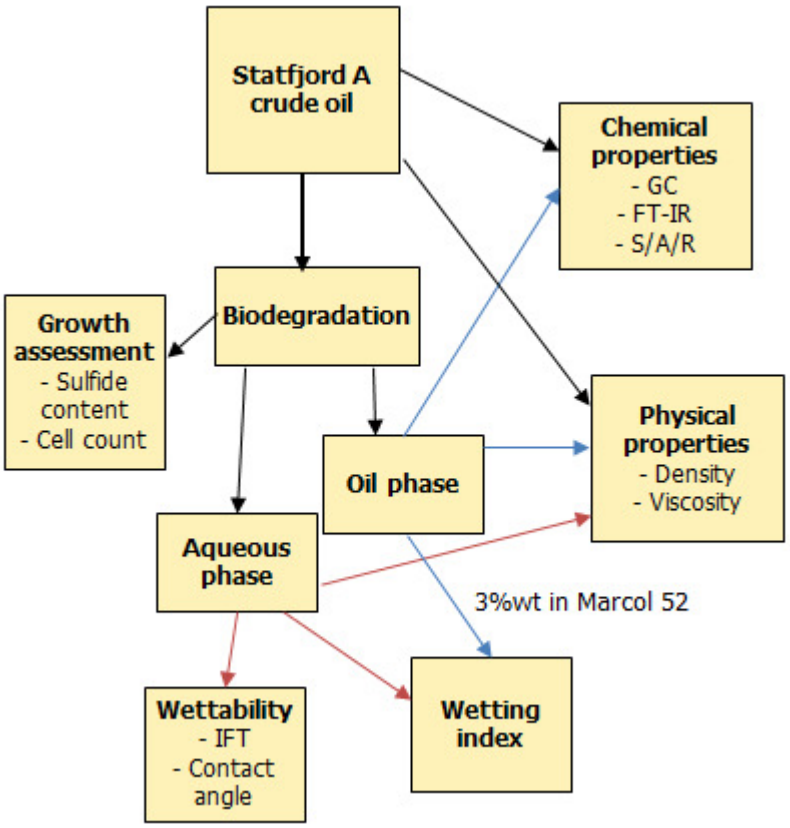

FIGURE 2.3: Flow chart of microbial degradation of Statfjord A crude oil and tests done.

A flow chart of the test done on the microbial degradation systems are shown in Figures 2.3 and 2.4.

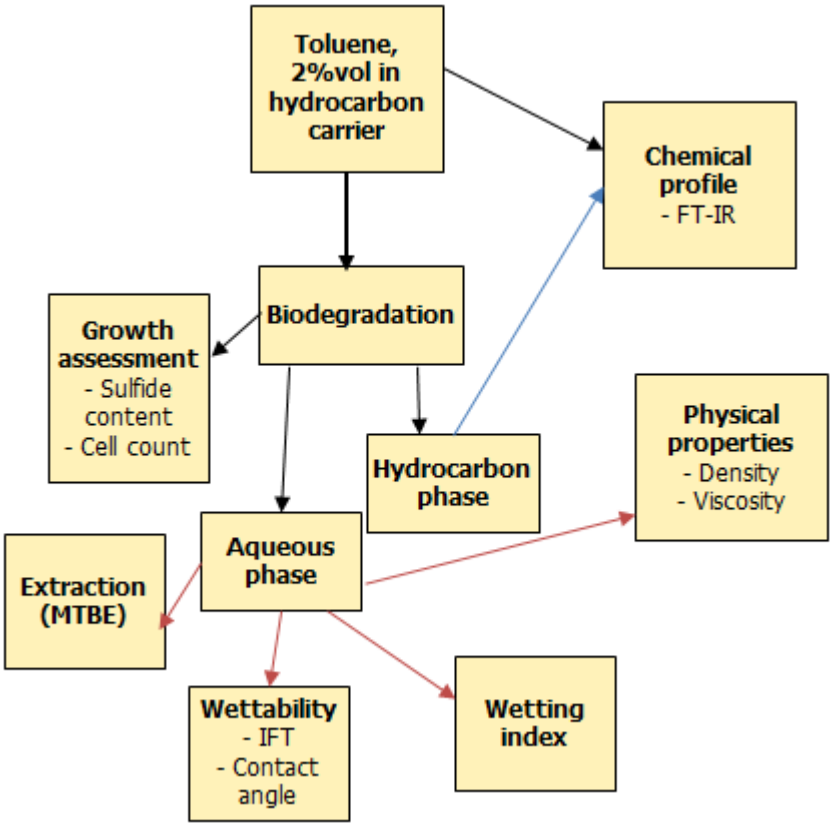

FIGURE 2.4: Flow chart of microbial degradation of toluene and test done.

2.4.1 Cultivation of *Desulfotignum toluenicum*

Two sets of samples were set up. One sample set was cultivated with only toluene, and one set was cultivated with crude oil from the Norwegian continental shelf, labelled S1. The crude oil was provided by the group of Professor Terje Torsvik, CIPR, Norway. Both the toluene and the oil was inoculated with an anaerobic bacterial culture. The anaerobic bacterium, *Desulfotignum toluenicum DSM 18732*, has been isolated and described by Ommedal and Torsvik.[5]

The crude oil incubation system consisted of 2 mL crude oil, 2 mL bacteria inoculum and 100 mL aqueous medium. The toluene incubation system consisted of 2 mL 2% v/v toluene in 2,2-4,4-6-8,8-heptamethylnonane, 2 mL bacteria inoculum and 100 mL aqueous medium. The low concentration of toluene was due to toxicity effects preventing growth at higher concentrations.[5] The medium used was 383a from Deutsche Sammlung von Mikroorganismen und Zellkulturen GmbH, with 2% NaCl.[49] The full content of the aqueous medium is attached in Appendix A. The incubation was carried out in 130 mL flasks, at 30°C, for a period of 10 months for the oil samples and 7 months for the toluene samples.

2.4.2 Sulfide content

The sulfide content of samples was measured spectrophotometrically according to the method explained by Cline.[50]

A 200-1000 μL sample of the aqueous medium, in parallels of two, was pipetted into a 50 mL volumetric flask containing 5 mL of 20 g/L ZnAc. The sample was added approximately 30 mL of distilled water, 5 mL *N,N*-Dimethyl-*p*-phenylenediamine dihydrochloride-solution (4 g/L of 6M HCl) solution and 0.5 mL $FeCl_3 \times 6H_2O$-solution (16 g/L of 6M HCl) and left to settle for 10 minutes.

The volumetric flasks were filled using distilled water, and the final solution was measured in duplicate at 670 nm using a UV-1800 Spectrophotometer from Shimadzu.

2.4.3 Cell count

Prior to preparation of object, 1-2 mL of aqueous culture media was removed using a syringe and fixated using 0.15 mL 25 % glutaraldehyde per mL culture media.

Objects for microscopic counting were prepared by filtering exactly 1 mL of medium through a GE polycarbonate black 0.2 μm over a Pall black polypropylene 10 μm. Prior to filtration, the sample was diluted to 10 mL using sterile phosphate buffered saline (PBS), and homogenized using a vortex mixer.

Subsequent to filtration, the filters were covered with DAPI-solution (4',6-diamidino-2-phenylindole)for staining DNA. This was left to react in darkness for 2 minutes, and the filters were then rinsed thrice using sterile PBS. The filters were transferred to a microscope slide with immersion oil underneath and on top of the filters, and covered with a cover slip. Prepared slides were kept cool and dark prior to counting.

For counting, a fluorescence microscope (Zeiss Axioplan) attached with a mercury lamp and a blue filter was applied. Wavelengths of <365 nm were injected, and fluorescing wavelengths observed was >395 nm, with a peak at 397 nm. The ocular used had a 10x magnification, while the objective was a 100x magnification Plan-APOCHROMAT. The factor $1{,}97 \times 10^4$ per 100 squares was used to relate the number of cells counted to the number of cells per mL sample.

2.4.4 Extraction of bacterial media

100 mL of bacterial media was extracted using one aliquot of 10 mL and one aliquot of 11 mL methyl-*tert*-butyl ether (MTBE). The solvent was evaporated under N_2-gas,

redissolved in a small amount of Folch solvent (chloroform:methanol 2:1 v/v) and transferred to a preweighed vial. The total volume in each vial was calculated using the density of the solvent divided by the total mass of the solution.

The relative content of extracted organic matter in the media was quantified by weighing 10 μL of the Folch solution on a Mettler Toledo XP2U microweight. The solvent was left for 20 minutes to evaporate, and the weight of the remaining organic material was recorded. Each weighing was done twice in order to ensure the results were within 10 % of each other.

The same procedure was repeated on 100 mL of medium filtered through a Whatman high efficiency Grade GF/F glass microfiber filter, although this sample was lost prior to weighing. A 100 mL sample of GF/F-filtered medium was adjusted from approximately pH 8 to pH 2.0 using hydrochloric acid and extracted using aliquots of 9 mL and 7 mL MTBE. Samples of medium filtered on other qualities were not possible to quantify using this method due to visible water pollution in the sample.

Chapter 3

Results

3.1 Introduction

The results of this work are organised in two sections: First, the model system and the results gained from this work are presented; second, the results attained from the microbial degradation systems are presented.

The discussion of the results is presented in Chapter 4.

3.2 Model system

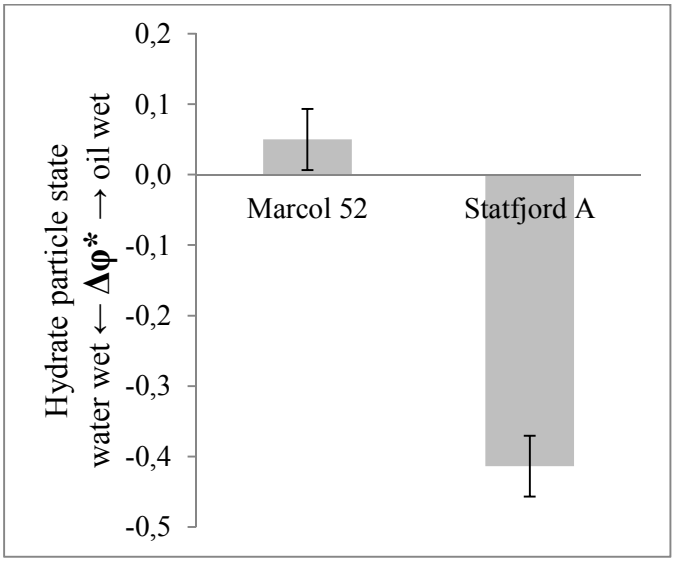

FIGURE 3.1: The wetting index of the model oils used. Negative to neutral wetting index indicates a high plugging tendency. A positive wetting index indicates a low plugging tendency.

Marcol 52 was selected as the model oil, and Statfjord A was used for crude oil tests. The chosen crude had a low Total Acid Number, 0.094 ± 0.0023 mg KOH/g oil and asphaltene content, 8.61 ± 1.49 mg/g oil. Figure 3.1 shows the wetting index of the model oils. As a model aqueous phase, 3.5 wt% NaCl in double-distilled deionized water was chosen. This is in agreement with the description in Høiland et. al. (2005).[16] As a concentration, 500 ppm was chosen. In previous works [19, 51], rhamnolipid biosurfactants have been tested and found to have an unusual high hydrate surface activity at concentrations as low as 500 and 50 ppm.

3.2.1 Naphthenic acids

The NA solution, listed in Table 2.1, was obtained as explained in section 2.3.5. Figure 3.2 shows the change in IR spectra from toluene extract into acid extract. Major peaks are listed in table 3.1. The acid extract was added to Marcol 52 in an attempt to modify initially intermediate wet and water wet hydrate surfaces to an oil wet state.

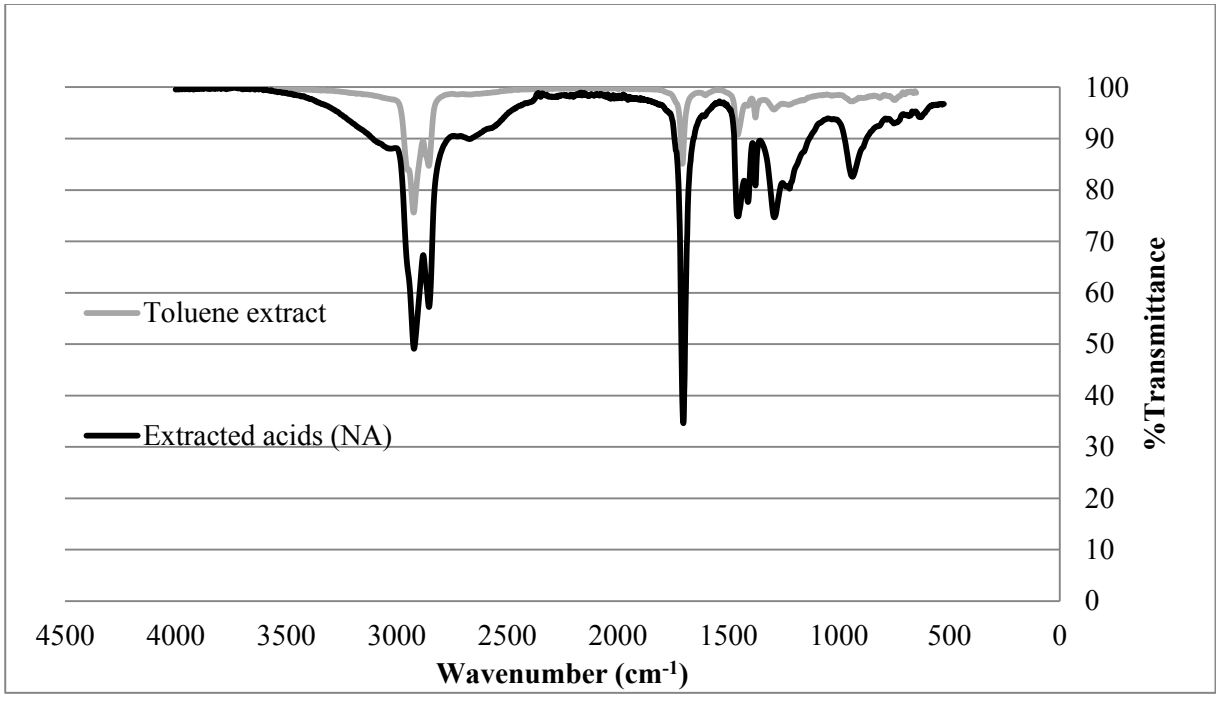

FIGURE 3.2: IR-spectra of toluene extracted naphthenate deposit and acids extracted from toluene extract.

Commercial naphthenic acids were obtained from Sigma-Aldrich, listed as a technical mixture of alkylated cyclopentane carboxic acids. The fourier transformed infra-red spectra of the two additives were recorded and compared. Figure 3.3 show that the FT-IR spectra are fairly similar.

Table 3.1: Main peaks of IR-spectra 3.2.

Possible source	**Main peaks**			
	NA	%Transmittance	Toluene extract	%Transmittance
C=O	1703	34,6	1707	85,1
Carboxylic acids O-H	2854	57,2	2854	84,7
Carboxylic acids O-H	2922	49,1	2924	75,6
Carboxylic acids O-H	2400-3300	85-95	2800-3000	85-95

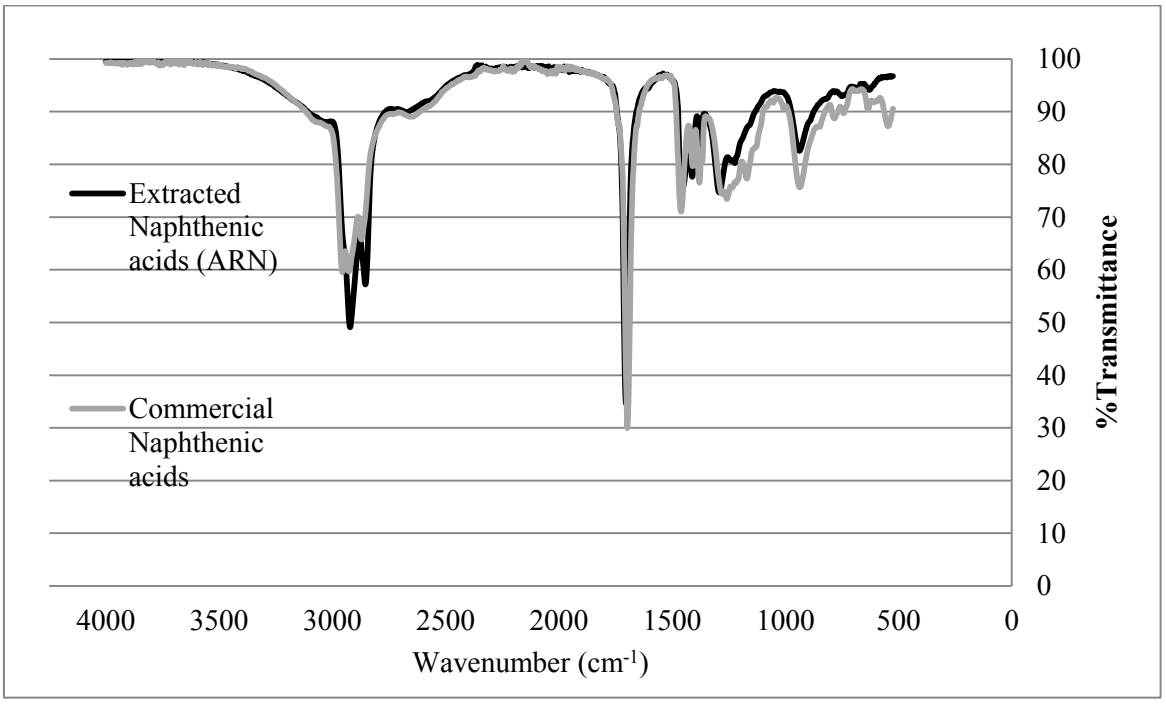

Figure 3.3: IR-spectra of extracted and commercial naphthenic acids.

Table 3.2: Main peaks of IR-spectra 3.3.

Possible source	**Main peaks**			
	NA	%Transmittance	NAC	%Transmittance
C=O	1703	34,6	1697,14	29,96
Carboxylic acids O-H	2854	57,22	2871,63	65,74
Carboxylic acids O-H	2922	49,09	2956,49	59,56
Carboxylic acids O-H	2400-3300	85-95	2980-3300	85-95

3.2.2 Wetting index

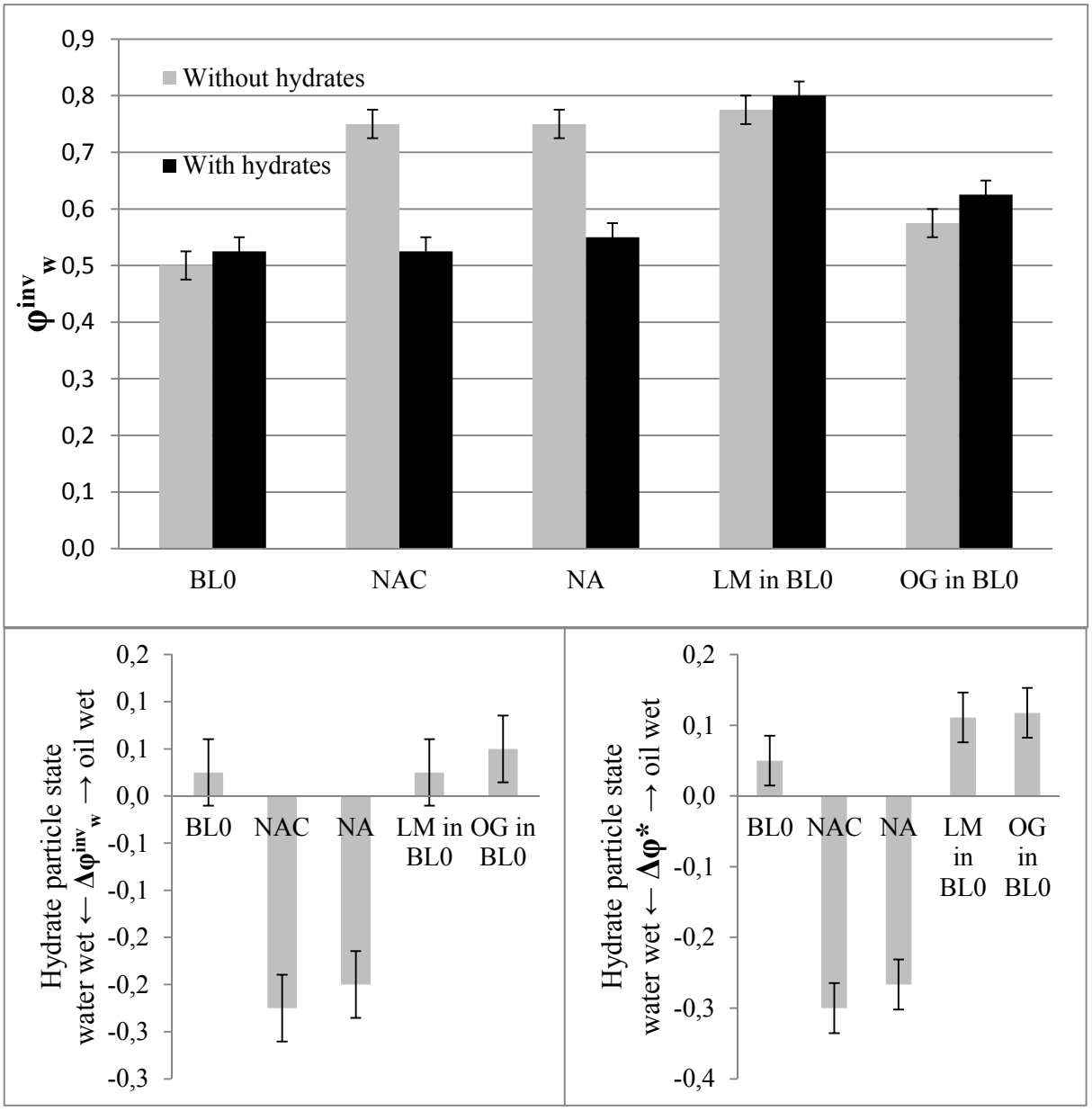

FIGURE 3.4: Top: Points of phase inversions for compounds added to model oil, down left: difference in points of phase inversions, down right: wetting index; difference in points of phase inversion, standardized according to equation 2.2. See Table 2.1 for explanations of labels.

As explained in Section 1.5.2, the wetting index can be interpreted as an indication of how easily plugs are formed in a system. Systems with a positive wetting index are assumed to be "non-plugging," and systems with neutral or negative wetting index are assumed to be plugging. Figure 3.4 shows the wetting index of the tested additives.

Table 2.1 explains the different labels in Figure 3.4. LM and OG are non-ionic biosurfactants, normally used as detergents [52]. The structures of the two alkylglycosides are shown in Figure 3.5.

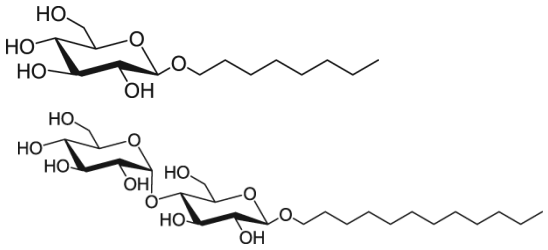

FIGURE 3.5: Upper: Octyl glucoside, lower: Lauryl maltoside. Taken from the suppliers website.[53, 54]

Initially, all additives were dissolved in Marcol 52 in order to test oil-soluble compounds. In the case of the two biosurfactants (figure 3.5), the solubility in Marcol 52 was quite poor, and stirring over night only seemed to disperse the compounds. Due to the good solubility in water, 50 mg/mL, the compounds were additionally dissolved in brine, 3.5 %wt and tested against blank Marcol 52 and a crude oil. A comparison of the plug index results of the glycosides is shown in Figure 3.6. Here it's seen that the system of Statfjord A and lauryl maltoside added to brine is the one that has had the largest change in wetting index, from a negative of -0.4 to a positive value of 0.25.

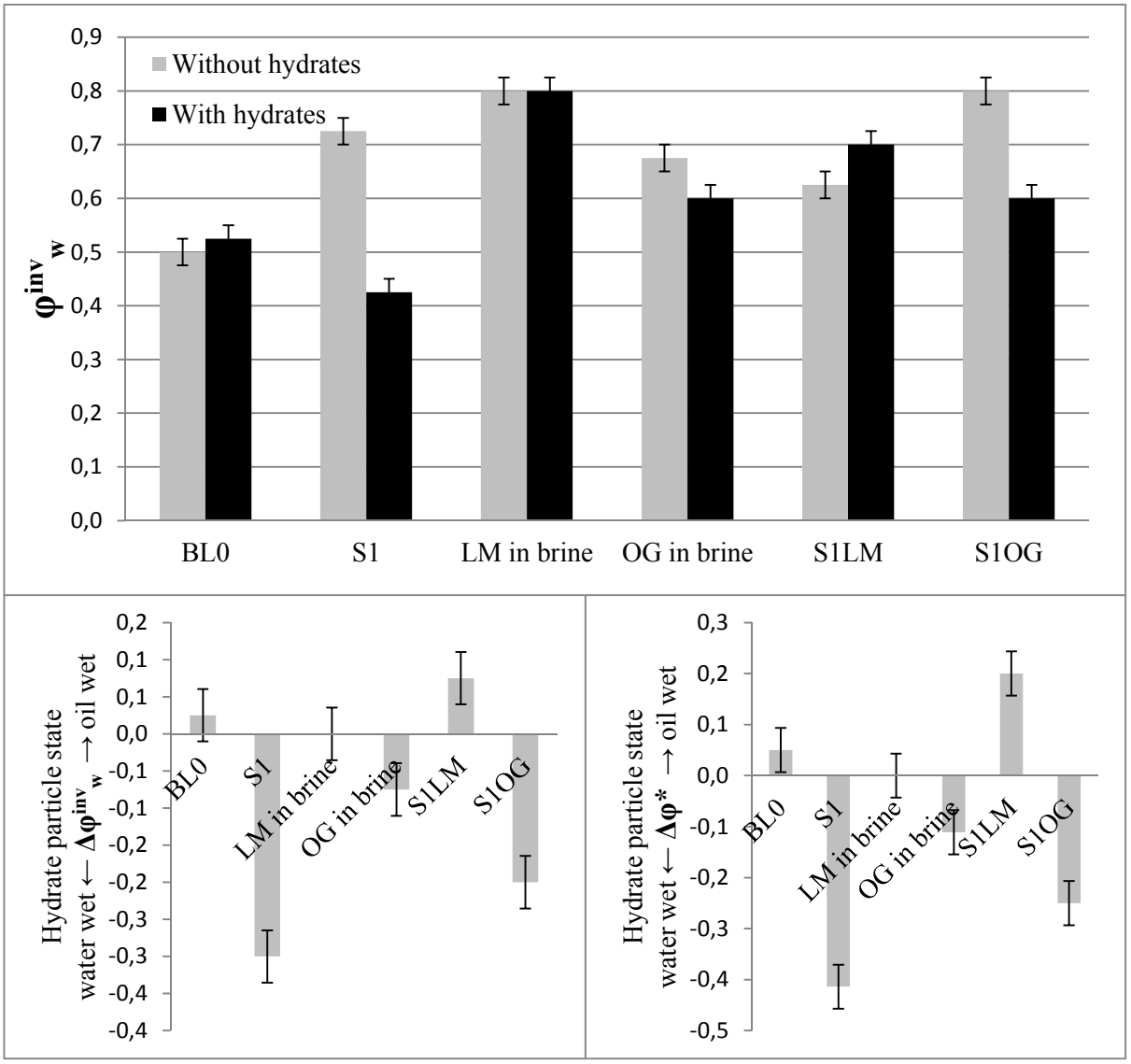

FIGURE 3.6: Comparison of efficiency of glycosides in model oil system and crude oil system. Top: Points of phase inversions with glycosides added to brine, down left: difference in points of phase inversions, down right: wetting index, difference in points of phase inversion, standardized according to equation 2.2. See Table 2.1 for explanations of labels.

3.2.3 Interfacial properties

Table 3.3 shows the interfacial tensions of the different model oil systems. Densities for the liquids used are listed in Appendix D.

Table 3.3: Interfacial tension between liquids of the model system, measured by pendant drop method.

Interface	**Interfacial tension (mN/m)**	**SD**	**%RSD**	**Number of parallells**
Brine, air	72.70	± 0.10	0.14	7
Brine, Marcol 52	13.56	± 0.26	1.94	2
Brine, NA-Marcol 52	10.60	± 0.36	3.41	5
Brine, NAC-Marcol 52	15.51	± 0.44	2.81	8
LM-brine, Marcol 52	0.41	± 0.07	16.43	6
OG-brine, Marcol 52	8.79	± 0.30	3.40	4

The interfacial tension was measured as a function of time, and the average value when the IFT vs time function was stable is listed.

Table 3.4: Contact angle values on stainless steel for model systems with various additives.

Drop, bulk phase	**Contact angle (°)**	**SD**	**%RSD**	**Number of parallells**
Brine, air	32.4	±1.3	4.0	4
Brine, Marcol 52	164	±1.0	0.6	3
Brine, NA-Marcol 52	164	±4.2	2.5	11
Brine, NAC-Marcol 52	145	±2.3	1.6	5
LM-Brine, Marcol 52	155	±2.3	1.5	5
OG-Brine, Marcol 52	166	±1.3	0.8	6

Table 3.4 shows the average values of contact angles measured, figure 3.7 shows representative pictures from analysis.

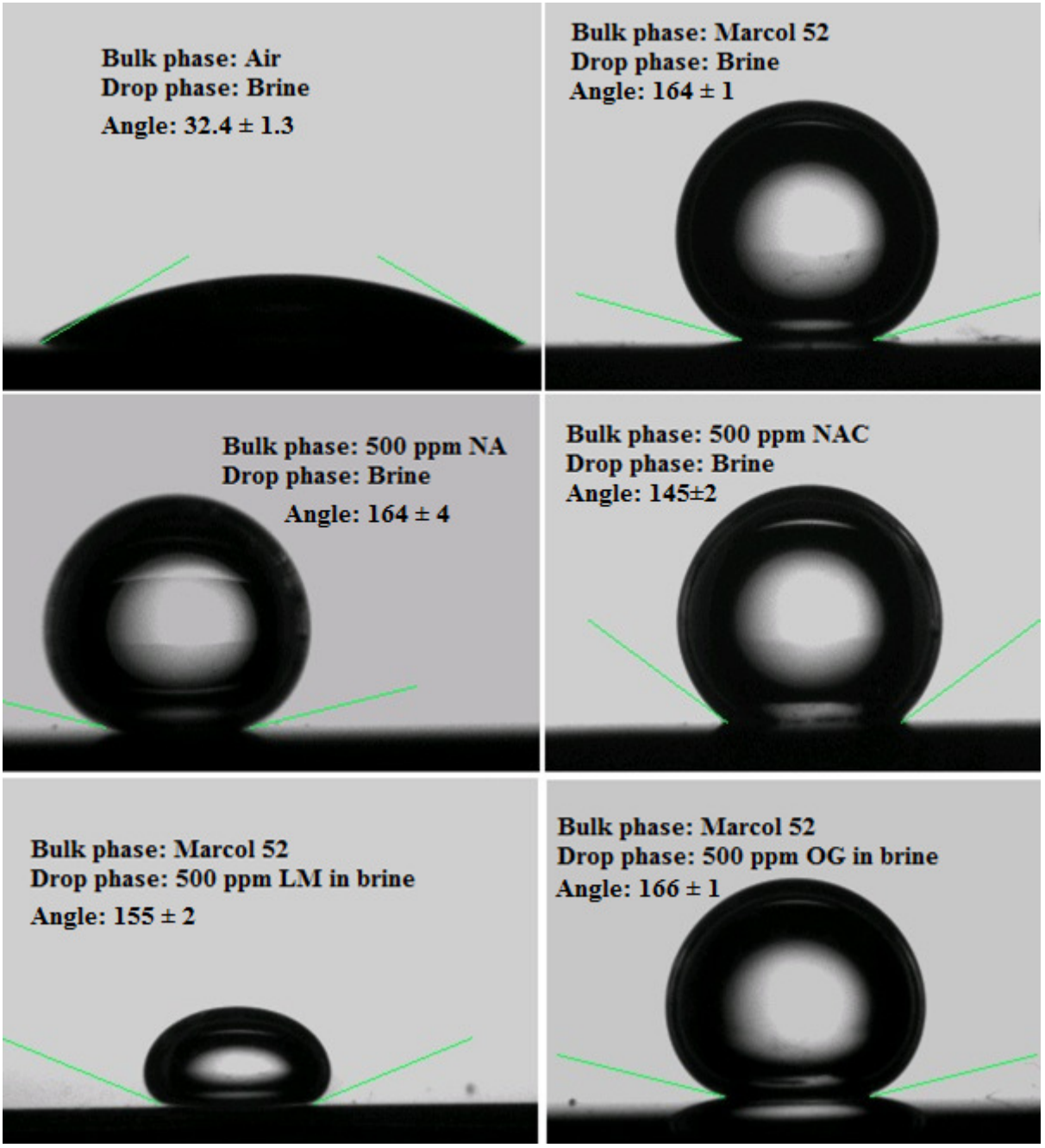

FIGURE 3.7: Example pictures of drops taken during contact angle measurements. All measured on stainless steel.

3.3 Microbial degradation

Results from the growth of the different systems are initially presented. Results from physical tests of the two systems of the microbial degradation are presented separately.

3.3.1 Bacterial growth

The first 5 months, the samples were monitored for sulphide content using Clines method (section 2.4.2). Sulphide content can be correlated with growth as a by-product from consumption. Figure 3.8 clearly displays the difference in growth rate between the oil degradation and toluene degradation. After 150 days, it was decided to air the sulphide due to possible toxic effect towards the bacteria. Samples of the medium were fixated at different dates between 5-10 months, in order to keep track of the growth.

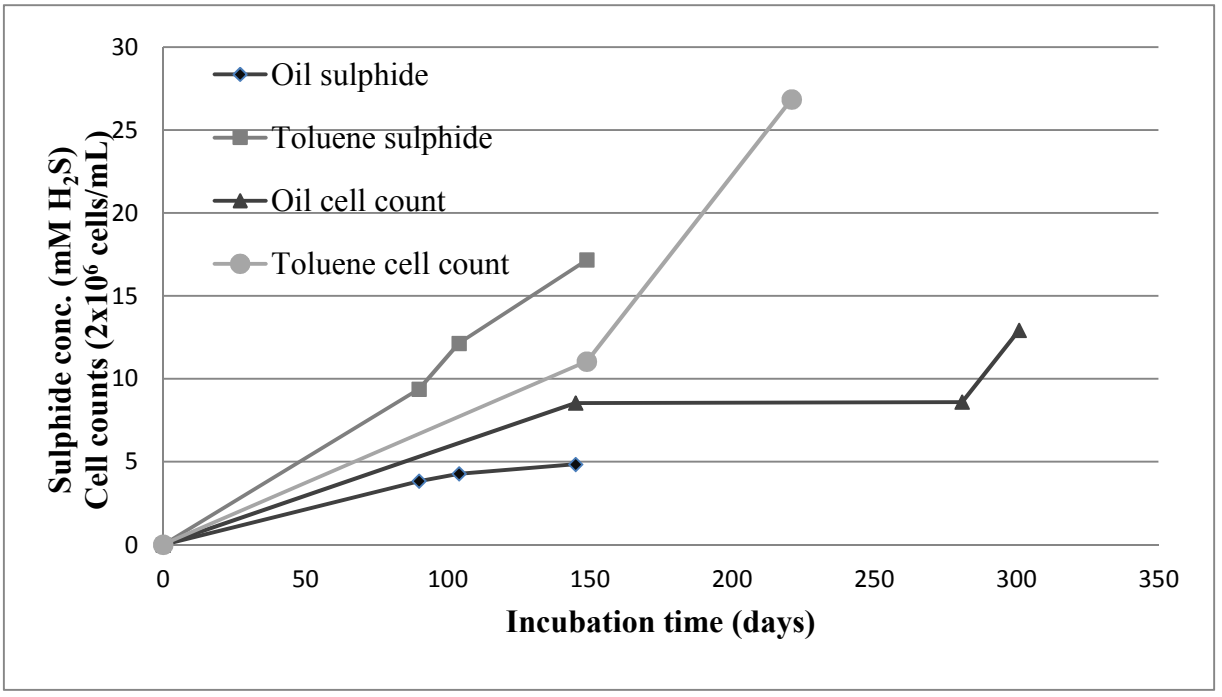

FIGURE 3.8: Growth of *Desulfotignum toluenicum*: Sulfide content measured by Cline's method and cell count for the two substrates.

When counting the cells (section 2.4.3), two observations were noted. One was that the residue of a thin, polymeric material that could be associated with biofilm formation[55, 56] was observed in the samples. Generally, it was difficult to uniformly suspend the bacterial cells on a filter for counting, as the cells seemed to grow in layers and stick together as blots on the filter paper. Figure 3.9 shows an example of the slides that were prepared for counting.

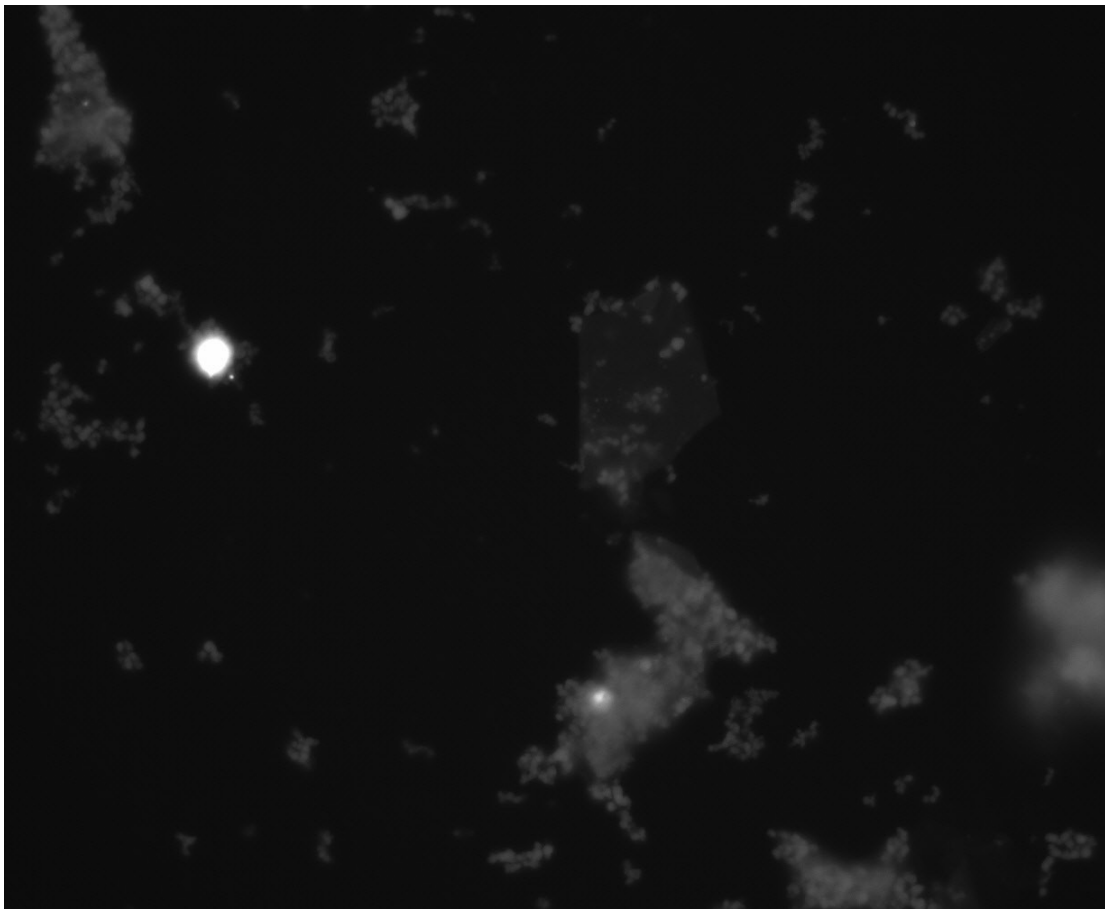

FIGURE 3.9: Picture of bacteria from collected from medium cultivated on oil for 281 days. The pictures shows that the bacteria are stuck together in layers, making the bacterial count difficult and leading to a probable underestimation of the number of cells.. A residue of a film is present in the middle of the pictures.

Another observation was that most of the cells observed were dead when looking at the samples, only a small fraction of the samples had their DNA intact when analyzing in the microscope. Table 3.5 shows the cell numbers observed when counting, and the corresponding fraction of DNA-containing cells.

TABLE 3.5: The number of cells counted in media, and the observed fraction of DNA-containing cells.

Cell count	**(crude oil**	**substrate)**			
Incubation time (days)	**No. cells / mL**		**Active cells**		**Fraction active cells (%)**
0	2.00E+04	±4.00E+03	2.00E+04	±2.00E+03	100 %
145	1.71E+07	±5.80E+05	2.34E+06	±2.15E+05	14 %
281	1.72E+07	±2.55E+06	2.25E+06	±3.30E+05	13 %
301	2.59E+07	±3.29E+06	1.80E+06	±4.52E+05	7 %
Cell count	**(toluene**	**substrate)**			
149	2.21E+07	±6.60E+05	5.43E+06	3.27E+05	25 %
221	5.37E+07	±4.60E+06	2.54E+06	±6.85E+05	5 %

3.3.2 Toluene biodegration system

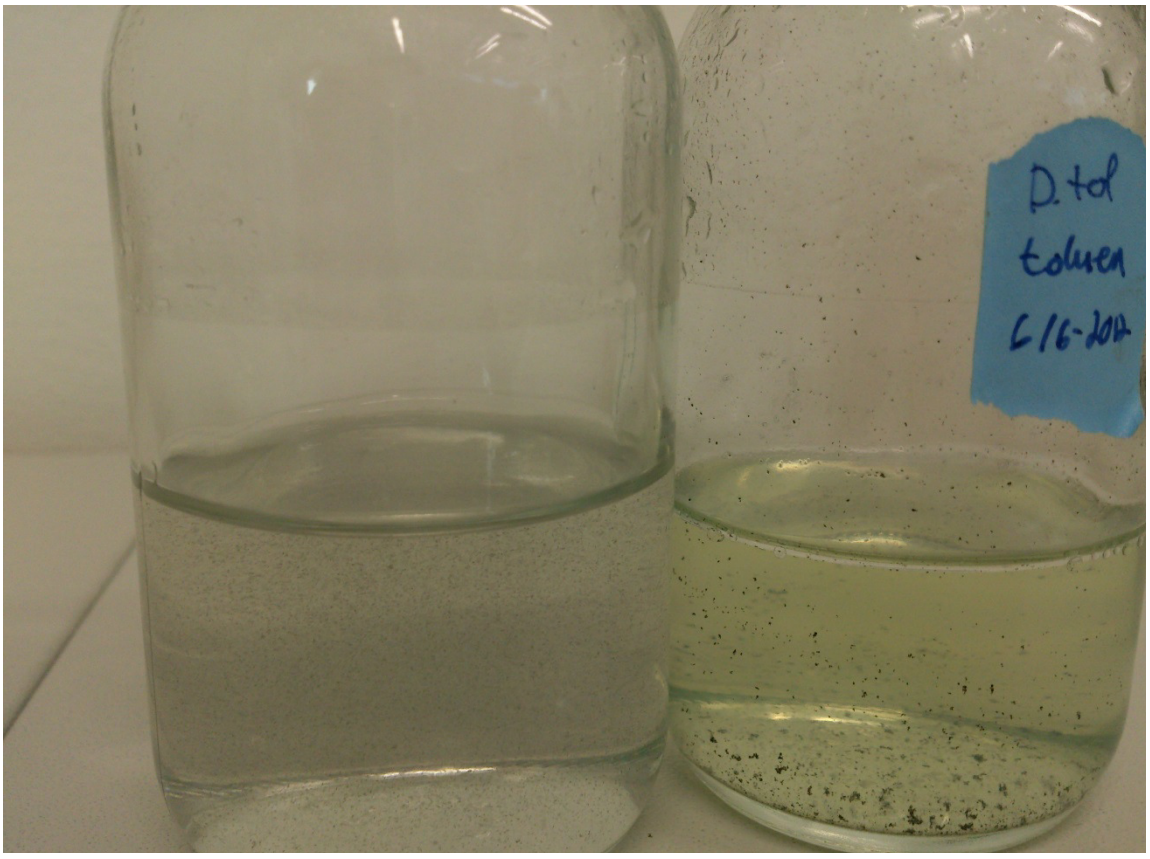

FIGURE 3.10: Pure medium (left) and medium containing *D. toluenicum* cultivated on toluene 7 for months (right.)

Figure 3.10 shows the difference of the medium before and after using toluene as a substrate for cultivation of *D. toluenicum* for 7 months. When visually comparing these, the medium after cultivation seemed to be more viscous and to contain more sulfide salts.

Wetting index of medium

The first toluene samples were collected after 3 months. Wetting index measurements of medium before and after filtration on 0.2 μm was performed, shown in figure 3.11.

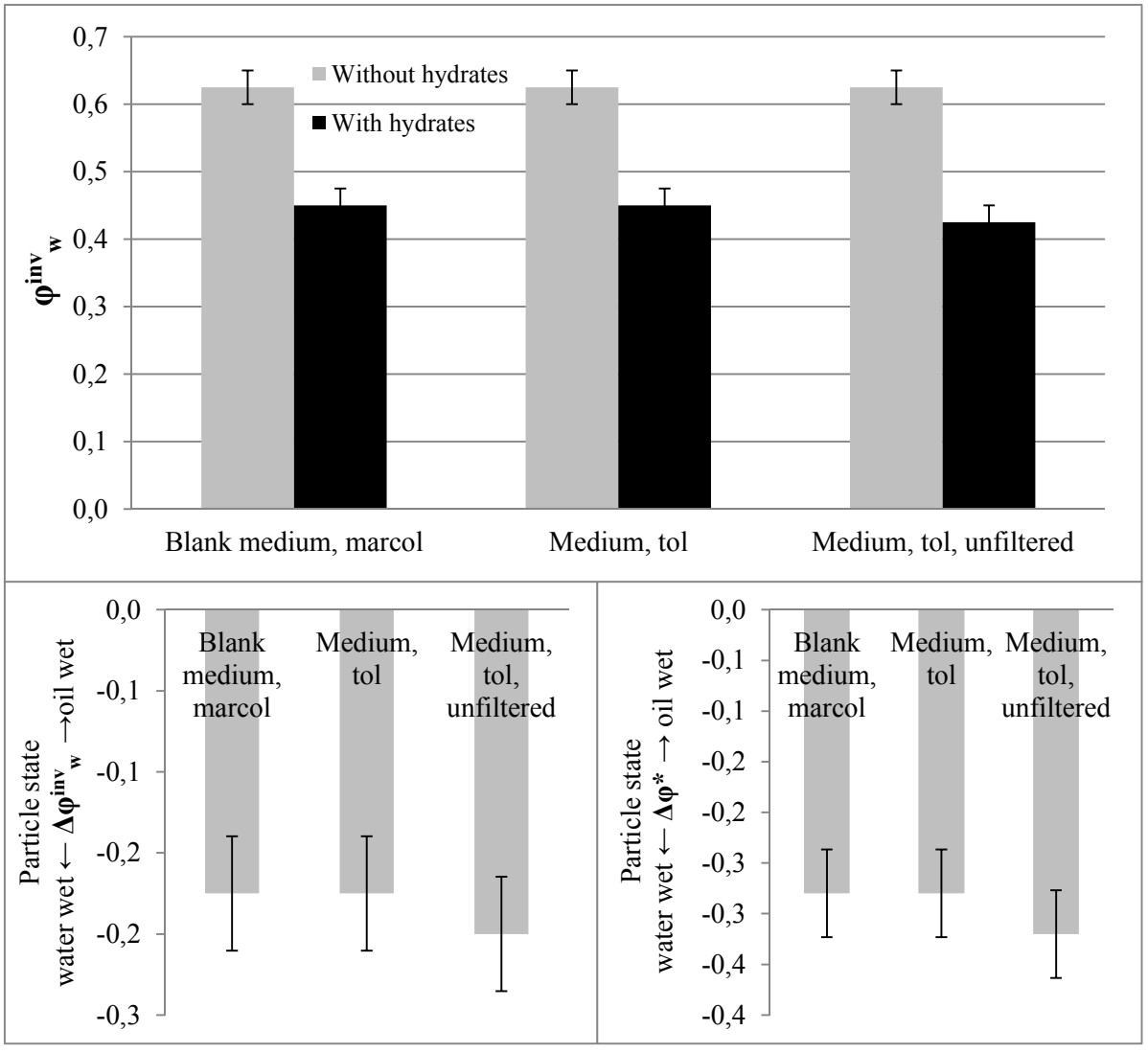

FIGURE 3.11: Upper: Points of phase inversions for bacterial media (3 months) in Marcol. Down left: difference in point of phase inversions, down right: wetting index, difference in points of phase inversion, standardized according to equation 1 (2.2).

Interfacial properties

Tables 3.6 and 3.7 lists average contact angles and interfacial tension for the blank medium and medium including bacteria cultivated on toluene. Densities are listed in Appendix D. Figure 3.12 shows example pictures of the different drops.

TABLE 3.6: Contact angles on stainless steel of blank medium and medium including bacteria cultivated with toluene as a substrate.

Drop / bulk phase	**Contact angle (°)**	**SD**	**%RSD**	**Number of parallells**
Blank medium / Marcol 52	129,7	±1,7	1,3	4
Bacterial medium cultivated on toluene / Marcol 52	145,6	±5,9	4,1	8

TABLE 3.7: Interfacial tension of blank medium and medium including bacteria cultivated with toluene as a substrate.

Interface	**Interfacial tension (mN/m)**	**SD**	**%RSD**	**Number of parallells**
Blank medium / Marcol 52	13,70	±0,23	1,6	5
Bacterial medium cultivated on toluene / Marcol 52	13,37	±0,44	3,3	3

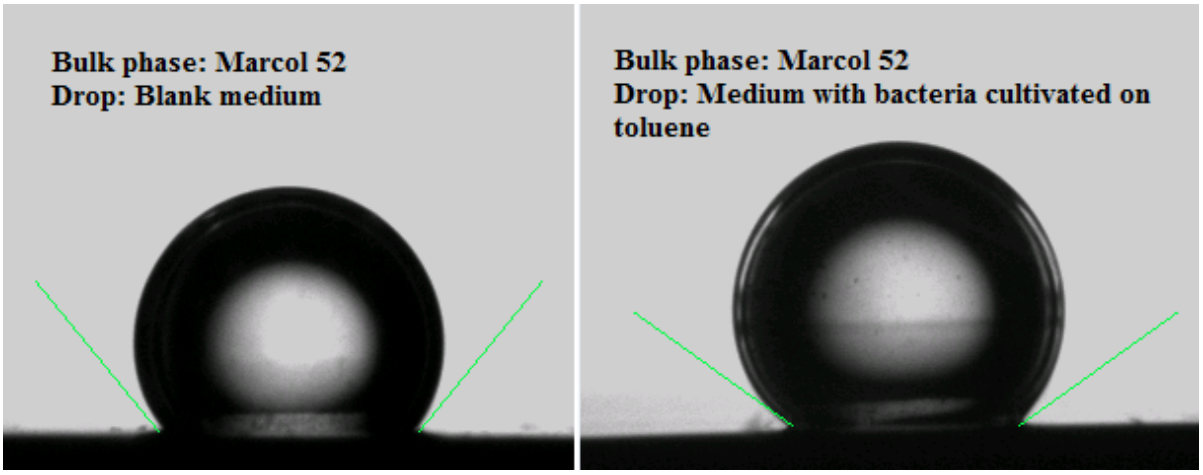

FIGURE 3.12: Representative pictures of contact angles on stainless steel for blank medium and medium including bacteria cultivated with toluene as a substrate.

Viscosity

The viscosity of the media were measured as a function of shear rate, shown in figure 3.13.

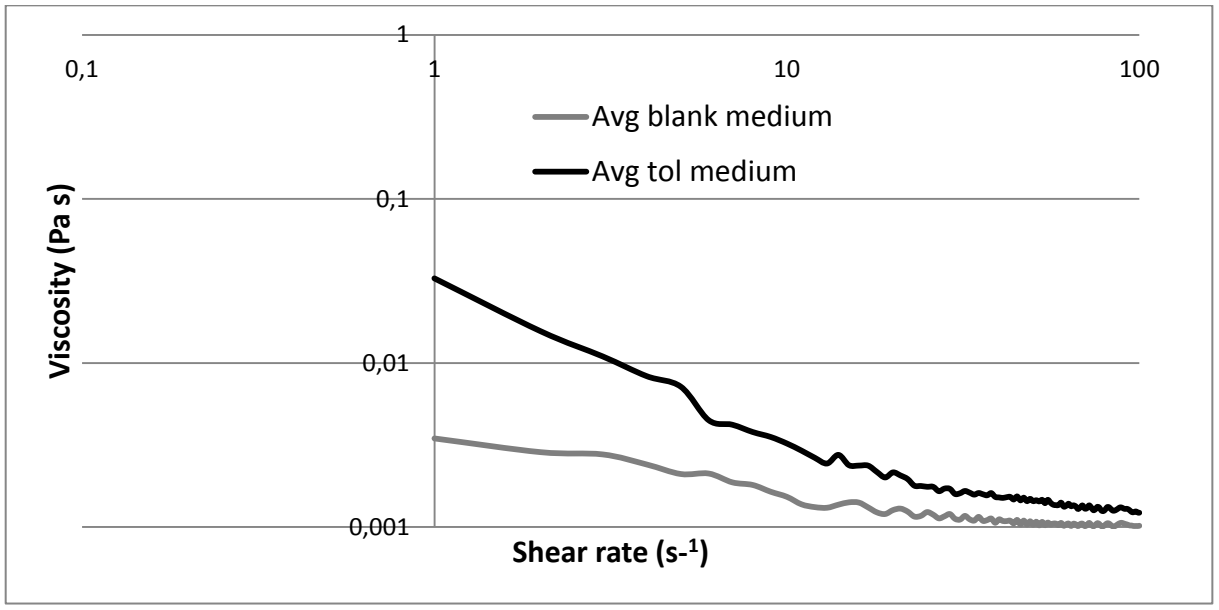

FIGURE 3.13: Average viscosity as a function of shear rate. The average of pure medium is based on 2 parallels, average of bacterial medium cultivated on toluene based on 4 parallels.

Biomass

After 7 months, the bacterial media cultivated on toluene were collected and extracted using methyl *tert*-butyl ether (MTBE), as explained in section 2.4.4, in order to establish the mass of MTBE-soluble components assumed to be possible biosurfactants. Table 3.8 lists the results. In order to separate possible water soluble biosurfactants from bacteria, filtration was performed on the media. Some bacterial mass was retained, and an FT-IR spectrum was obtained, appendix C, in order to confirm the presence of organic material.

TABLE 3.8: Results from extraction using MTBE of media from biodegradation of toluene. The obtained mass is calculated from gravimetric analysis, method described in methods section 2.4.4.

Sample	**Mass in 100 mL medium (mg)**	**Concentration of MTBE soluble compounds in medium (mg/mL)**
Unfiltered medium	19.439	0.19439
Acidified to pH 2, 0.7 μm filtered	2.5184	0.02518

An observation to note was that polycarbonate filters with uniform pore diameters were quickly clogged, giving flow rates of 0.6 mL/min when changing filters every 100 mL. When filtered using a Whatman high efficiency Grade GF/F glass microfiber filter, the flow rate was increased to 20 mL/min without having to change filters. However, using glass microfiber filters made it very difficult to remove and sample the bacterial mass from the filter.

3.3.3 Crude oil biodegradation system

FIGURE 3.14: Pure medium with non-degraded Statfjord A (left) and biodegraded Statfjord A and medium containing *D. toluenicum* cultivated on crude oil for 10 months (right.)

Figure 3.14 shows the biodegradation system before and after cultivation of *D. toluenicum* for 10 months.

3.3.3.1 Crude oil phase

The biodegraded crude oil phase was collected by separating out and adding all the crude oil phases from each of the flasks together. This was done due to the small amount of crude oil in each sample flask.

Table 3.9 lists the difference in some properties of the crude oil before and after biodegradation. No sterile control was done, so the effect of evaporation cannot be assessed.

TABLE 3.9: Density and composition of Statfjord A oil before and after biodegradation.

Statfjord A crude oil	**Non-biodegraded**		**Biodegraded 10 months**	
	Result	**SD**	**Result**	**SD**
Density (g/mL)	0.734	±0.013	0.855	±0.001
Saturates (mg/g oil)	557	±10.1	574	±3.7
Aromatics (mg/g oil)	36.5	±1.0	86.5	±0.53
Resins (mg/g oil)	28	±0.90	50.6	±1.6

Chromatographic profile

Appendix B shows the whole-oil chromatograms of the Statfjord A crude oil before and after biodegradation.

Figure 3.15 shows the separate peak areas normalized to pristane. Pristane is a branched, long-chained alkane that is generally assumed to be relatively inert towards biodegradation.[57]

Peaks in figure 3.15 are assigned based on comparison with NSO-1 from NIGOGA. [44] The lower mass peaks were difficult to identify due to the use of a shorter temperature program than the standard.

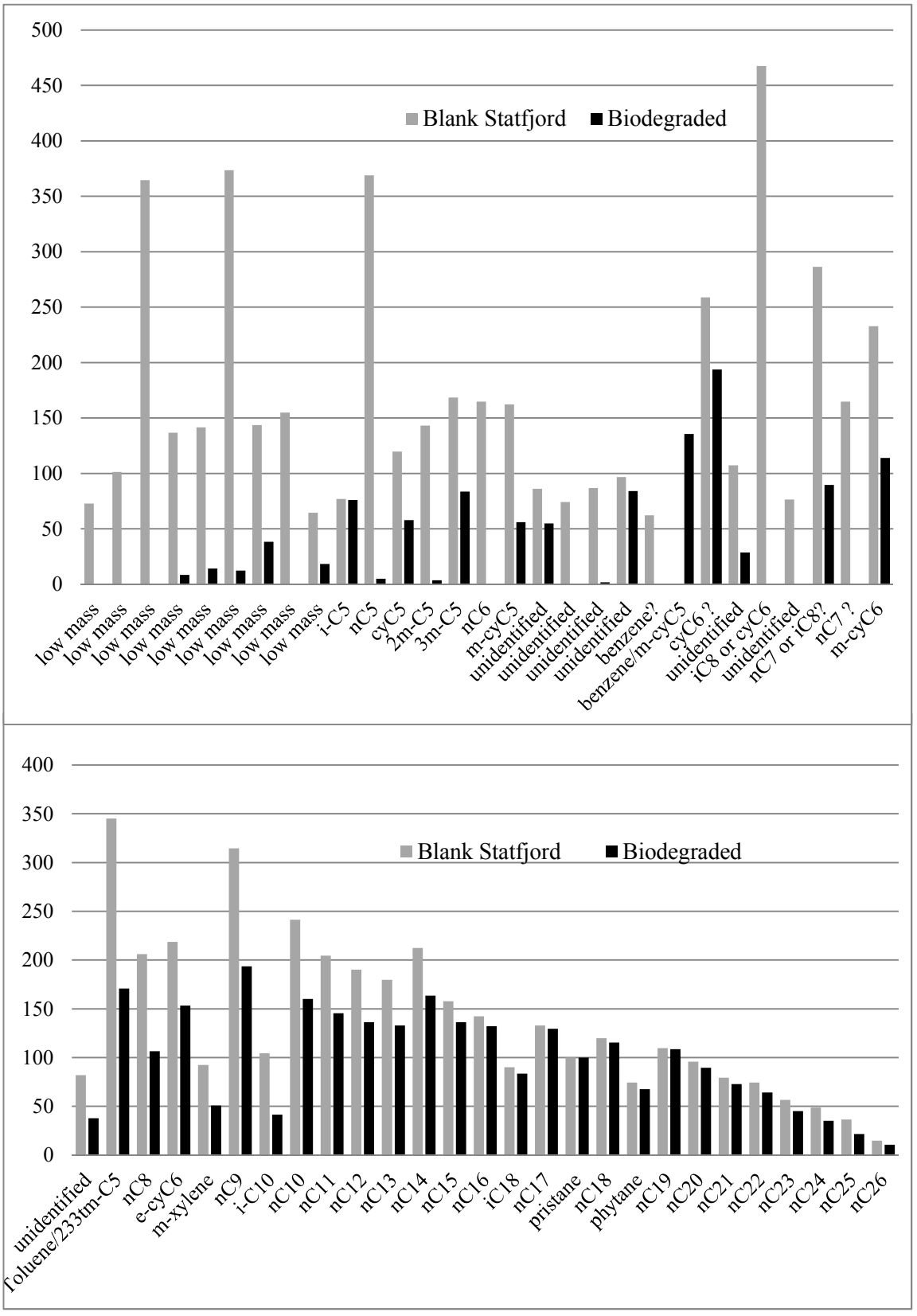

FIGURE 3.15: Comparison of the separate peak areas prior to and subsequent to biodegradation, normalized to pristane. Retention times from low to high. Peaks are assigned based on comparison with NSO-1 from NIGOGA. [44] Blank Statfjord is here the crude Statfjord A oil prior to biodegradation.

Fourier Transform Infra Red Spectroscopy

Figure 3.16 shows the FT-IR spectra of the crude oil before and after 10 months biodegradation using *Desulfotignum toluenicum*, with the main peaks listed in table 3.10.

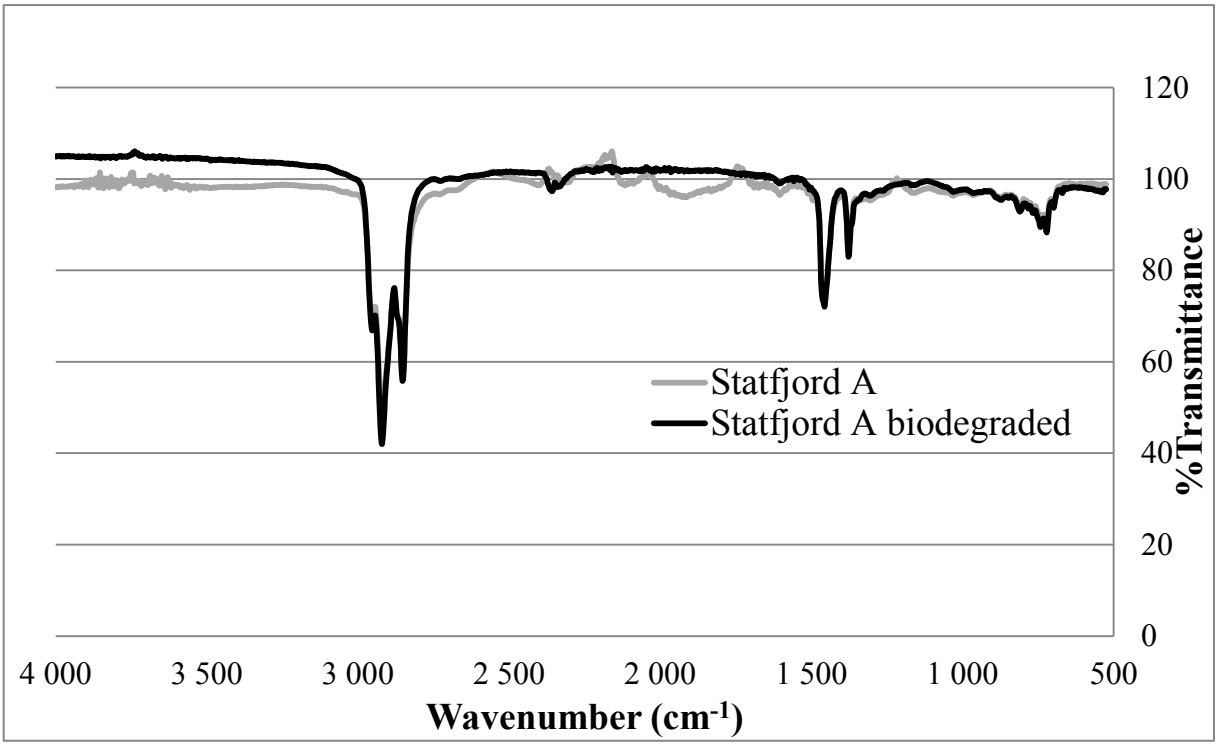

FIGURE 3.16: FT-IR spectra of crude oil prior and subsequent to 10 months biodegradation using *D. toluenicum*.

TABLE 3.10: Main peaks from FT-IR spectra of Statfjord A (figure 3.16.)

Possible source	**Main peaks (cm^{-1})**	**Intensity**
Aromatic C-H	722	88
C-H (methyl, rock)	1377	82
C-H (alkanes, scissoring)	1456	71
C-H (alkanes, stretch)	2852	56
C-H (alkanes, stretch)	2921	41
C-H (alkanes, stretch)	2953	66

Viscosity

Figure 3.17 shows viscosity as a function of shear rate, before and after 10 months biodegradation using *Desulfotignum toluenicum*.

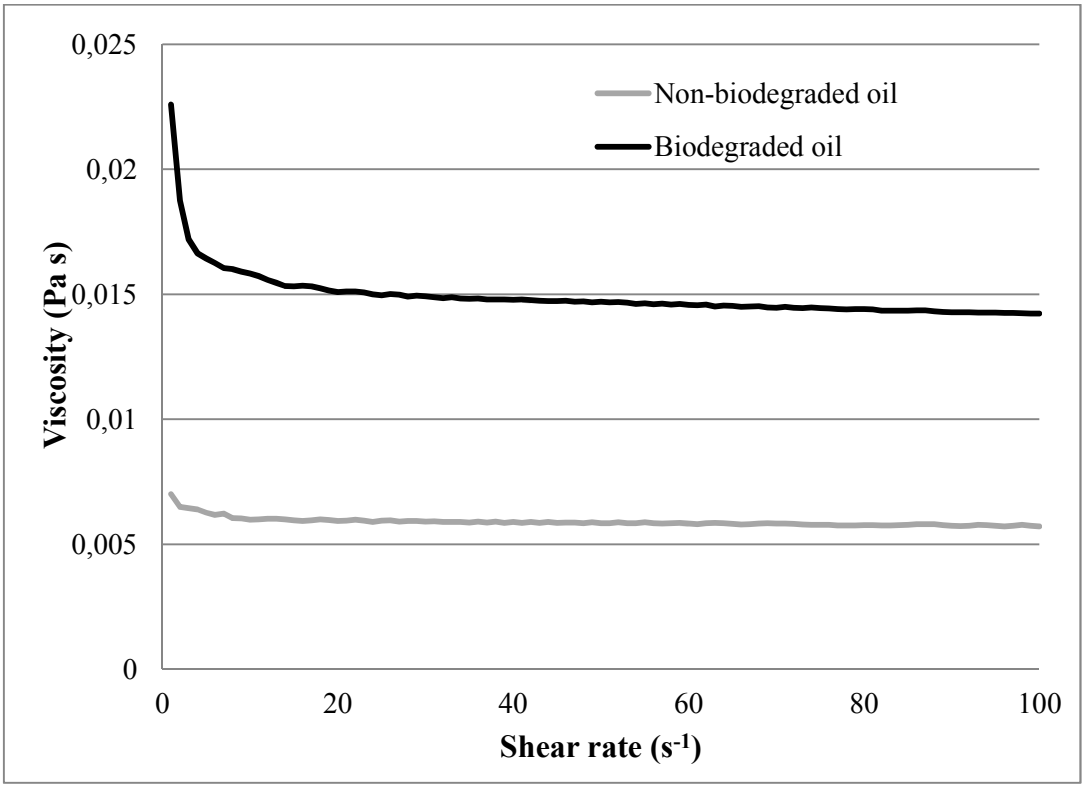

FIGURE 3.17: Viscosity as a function of shear rate of Statfjord A crude oil prior and subsequent to 10 months biodegradation using *D. toluenicum*.

TABLE 3.11: Average viscosity of Statfjord A crude oil prior and subsequent to 10 months biodegradation using *D. toluenicum*, shear rates 50-100 s^{-1}.

Non-biodegraded		**Biodegraded**	
Viscosity (Pa s)	**SD**	**Viscosity (Pa s)**	**SD**
0.0058	±0.0006	0.0144	±0.0005

Wetting index

After 3 months, one batch of biodegraded oil was collected and mixed with Marcol 52 into a 3 %wt crude oil in Marcol-mixture. The same was done after 10 months. A standard of 3 %wt non-biodegraded Statfjord A oil in Marcol 52 was made and tested for comparison. Figure 3.18 shows the result when measuring the wetting index of this versus the blank medium.

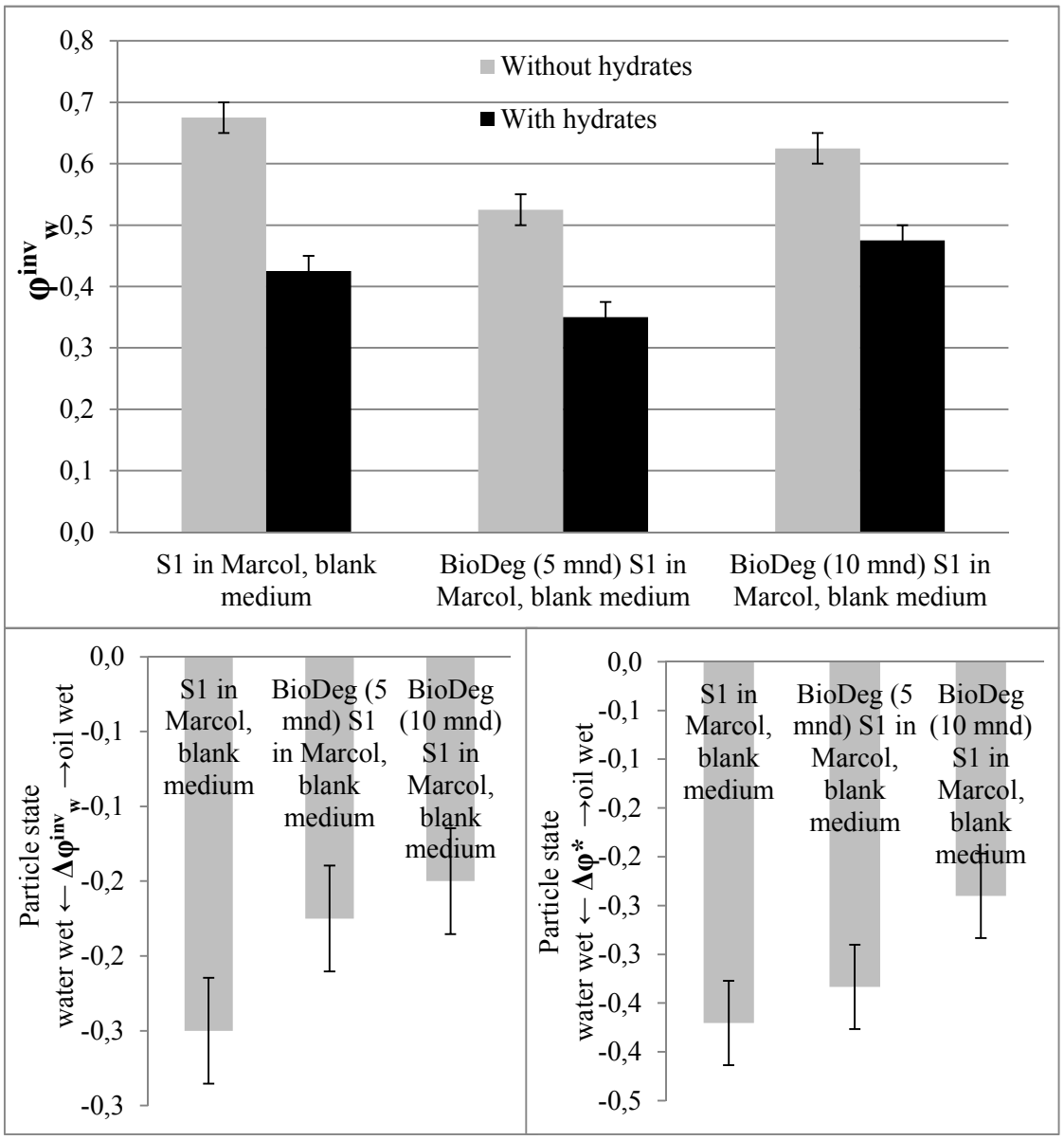

FIGURE 3.18: Wetting index of 3 %wt Statfjord A crude oil in Marcol 52, prior and subsequent to 3 months and 10 months biodegradation using *D. toluenicum*. Upper: Points of phase inversions. Down left: Difference in point of phase inversions, down right: wetting index, difference in points of phase inversion, standardized according to equation (2.2).

3.3.3.2 Aqueous phase

The medium from the crude oil biodegradation was collected and tested. This was not filtered or altered in any way prior to testing.

Wetting index

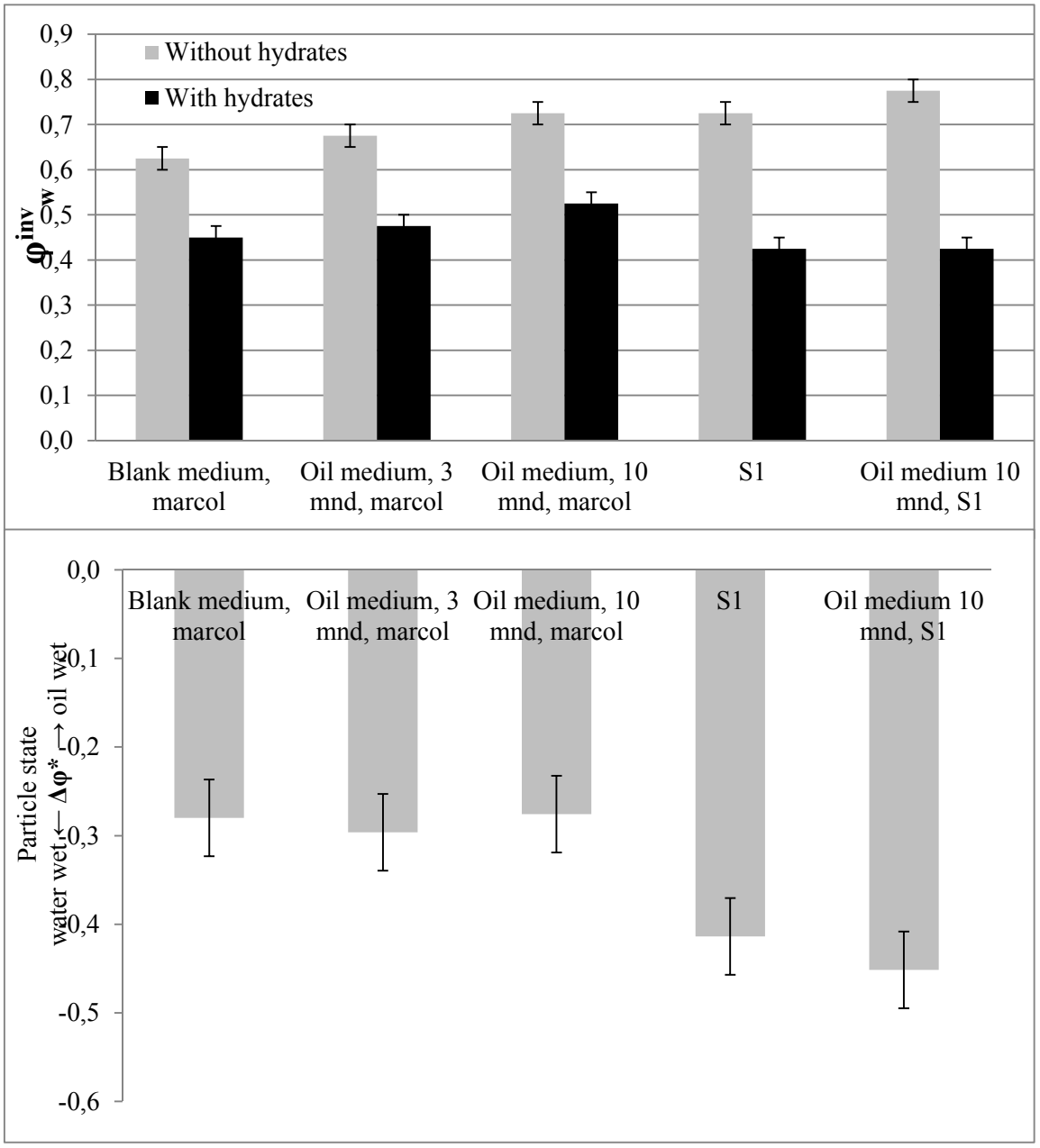

FIGURE 3.19: Wetting index medium from cultivation of *D. toluenicum* with crude oil as a substrate. Upper: Points of phase inversions. Lower: wetting index, difference in points of phase inversion, standardized according to equation 2.2.

The medium was tested against Marcol 52 in wetting index measurements after 3 months and 10 months. The medium was also tested against Statfjord A crude oil after 10 months. Figure 3.19 shows the results.

Interfacial properties

Tables 3.12 and 3.13 lists average contact angles and interfacial tension for the blank medium and medium including bacteria cultivated on crude oil as substrate. Densities are listed in Appendix D. Figure 3.20 shows representative example pictures of the different drops.

TABLE 3.12: Contact angles on stainless steel of blank medium and medium including bacteria cultivated with crude oil as a substrate.

Drop / bulk phase	**Contact angle (°)**	**SD**	**%RSD**	**Number of parallells**
Blank medium / Marcol 52	129,7	±1,7	1,3	4
Bacterial medium cultivated on crude oil/ Marcol 52	153.9	±2,0	1.3	5

TABLE 3.13: Interfacial tension of blank medium and medium including bacteria cultivated with crude oil as a substrate.

Interface	**Interfacial tension (mN/m)**	**SD**	**%RSD**	**Number of parallells**
Blank medium / Marcol 52	13.70	±0.23	1.6	5
Bacterial medium cultivated on toluene / Marcol 52	8.55	±0.53	2.5	6

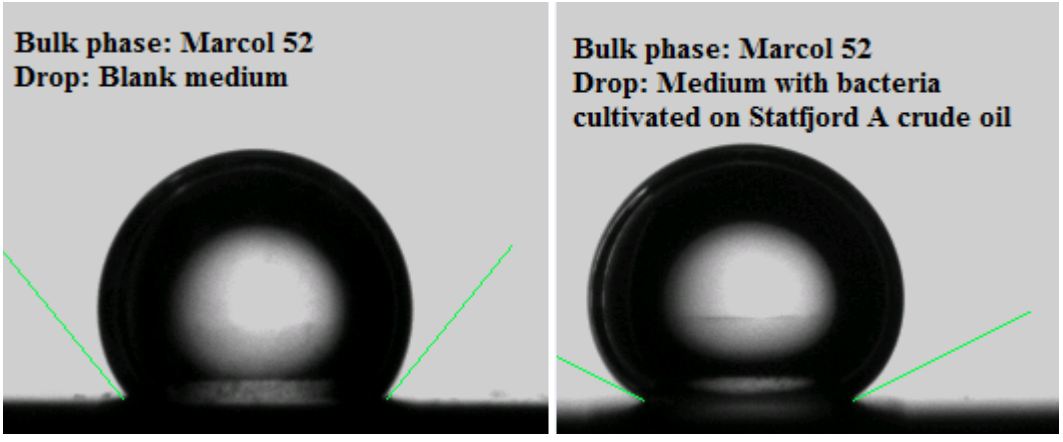

FIGURE 3.20: Representative pictures of contact angles on stainless steel for blank medium and medium including bacteria cultivated with crude oil as a substrate.

Viscosity

Figure 3.21 shows viscosity as a function of shear rate for blank medium and medium including *Desulfotignum toluenicum* cultivated on Statfjord A crude oil for 10 months.

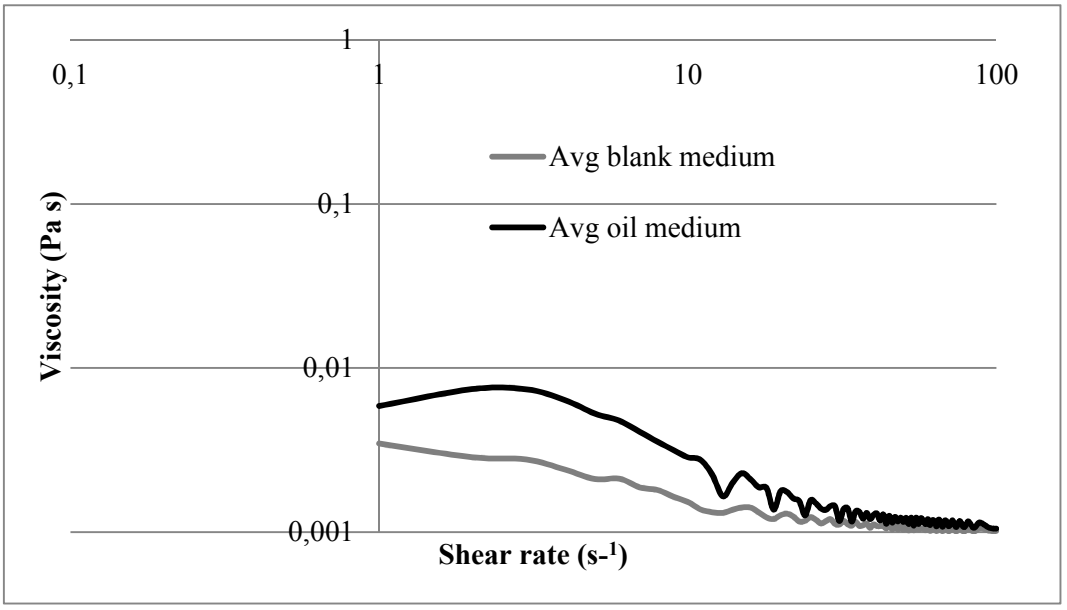

FIGURE 3.21: Viscosity as a function of shear rate for blank medium and medium including *Desulfotignum toluenicum* cultivated on Statfjord A crude oil.

Chapter 4

Discussion

4.1 Introduction

In the following chapter, results presented in chapter 3 are discussed. A discussion of separate results will be laid out in a similar format as in chapter 3, followed by a discussion of possible correlations, implications and applications.

In order to properly discuss the results from the wetting index method, an understanding of the underlying theory is essential.

The wetting index value is defined as the standardized difference in the points of phase inversion between a Freon hydrate-containing sample and blank sample, in accordance with equation 2.2.

The emulsion state of an oil/water mixture is dependent on the water cut, and the water cut (between 0.05-0.95) where the emulsion state changes from water-in-oil to oil-in-water, is considered the catastrophic point of phase inversion.[58]

As the wetting index is presented as a difference in this point of phase inversion, this means that the addition of Freon hydrates is expected to make a change in the emulsion state. According to previous research discussing emulsion behaviour of crude oil/water-mixtures and the addition of hydrates, [16, 19, 48, 59] the difference in the point of phase inversion can be correlated to the tendency of forming an emulsion with finely dispersed hydrate particles, as opposed to the phases separating and the hydrate particles agglomerating.

The difference in point of phase inversion upon addition of Freon, is due to the effect hydrates have as particles in the emulsion. Particles may alter the emulsion state and thus the point of phase inversion. [30, 60, 61] Table 4.1 gives an overview of possible

wetting states of hydrate particles in different emulsion states, and the expected effects on further hydrate growth.

TABLE 4.1: An overview of different emulsion states with particles of different states, and its effect on hydrate growth. Adapted from Fotland and Askvik (2008). [59]

Initial state Emulsion	**Particle (hydrate)**	**Water wetted**	**Oil wetted**
Water-in-oil		Destabilizing, separation, inversion to oil-in-water. Inhibits hydrate growth before inversion. Aggregate formation likely	Stabilizing, break up of droplets and more interface generated. Hydrate growth is instantly promoted. Dispersion is probable.
Oil-in-water		Stabilizing and possible break up of droplets. New interface forms in water and hydrate growth will probably accelerate. Eventual aggregation is likely	Destabilizing, droplets will grow and oil separate from water. Eventually inversion may occur. Initially hydrate growth is inhibited due to decreasing interfacial area
Separated/stratified		Oil-in-water emulsion may form. Interfacial area increases thus hydrate growth is promoted. Aggregation is likely	Water-in-oil emulsions may be generated. Increasing interfacial area promotes hydrate growth. Dispersions due to oil wetting is likely.

When the addition of Freon hydrates to an oil/water mixture leads to a higher point of phase inversion than the blank, it indicates that the Freon hydrates become oil wetted, due to a net stabilization of the water-in-oil emulsion state.

In effect, this means that a positive wetting index indicates oil wetted hydrate particles and probable dispersion of hydrates rather than agglomeration. A negative wetting index, where the addition of Freon hydrates decreases the initial point of phase inversion, indicates a destabilization of the water-in-oil emulsion state and thus indicates water-wet hydrate particles that can serve as nucleation sites for further hydrate agglomeration.

4.2 Model system

From figure 3.1 it is shown that the wetting index of the model oil Marcol 52 is neutral to slightly positive. This means that Freon hydrates in this system can be assumed as intermediate to oil-wet. The wetting index of the Statfjord A crude oil is negative, and indicates that added Freon hydrate particles will be water-wet and promote hydrate aggregate formation. The crude oil used in this work was selected due to the negative

wetting index value, so that the net effect of additives and biodegradation would be easily seen should they give more oil-wet hydrates.

Marcol 52 was mainly chosen due to its availability, non-reactivity and functionality in wettability studies additionally, additives to an initially neutral wetting index might give a clear net effect to the wetting index in both directions.

4.2.1 Additives

The chosen additives were based on the indication from previous works where petroleum acids and biosurfactants have been found to have an anti-agglomerating effect when added to or naturally present in crude oil [2, 3, 19, 48, 62] or model oils.[23, 51] Commercial napthenic acids and naphthenic acids extracted from different crude oils, have been previously tested at concentrations in the oil phase from 0.65-5 %wt using the wetting index method and a high pressure/low temperature sapphire cell.[19, 23]

4.2.2 Extraction of acids

Baugh og Mediaas et.al. [63] have discovered calcium naphthenate deposits to contain high molecular weight naphtenic acids, called *ARN* acids. *ARN* acids is a family of 4-protic carboxylic acids containing 4 - 8 unsaturated sites (rings) in the hydrocarbon skeleton, with molecular weights in the range of 1227 - 1235 g/mol. In this work, the goal was to test *ARN*-acids,[63] which were isolated from a toluene extract of a calcium naphthenate deposition. The acids were isolated using the Acid-IER method (section 2.3.5), the same procedure as applied in the original discovery of these acids.[63]

The IR spectra in figure 3.2, shows that the intensity of the carboxyl bond C=O at 1703 cm^{-1} is greatly increased, and the peaks identified as C-H stretch in the original toluene extract, have in the extracted acids been overlapped by the broad peak from the O-H bond ranging from 2400-3300 cm^{-1}, indicating a high concentration of carboxylic acids.[42] A similar FT-IR spectrum is found in published data, when applying the same extraction method for isolating *ARN*-acids.[64] Further analysis in order to ensure the identification of *ARN*-acids was deemed unnecessary.

The same acid extraction method has previously been applied by Erstad et.al. to extract acids from crude oils. The extracted acids were used to modify crude oils at different concentrations, and the tendencies to form gas hydrate plugs or dispersions were compared using the wetting index method[62] and a high pressure sapphire cell.[7]

This work indicated that there was a clear difference in the efficiency of the extracted acids for the application of creating hydrate dispersions, naming the source of the acids as a more important factor for efficiency than the concentration.

Although the acid-IER method has mainly been applied to extract ARN-acids,[64–68] the composition of the acid extract is very dependent on the source oil.[62, 69–71]

The IR spectra seen in figure 3.3 show the same major peaks of the extracted *ARN*-acids and the commercial naphthenic acids, which probably indicates that both samples have a high concentration of saturated carboxylic acids.[42] Since an IR spectrum reveals the main functional groups, and both of the samples have a high concentration of the same functional group, similar spectra can be expected. From the fingerprint region, slight differences can be seen, giving a clue that there are some compositional differences between the samples.

The commercial naphthenic acid obtained from Sigma-Aldrich is listed as a technical mixture of alkylated cyclopentane carboxic acids,[72] extracted from several crude oils. More information on naphthenic acids can be found in a review article by Clemente and Fedorak.[73] This commercial mixture of naphthenic acids has previously been used by Aspenes et.al.,[4, 74] to assess the effect on the wetting properties of different pipeline materials using petroleum ether as a model oil.

4.2.3 Wetting index

Limitations

Prior to a discussion of the results from the wetting index measurements laid out in this thesis, some limitations based on results from previous work must be assessed:

1. All previously published wetting index measurements are based on crude oils.[16, 19, 48, 62, 75, 76]
2. A previous study on model additives,[19] showed that the same additive could change the wetting index value of crude oils with similar properties in completely different directions, making the results of the wetting index measurement system dependent.
3. The same study showed that the wetting index was not in all cases directly correlated to the effects at realistic conditions.
    (a) In this study, it was hypothesized that in cases with low interfacial tension between the oil and aqueous phase, the effect on the IFT from the hydrate

former (Freon R11) itself might give less comparable results to natural gas as a hydrate former in realistic conditions.

(b) A study using different approaches to gain realistic laboratory conditions, such as high pressure sapphire cell, a Wheel shaped Flow Simulator and a high pressure flow loop,[18] indicated that the water cut influenced the hydrate dispersion ability, and that crude oils with wetting indexes around zero would start to form aggregates at lower water cuts than a crude oil with a higher wetting indexes.

Naphthenic acids

Looking at the wetting index results from the model system, some interesting comparisons can be made. Figure 3.4 show that the wetting index of the model oil, Marcol 52, is altered when different additives are used. Previous works[2, 3, 19, 48, 62] have correlated the differences in gas hydrate plugging tendency of crude oils with their acid content and degree of biodegradation.

The acids used in this research are extracted ARN-acids and commercial naphthenic acids from Sigma-Aldrich. From figure 3.4, the two samples are found to change the wetting index value of pure Marcol 52 from slightly positive into negative, indicating water wet hydrate particles and a tendency to create hydrate plugs. This is contradictory to previous research on the plugging tendency when adding naphthenic acids,[7, 19, 23, 48, 62, 77]

On the other hand, published results cannot be directly compared to these results, mainly due to the fact that the concentration used in this work is 0.05 %. In published results adding naphthenic acids to a model oil to test some hydrate agglomeration-related property, around 0.6-5 %wt have been added.[23, 77]

Several of the studies have also applied crude oil rather than a model oil [7, 19, 48, 62] a crude oil is a much more complicated matrix and might contain compounds that co-influences the effect of added acids.

In the work done by Høiland et.al.,[19] the effects of naphthenic acids were not consistent. The same acids were added to two similar crude oils 0.65 %wt, and one of the crude oils ended up with a negative PI value, while the other increased to a positive PI value. The efficiency was also increased with a doubled concentration of the added acids.

As this thesis mainly aimed to evaluate efficiency at low concentration, with a focus on biosurfactants which have been found efficient at concentrations lower than 0.05 %wt,[19, 51], a further evaluation of the naphthenic acids at higher concentrations was

not prioritized. Several studies have related the acidic content of different crudes to their plugging tendency,[4, 18] but the downside of having naphthenic acids as natural inhibiting compounds is the corrosiveness of an acidic oil.[78] The anti-agglomerating effects of naphthenic acids have also been found to be reduced with increased salt content and removed by high pH.[79] The *ARN*-acid family are also the ones that are linked to calcium naphthenate deposition, so even if these acids were efficient anti-agglomerants at a higher concentration, they are not a desirable component of crude oil.[63, 65, 66, 68]

Glycosides

Figure 3.4 shows the wetting index of Marcol 52 added 0.05 %wt lauryl maltoside and octyl glucoside. As the two compounds created a dispersion in marcol 52, it made more sense to dissolve the compounds in the aqueous phase. Figure 4.1 shows a comparison of the points of phase inversion, difference in points of phase inversion and normalised difference in point of phase inversion (wetting index).

Looking at the wetting index values compared in figure 4.1, the wetting index of especially octyl glucoside, is different when added to the different phases. When looking at the points of phase inversion, it can be seen that the point of phase inversion increases from a water cut of 0.575 to a water cut of 0.675. This could be due to the compound being more available to the oil/water interface when dissolved in the aqueous phase. A higher point of phase inversion means that the water-in-oil emulsion is stable at higher water contents, where drops of water are dispersed in the oil continuous phase. When the surfactant is dissolved in the aqueous phase, it can be assumed that when agitation is kept constant, more interfacial area will be available than if the compound is added to the continuous phase.

In addition, there is also a difference in the effective concentration. Since brine has a higher density than Marcol 52, when the compounds are added to the different phases in wt%, and the wetting index measurement adds the different phases according to volume, this means that when the compound is added to brine, more of the compound is in the total emulsion. For a 50/50 marcol/brine emulsion, the difference will be 48 mg. Since the water cut in this case is even higher than 50 %, the difference will even larger. This indicates that OG could be more dependent on concentration. For the case of LM, the only difference when added to the separate phases is in the point of phase inversion for the non-hydrate containing emulsion, and is within the standard error.

In order to further test these biosurfactants as possible anti-agglomerants, the Statfjord A oil was investigated. Previous studies have shown that when using a model oil poor

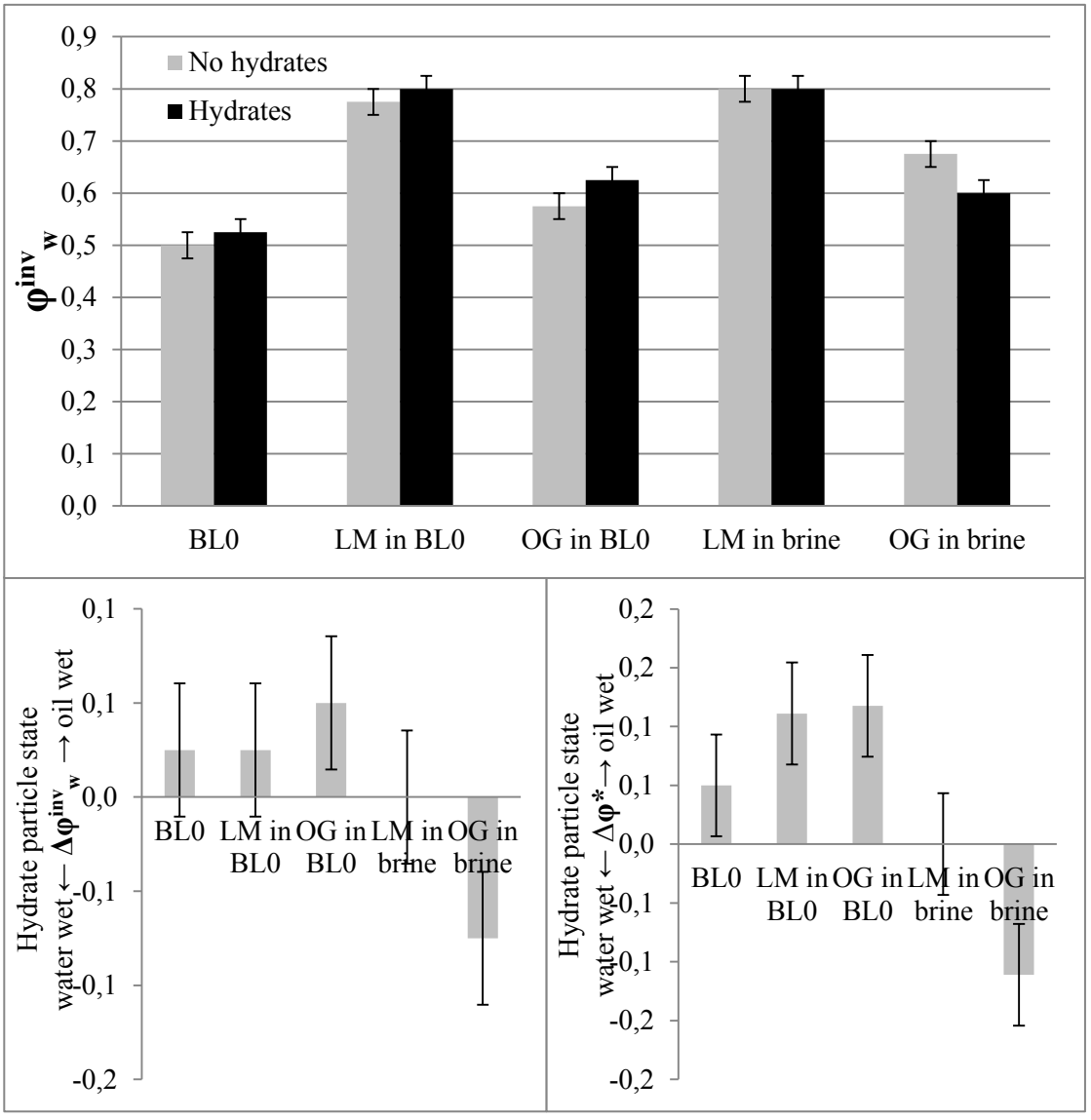

FIGURE 4.1: Upper: Points of phase inversion of blank Marcol 52 and LM and OG dispersed/dissolved in the difference phases. Lower left: Difference in point of phase inversion. Lower right: Normalised difference in point of phase inversion (wetting index). See Table 2.1 for explanations of labels.

in natural surfactants, like Marcol 52, the concentration of applied anti-agglomerants necessary for efficiency will decrease when mixing with a crude oil.[80]

This indicates that the application of anti-agglomerants to a crude oil system will be more efficient than when applied to a model oil system. Looking at figure 3.6, the wetting index of the Statfjord A oil increases from negative to positive when lauryl maltoside is applied. When octyl glucoside is applied, the PI value also increases, but not as dramatically.

The reason behind this increase in wetting index value can be seen from the shift in point of phase inversion. Lauryl maltoside added to the brine increases the point of phase inversion when Freon hydrates are added, from a water cut of 0.425 v/v to a water cut of 0.7 v/v, which is higher than the point of phase inversion for the emulsion without hydrates. This indicates that the wetting of the Freon hydrates have changed from water-wet to oil-wet in this emulsion.

For the system of Statfjord A and brine with added octyl glucoside, the point of phase inversion increased both with and without Freon hydrates. The difference in points of phase inversion increased somewhat from the blank Statfjord A/brine system, but a negative wetting index still indicates water wet Freon hydrates. As discussed previously in this section, octyl glucoside might be more efficient at higher concentrations.

4.2.4 Interfacial properties

From table 3.3, the interfacial tension between the blank marcol/brine system and the systems with additives can be compared. The systems with added biosurfactants clearly stand out with much lower interfacial tensions than the systems with added acids. Marcol 52 with added *ARN*-acids (NA) had a somewhat lower interfacial tension with brine, than blank Marcol 52 and Marcol 52 with commercial naphthenic acids (NAC). The addition of 500 ppm commercial naphthenic acids to Marcol 52, did not seem to have much effect on the interfacial tension.

Table 3.4 lists the observed contact angles from the model systems. In air, it can be observed that stainless steel is wetted by brine, through a contact angle $< 90°$. In the work of Aspenes et. al.,[40] naphthenic acids added to petroleum ether was found to increase the contact angle between a buffer solution and stainless steel by increasing concentration. The smallest concentration tested was 700 ppm, which gave an increase of 4°, but within the standard error. The largest increase in contact angle was found in the concentration range 1000-1500 ppm.

In this work, the contact angle of brine on the same steel plate in presence of Marcol 52 decreased from 164° to 145° when adding 500 ppm of the same commercial naphthenic acids. The system tested by Aspenes et.al.[40] used a similar light phase to Marcol 52, petroleum ether, and the same steel plates, but a buffer solution was used as the heavy phase in order to control the pH. The contact angle is highly dependent on pH value,[81] and in order to get similar systems as tested in the wetting index-method, the pH was not controlled in this work. This means that the results are not directly comparable.

The two biosurfactant systems tested, show a great decrease in interfacial tension. There is not much difference in the contact angle, except for lauryl maltoside. For lauryl maltoside in brine, the contact angle on stainless steel in Marcol 52 was decreased with about 10°, indicating a more water wet surface.

When both interfacial tension between the two liquids and the contact angle is known, this can be used to calculate the adhesion energy. The work of adhesion is calculated from the Young-Dupré equation[82] (equation 4.1), a rewriting of Young's equation (equation 1.1).

$$W_{swo} = \sigma_{wo}(1 + cos\theta) \tag{4.1}$$

The adhesion energy W_{swo} is given as energy per unit area of a solid surface (s) and water (w) adhering in oil. It gives a relationship between the interfacial tension and contact angle. Table 4.2 lists the calculated adhesion energies for the systems tested.

TABLE 4.2: Adhesion energies on stainless steel, calculated for model systems using Young-Dupré equation (equation 4.1).

System	**Adhesion energy (mJ/m^2)**
Marcol 52, brine	0.510 ±0.527
NA-Marcol 52, brine	0.392 ±0.721
NAC-Marcol 52, brine	2.743 ±0.872
Marcol 52, LM-Brine	0.039 ±0.134
Marcol 52, OG-Brine	0.261 ±0.598

The calculated adhesion energies of the systems tested are listed in table 4.2. The LM-added system observed a decrease in contact angle, but attained the lowest adhesion energy.

When applied to crude oil systems, Aspenes et.al found a slight correlation between a high contact angle and a positive wetting index of systems tested.[83] An even better correlation was obtained when relating the adhesion energy to the wetting index. Figure

4.2 illustrates the adhesion energy of the different systems tested in this work, as a function of the obtained wetting index.

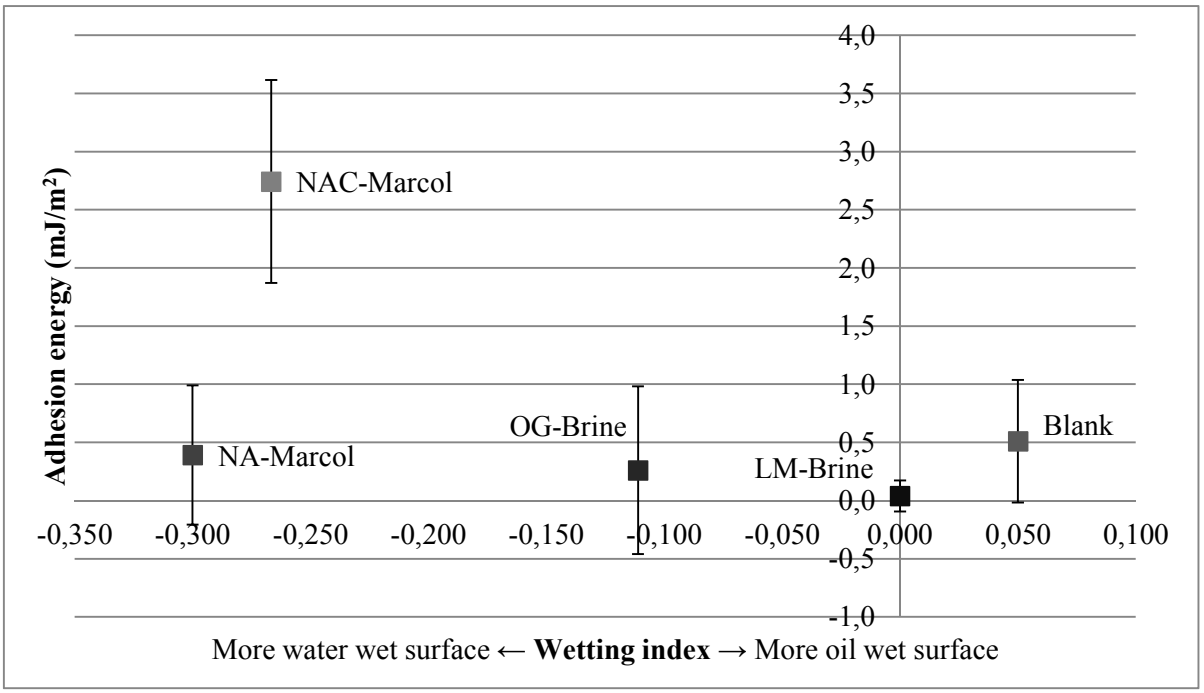

FIGURE 4.2: The adhesion energy of tested model systems as a function of wetting index. All tests are done with drops of aqueous phase on a pre-aged stainless steel-plate in the presence of the light hydrocarbon phase. A high wetting index indicates a more oil wet surface of Freon hydrates, low adhesion energy indicates a more oil wet steel surface.

The results from the wetting index are previously discussed, and a probable reason for the lack of increase in this value is the low concentration of additives. The contact angle and interfacial tension measurements might be more sensitive to additives than the wetting index measurement. When tested against a crude oil, the wetting index increased for the biosurfactant systems (see figure 3.6). When assuming that the adhesion energy on steel in crude oil is similar to the model system, the low adhesion energies obtained for the biosurfactant systems indicates a more oil wet behaviour of the steel surface, making gas hydrates less likely to adhere to the surface and agglomerate.

4.3 Microbial degradation

4.3.1 Bacterial growth

The sulphide content of the bacterial medium at different time intervals can be used as an indirect measure of bacterial growth. Optimum growth will occur when optimum conditions are kept. The purpose of this cultivation was not to promote optimum growth,

but to see what effect the bacteria have on the aqueous media when subjected to the different substrates toluene and crude oil. All other optimum conditions were kept in order to promote growth using these substrates, as described in the methods section 2.4.1.

From figure 3.8, it is clear that using toluene as a substrate, promotes more growth than using crude oil. The sulphide concentrations show similar growth rates as found by Ommedal et al.[5] This might be due to toluene being somewhat soluble in water (515 mg/L, at 1 atm and room temperature[84]) and more available than less soluble compounds in the crude oil.

From the amount of toluene added, an approximation of maximum attainable concentration of biomass can be done based on the amount of available carbon. Most of the toluene substrate is used as energy and broken down to CO_2.[35] Rabus et al. reported that the dry mass per mol toluene dissimilated by the sulfate reducing bacteria *Desulfobacula toluolica* yielded 29 g,[85] and assuming a general formula for biomass as CH_2O, this gives a yield of 14 %wt conversion of the carbon in toluene into biomass. Using this number as a maximal yield for biomass conversion, table 4.3 lists the theoretical concentration attainable.

TABLE 4.3: Theoretical calculation of maximum concentration of biomass based on the amount of toluene substrate added. Density of aqueous medium is assumed to be 1 g/mL for simplification.

Maximum theoretically attainable concentration of biomass	
Mass of added toluene in 100 mL aqueous medium (g)	0.0347
Mass of carbon from added toluene (g)	0.0316
%Yield of carbon converted to biomass from anaerobic degradation of toluene [86]	13.8 %
Mass of carbon available for biomass (g)	0.00436
Mass of maximum possible biomass with general formula CH_2O (g)	0.0113
Maximum concentration of biomass in aqueous medium (ppm)	113

Taking into consideration the maximum cells counted (figure 3.8), and assuming the dry mass of one cell to be 10^{-13} g, an approximation of the obtained biomass concentration is calculated in table 4.4.

TABLE 4.4: Theoretical calculation of concentration of biomass in the media based on the amount of cells counted.

Maximum attained concentration of biomass	**Toluene substrate**	**Crude oil substrate**
Dry mass of cell (g)	1.0E-13	1.0E-13
Maximum cells counted (mL^{-1})	5.4E+07	2.6E+07
Total mass in 100 mL (g)	5.4E-04	2.6E-04
Attained concentration (ppm)	5.4	2.6

Table 4.4 does not take into consideration other byproducts and types of biomass other than cells. When extracting the media with MTBE, it was found to contain 194 ppm organic mass (table 3.8). This could indicate that a lot of organic material besides the microbial cells is produced in the media.

An observation mentioned in results section 3.3 when analyzing the bacterial suspension using a microscope (see methods section 2.4.3), was the occurrence of a polymeric material indicating biofilm formation, see picture 3.9. Biofilms are microbial communities adhering to an interface, generally solid-water, usually encased in hydrated extracellular polymeric substances (EPS): polysaccharides, proteins, nucleic acids and lipids.[56, 87] Biofilm formation is often associated with infectious diseases caused by pathogenic bacteria,[88–90] but has been found to occur with many different bacterial strains when specific conditions are met, including sulfate reducing bacteria.[55, 91, 92]

In the petroleum industry, biofilm formation has been applied to microbial enhanced oil recovery (MEOR) in order to form polysaccharide plugs of zones with less oil, and to alter wettability of surfaces.[93] Biofilm formation on metal surfaces has also been studied with respect to corrosion inhibition.[91, 92, 94]

The EPS from a biofilm are indicated as being hydrogels, polymers that can take up and trap water many times their mass within their matrix.[56] If these substances are extracted with the MTBE, water pollution could increase the obtained weight of organic material when gravimetrically determining the concentration using microweight (methods section 2.4.4). This could explain the obtained concentration of 194 ppm organic material in the toluene degradation system, when expected maximum concentration based on added substrate was 113 ppm. Another explanation could be that the extracted organic mass includes more oxygen or nitrogen than the general formula CH_2O predicts.

TABLE 4.5: Calculation of how much toluene is oxidized in order to create the measured amount of H_2S.

Inoculation time (days)	**Sulphide content (mol/L medium)**	**Sulphide content in 100 mL medium (mol)**	**Toluene oxidized (mol)**	**%Reacted, of toluene added**
0	0	0	0	0 %
90	9.38E-03	9.38E-04	2.09E-04	55.4 %
104	1.21E-02	1.21E-03	2.70E-04	71.7 %
149	1.72E-02	1.72E-03	3.82E-04	101 %

Using the chemical reaction for sulfate reduction into H_2S with toluene as a substrate (equation 1.2), the H_2S measurements can give an indication of how much toluene has

been broken down to energy and CO_2. Table 4.5 gives an overview of the amount of toluene expected to have been oxidized for energy.

From table 4.5, the measured H_2S-levels indicate that all of the added toluene substrate was broken down after 5 month. When most of the toluene is used for creating energy rather than biomass, it can be expected to count a low number of cells. Table 4.6 lists the yielded biomass calculated from the cells counted at 5 months.

TABLE 4.6: The yield of biomass formed from added toluene substrate calculated from cell count at 5 months.

%Yield of biomass from added toluene substrate	
Dry mass of cell (g)	1.0E-13
Cells counted at 5 months (mL^{-1})	2.2E+07
Total mass in 100 mL (g)	2.2E-04
Amount biomass with general formula CH_2O (mol)	7.3E-06
Amount carbon (mol)	2.9E-06
%Yielded from added toluene	0.11 %

It was found from figure 3.8 that the number of cells counted increased after 5 months. This has probably to do with the sampling method. When medium was removed from the culture flasks, the flask was turned upside down and a sample was taken from the bulk, away from the interface. This means that the samples are representative for the bacterial concentration in the bulk aqueous phase. If the bacteria grow as a biofilm, this will be at the water/hydrocarbon interface, meaning that the concentration of bacteria in the bulk water phase is much lower than at the interface. When there is crowding and lack of substrate for the bacteria, many bacteria die and might be dispersed into the bulk aqueous phase from the biofilm. This could also explain the low and decreasing fraction of DNA-containing cells found in the bulk aqueous phase.

The amount of organic material extracted using MTBE (table 3.8) is difficult to explain when assuming that most of the substrate has been used for energy. MTBE is slightly soluble in water, so an extraction using this solvent, as described in section 2.4.4, gives some water in the organic phase. To cope with this, the organic phase was dried using N_2-gas prior to dissolution in Folchs solvent and gravimetric determination. If the extracted organic material has hydrogel properties and water trapped, N_2-gas might not be efficient enough to dry it completely. A viable explanation could be that the extracted organic material does contain some water that could influence the mass.

As mentioned in section 3.3.2, the medium with toluene as substrate was filtered prior to extraction with MTBE. The reasoning behind filtration was to separate possibly water soluble biosurfactants from the bacteria itself, so that chemical techniques could be applied to a cleaner sample. The size of *Desulfotignum toluenicum* is 0.6-1 μm in

diameter, 1.4-2.5 μm in length,[5] so all bacteria would be expected to be retained on a filter with a pore size smaller than 0.6 μm.

The experience was that polycarbonate filters were clogged within a few minutes, giving unexpectedly slow flow rates. The presence of EPS could explain this observation, polysaccharides would be too large to flow through small pores, and would clog them. Due to the irregular pore shapes and the thickness of glass microfiber filters, these are not as easily clogged by large molecules, especially when vacuum is applied, although the material left on the filter cannot be recovered as from polycarbonate filters.

4.3.2 Physical properties of media

Wetting index

Figure 3.11 and 3.19 shows that the wetting index did not change when bacteria was present in the medium. For the toluene degradation system, each culture was added the fixed amount of $3.8\text{x}10^{-4}$ mol toluene. Assuming all other essentials, like nutrients and sulphate, are available in excess, the amount of substrate will limit carbon and energy available for growth of bacteria and production of possible biosurfactants,[95] as table 4.3 lists.

Assuming that only a fraction of this biomass can exhibit surface active properties, and that surface active compounds would mainly be present in the interface rather than the bulk aqueous solution, the effective concentration of any surfactants in the medium is probably too low to have any impact on the wettability of Freon hydrates in the emulsion.

For the crude oil degradation system, more substrate is potentially available. The availability of substrate compounds is here limited by the surface area and time. Figure 4.3 shows a comparison of the blank medium and the media cultivated using toluene and crude oil as substrate, respectively.

Figure 4.3 shows that the wetting indexes are within the standard error of each other. When testing the medium where crude oil was the substrate, the point of phase inversion was increased for both the emulsion with and without Freon hydrates, indicating a more stable water-in-oil emulsion.

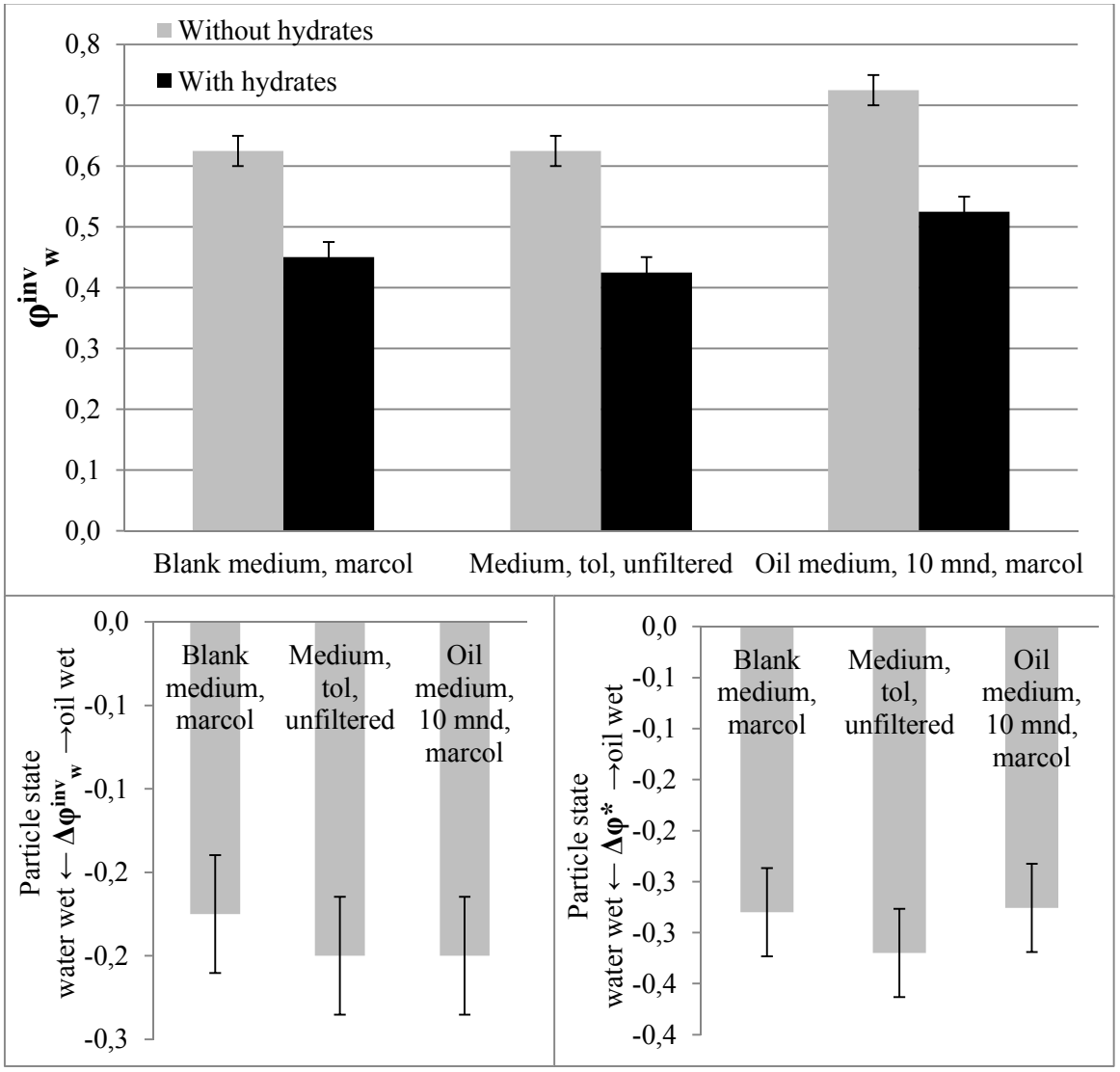

FIGURE 4.3: Top: Points of phase inversions for the different media, down left: difference in points of phase inversions, down right: Wetting index, difference in points of phase inversion, standardized according to equation 2.2.

Interfacial properties

Tables 3.7 and 3.13 shows that the interfacial tension of the media decreased for the crude oil-substrate medium, while remaining within the standard error for the toluene-substrate medium. The contact angle of the medium on a steel plate in Marcol 52 increased with bacteria cultivated on both substrates. Figure 4.4 shows representative pictures of the drops for comparison.

When calculating the adhesion energy, the reduction in adhesion energy clearly indicates a change in wettability of the steel plate to a more oil-wet state (figure 4.5).

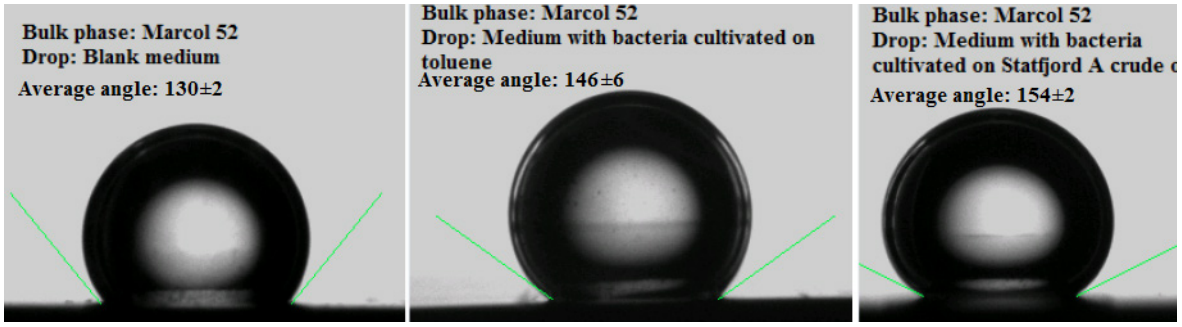

FIGURE 4.4: Representative pictures of drops from media cultured using diffs erent substrates, on stainless steel in Marcol 52.

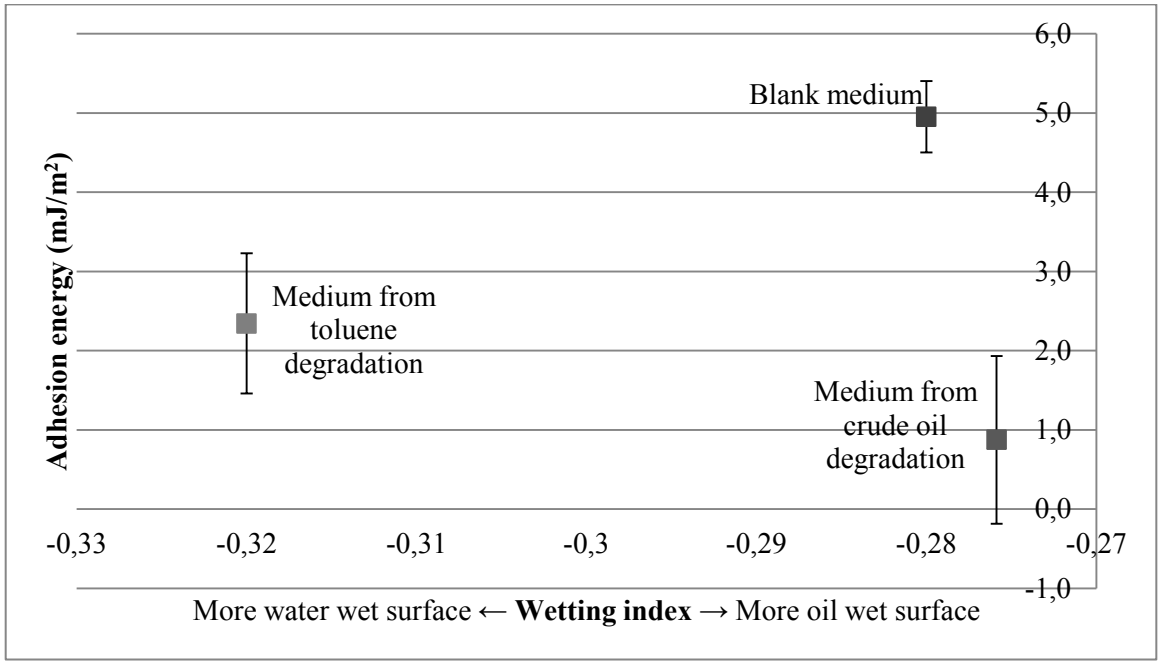

FIGURE 4.5: The adhesion energy of the medium with and without bacteria cultivated on toluene as a function of the wetting index. Note that the wetting indexes of each of the samples are within the standard error of each other, as discussed in section 4.3.2. All tests are done with drops of aqueous phase on a pre-aged stainless steel-plate in the presence of the light hydrocarbon phase. A high wetting index indicates a more oil wet surface of Freon hydrates, low adhesion energy indicates a more oil wet steel surface.

Viscosity

The medium with bacteria cultivated on toluene, had a clear viscosity change seen in figure 3.13. The crude oil-substrate medium, also showed a change in viscosity, but to a lesser degree (figure 3.21). The viscosity is still quite low, but the largest difference in viscosity can be seen at low shear. A comparison of the media is presented in figure 4.6. Especially the media cultivated on toluene showed a shear thinning behaviour.

The EPS from biofilms are considered to have viscoelastic properties,[56] so the shear thinning behaviour observed could be due to the presence of EPS in the aqueous media.

An explanation of why this behaviour is most clear for the medium where toluene was the substrate, could be the observation done in section 4.3.1, that the toluene substrate seemed to be exhausted. When there is lack of substrate and bacterial cells die, there might be an increase of biofilm dispersal,[56] causing a higher concentration of EPS in the bulk medium which would lead to a higher viscosity at low shear. Some natural polysaccharides exhibit shear thinning properties at dilute concentrations, and at higher concentrations of this is even more common.[96]

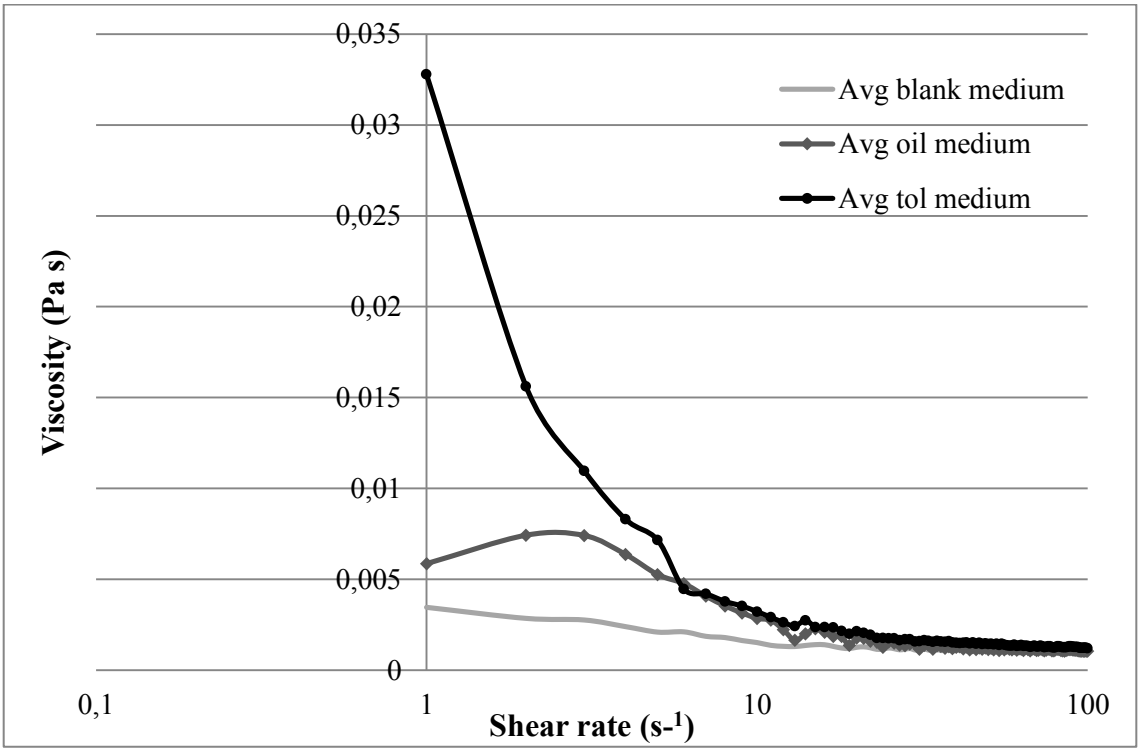

FIGURE 4.6: The viscosity of the different media as a function of shear rate. Note that the viscosity in this graph is not presented logarithmically as in figures 3.13 and 3.21. This is to give a clearer picture of the shear thinning property of the media cultivated with bacteria.

4.3.3 Properties of crude oil phase

Fractional composition

In table 3.9, some properties of the crude oil before and after biodegradation is listed. The change in density can be attributed mainly to evaporation of light, low density compounds. An observation done when measuring the density of the non-biodegraded crude oil was that when parallels were measured when the oil was left in open for 10-15 minutes, the density attained was higher and not within 10 % of the value attained from a sample in a closed container.

TABLE 4.7: An overview of the change in fractional distribution based on S/A/R-analysis (section 2.3.3, and a calculation of the difference between the obtained result and the result if the fractional composition had remained unchanged.

Statfjord A crude oil	**Non-biodegraded**		**Biodegraded 10 months**		**If same distr.**	**Diff. in res.**
	Result	**Fraction**	**Result**	**Fraction**	**Result**	
Saturates (mg/g oil)	557	89,6 %	574	80,7 %	637	63,3
Aromatics (mg/g oil)	36,5	5,87 %	86,5	12,2 %	41,8	-44,7
Resins (mg/g oil)	28,0	4,51 %	50,6	7,12 %	32,0	-18,6
Total:	622	100 %	711	100 %	711	0,00

The total content of saturates, aromatics and resins of the non-biodegraded crude oil gives a yield of 62 %wt of the original sample of oil fractioned, while the yield is 71 %wt in the biodegraded oil. Table 4.7 gives an overview of the change in fractional distribution, and a calculation of the difference between the obtained result and the result if the fractional composition had remained unchanged. The decrease in content of saturates is to be expected due to evaporation, and this would increase the relative mass of the other fractions. The decrease in mass from the saturated fraction is not evenly distributed among the resins and aromatics, and it might look like more of the aromatics than resins are accumulating, indicating that more resins are degraded rather than aromatics. This is a little bit surprising, since the bacteria are known to degrade the aromatic toluene. It might be that when presented with alternative substrates in a crude oil, aromatics are not the preferred substrate.

Note that the asphaltene content was not determined for the biodegraded crude oil, and is therefore omitted in the calculation. This could also influence the fractional distribution, but the initial content was quite low so it might not have changed significantly. In the work by Erstad et.al., the S/A/R-distribution in the oil used for anaerobic degradation with the *D. toluenicum* bacteria, was measured by Iatroscan. The distribution was found quite unchanged through that method.[7] This lack of change in distribution could indicate that there is better reproducibility in Erstads method in comparison to the solid phase extraction method applied in this work. In the work by Erstad, the original oil contained less saturated components from the beginning, A consequence of this could be that there were less light components that could evaporate and influence the result.

The initial total acid number gave a low acid content of the oil. High acid content has previously been correlated with low plugging tendency and high degree of biodegradation,[3] so the low acid content might explain why the Statfjord A oil initially was found to have a low wetting index. The acid number after degradation was not measured due to problems with the equipment.

Gas Chromatographic profile

Figure 3.15 shows the difference between the highest peak areas from the chromatograms of non-degraded and biodegraded oil. The most volatile compounds were difficult to identify due to a quicker temperature program than the NIGOGA standard. The most volatile compounds are probably irrelevant, due to quick evaporation rather than biodegradation. To assess the degree of biodegradation versus evaporation, a sterile system treated the same way as the degradation system, would have had to be set up and compared. From nC8 and higher, biodegradation can be assumed as the cause of change (Barth, T., personal communication). All identified compounds up to nC15 seem to have experienced some biodegradation, indicating that the bacterium utilizes a wide range of compounds when presented with a mixed substrate.

FT-IR

The FT-IR spectra (figure 3.16) of the non-biodegraded and biodegraded oils does not show any significant changes to the oil phase.

Viscosity

Figure 3.17 shows that the viscosity of the biodegraded oil has increased somewhat. This is probably due to the evaporation and degradation of light, non-viscous components in the oil. There is a slight indication of some shear-thinning effect in the biodegraded oil. One explanation of this could be that some of the EPS components could have gone into the oil phase.

Wetting index

Figure 3.18 shows a clear tendency of the wetting index to increase from a standard of marcol 52 mixed with non-biodegraded oil and the biodegraded oil at different incubation times. The oil was diluted to a 3 %wt mixture with Marcol 52, so a change in the wetting index at such a low concentration would indicate high efficiency of surface-active components in the oil sample. A higher concentration or longer degradation time could give more changes.

4.4 Implications

The wetting index-test with a model oil show that it is difficult to get major results without testing other variables like concentration, and that the results are not directly comparable to a crude oil. The wetting index was developed for crude oils,[16] and it is likely that a system using a model oil with a low content of natural surfactans, such as Marcol 52, will need an increased concentration of additives than the low concentrations that are preferred. The test requires about 50-100 mL of sample for both the hydrocarbon and aqueous phase to get a reliable result, so it is difficult to apply for small sample volumes.

The mixing of a crude oil into a model oil with a low content of natural surfactans and its effect on the efficiency of commercial anti-agglomerants was discussed in a paper by Moradpour et.al. [80] It was found that in diesel oil, the concentration of the commercial anti-agglomerant needed to be higher than in crude oil systems in order to attain wanted result.

The wettability tests done on the systems might give an indication of the likelihood for adhesion to the pipeline wall, which could be a simple and useful test in order to rule out possible anti-agglomerant candidates. In order to assess potential anti-agglomerant properties of a system, tests in more realistic conditions are necessary. An important advantage of the method compared to the wetting index-method, is that it does not need large sample volumes.

It is important to note that pipeline walls are usually not plain, smooth stainless steel surfaces, as they are usually subject to mechanical wear and depositon of for example wax- and scale.

Biosurfactants are an interesting category of substances for further research in this area. The two glycosides tested in this thesis, octyl glycoside and lauryl maltoside (figure 3.5), seem to differ in their efficiency of exhibiting surfactant properties. The two molecules differ in both molecular mass and critical micelle concentration.

At the concentration of 500 ppm in water, the concentrations of octyl glucoside and lauryl maltoside are 17 and 9.8 mM, respectively. With reported cmc values of 24-26 mM[97] for octyl glucoside and 0.16 mM for lauryl maltoside,[98] the concentration applied was below cmc for octyl glucoside and above cmc for lauryl maltoside. Looking at biosurfactants with low cmc values could be a reasonable strategy if more biosurfactants were to be tested for anti-agglomerating properties.

The degradation using *Desulfotignum toluenicum* bacterium does seem to have some impact on the crude oil phase, this could imply that surface active compounds produced

by the degradation process mainly resides in the oil phase. In order to note any effect from possible compounds in the aqueous phase, either other methods should be applied, or a sample would have to be made more concentrated. The adhesion energy for the system did decrease, especially for the crude oil substrate-system.

Spectroscopic techniques have previously been applied to analyse EPS, a small overview is found in a review article by Sheng et.al.[99] When separated from the bacterial cells, this is found to be a complicated matrix, including carbohydrates, proteins and some nucleic acids. Extracting and separating specific surfactant molecules from this matrix might prove difficult. A study comparing the surface adhesion of bacteria to the composition of their external layers, correlated hydrophobicity with a high content of proteinaceous materials, while hydrophilicity was correlated with oxygen functions (polysaccharides).[100]

Assuming that both of these categories of compounds are present in the EPS of *Desulfotignum toluenicum*, it is probable that the polysaccharides will reside in the aqueous phase, while the protein functions might reside in the oil phase. It has also been demonstrated that some bacterial strains produce biosurfactants in their biofilms, affecting the architechture and cell-to-cell interactions.[101]

Separating out possible anti-agglomerating compounds in this extracellular matrix might be difficult, but the change in the wetting index of the crude oil phase mixed with Marcol 52, seen in figure 3.18, but not from the medium, might lead the assumption to expect that the more hydrophobic compounds are more efficient anti-agglomerants. In her thesis, Erstad found one fraction of compounds from the oil phase more efficient at low concentrations than other fractions when applying a low temperature/high pressure sapphire cell.[2]

4.5 Applications

When considering to apply the results, an important thing to keep in mind is the low efficiency and high cost of extraction of biosurfactants. Table 4.8 gives a simplified picture of the costs associated with using the common thermodynamic inhibitor ethylene glycol (MEG) compared to applying a commercial anti-agglomerant or the glycoside, lauryl maltoside, applied in this work. The data is based on the Ormen Lange gas field,[1] which is a worst case scenario for the amount of MEG applied, since it is operated in subzero water temperatures.

From this scenario, it might seem that applying biosurfactants would be less costly, but this calculation uses an unrealistically high price and quality of MEG, which will

TABLE 4.8: Simplified cost scenario from Ormen Lange field[1] comparing current thermodynamic inhibitor usage with commercial anti-agglomerant and biosurfactant. Several simplifications are done: The water cut has not been considered, the %wt is assumed of the whole mass flow. Density of Span-20 is simplified to 1 tonne/m^3. Prices are collected from supplier websites, per anno quality, ignoring discounts, and are probably unrealisticly high. Ormen Lange is a gas field, and applicability for AA is minor, see discussion text.

Worst case scenario, Ormen	**Lange**	
Fraction of MEG required	70	%wt
Corresponding to	6	m^3/MMSCF
	6.66	tonnes/MMSCF
Cost of MEG (Sigma-Aldrich[102])	295 375	NOK/m^3
	266 104	NOK/tonne
Total cost	**1 772 250**	**NOK/MMSCF**
Fraction of Span-20 required[103]	3	%wt
Corresponding to	2.85E-01	m^3/MMSCF
Cost of Span-20 (Sigma-Aldrich[104])	1 096 490	NOK/m^3
Total cost	**312 970**	**NOK/MMSCF**
Fraction of LM required	0.05	%wt
Corresponding to	4.76E-03	tonnes/MMSCF
Cost of LM (Avanti[54])	283 200 000	NOK/tonne
Total cost	**1 347 223**	**NOK/MMSCF**

probably be lower due to discounts for the large volumes required. Another factor that is left out, is the possibility of recycling MEG, which would further bring down the costs. Comparing the biosurfactant to the commercial anti-agglomerant, the biosurfactant is more than four times as expensive to apply. The benefit of a biosurfactant is its non-toxicity and biodegradability. A problem with commercial anti-agglomerants has been its environmental toxicity due to the low biodegradability and the release through the water phase in a relatively high concentration.[105]

The comparison to the Ormen Lange-field is not realistic for the application of anti-agglomerants, but used to show the worst case scenario of the costs of applying thermodynamic inhibitor. The application of anti-agglomerants will not work without a hydrocarbon fluid for transporting the small hydrates that are formed. In a gas field, the small amount of condensate present is not sufficient to form the oil-continuous hydrate slurry that is necessary to prevent agglomeration of hydrates. The typical conditions for the application of anti-agglomerants is in a multiphase oil-dominated flowline with a water cut of 30 %vol.[1]

In order for biosurfactants to be viable solution, the costs of production must be brought down. An alternative is to avoid extraction of the surfactants and look into the use of the bacterial culture instead, where the non-refined mixture of dead bacteria and surfactants would work as well as the refined surfactant and at low concentrations. A third option

is the injection of a bacterial culture in situ, that grow on the crude oil to change its composition and/or make biosurfactants. The last option seems unrealistic, mainly due to the slow growth of anaerbic bacteria using crude oil as a substrate, compared to production of oil. It is also difficult to control conditions in order to optimize growth of the correct bacteria.

Biofilm formation is applied in microbial enhanced oil recovery today. As the bacteria tested in this work is a sulfate reducing bacteria producing H_2S-gas, it is a bacterium that is best avoided in an oil production setting. In microbial enhanced oil recovery, sulfate reducing bacteria are considered the "notorious villains" (Sen, 2008[93]), as they lead to reservoir souring and have simple growth requirements. They thrive especially when sea water is injected, as the content of sulfate in sea water is high. Efforts are made to kill populations of these using injection of chemicals or nitrate reducing bacteria to outcompete the sulfate reducing bacteria.[93]

The application of *Desulfotignum toluenicum* should be limited to lab scale research, and a longer time frame should be applied. Erstad discusses the incubation time of 10 months laboratory degradation as an insuffient time scale to produce enough of the desired compounds in the oil phase.[7] This seems to be an insufficient time scale to produce sufficient amount of any desired compounds in the aqueous phase as well. However, the application of toluene as a carbon source could have provided more biomass in the aqueous phase in a shorter amount of time if there was a continuous addition of toluene and flushing of hydrogen sulfide. It is difficult to conclude whether EPS produced by the bacteria during toluene degradation would have any effect at higher concentrations.

Chapter 5

Conclusion and suggestions for further work

5.1 Conclusion

The main purpose of this work was to assess the efficiency of biosurfactants in the context of preventing gas hydrate agglomeration, and see whether the bacterium *Desulfotignum toluenicum* produced water soluble compounds with anti-agglomerating properties. The conclusions to be drawn from the work can be summarized as follows.

Naphthenic acids extracted from petroleum, have previously been demonstrated to contribute as natural anti-agglomerants in crude oil at higher concentrations. At the concentration applied in this work, 500 ppm in a model oil, these compounds are found to be inefficient anti-agglomerants in a model oil system.

From the two commercial biosurfactants tested at 500 ppm in brine, octyl glucoside and lauryl maltoside, the latter was found efficient in changing the wetting index of a crude oil from negative to positive, in effect changing the wettability of Freon hydrates from water-wet to oil-wet, possibly changing the plugging potential of the crude oil system. This compound was added in a concentration above its critical micelle concentration, and showed particularly low interfacial tension and adhesion energy. Octyl glucoside was added at a concentration below its cmc, and assumed to be tested at a too low concentration to conclude regarding anti-agglomerating properties.

The commercial biosurfactants tested did not show any effect on the wetting index of the model oil, but both compounds decreased the interfacial tension and adhesion energy on stainless steel. This observation adds on previous observations that additives can

behave differently when applied to different systems, probably due to differences in oil composition (section 4.2.3).

The aqueous phase from the biodegradation setup showed no influence on the wetting index of the model oil system or the crude oil system. The aqueous phases changed the wettability of stainless steel by increasing the contact angle and lowering the adhesion energy. The aqueous phase from the crude oil degradation also reduced the interfacial tension from the blank. Any possible anti-agglomerants present would be at a too low concentration to be efficient in changing the wettability of hydrates.

The biodegraded crude oil phase showed some increase in wetting index when diluted in the model oil, indicating a change in the composition of the oil. The increase in wetting index was not enough to conclude that wettability of hydrate particles would change from water-wet to oil-wet, but this effect might have decreased due to the dilution.

D. toluenicum is a slow growing bacteria on crude oil, and the time frame used in this work was probably insufficient to attain the same efficient change of wetting index as naturally biodegraded oils.

Observation in microscope, viscosity changes and filter plugging leads to the conclusion of the growth of the *D. toluenicum* bacteria as a biofilm in the oil/water interface. This leads to an inefficient extraction of the aqueous phase for biomass analysis, and difficulty in counting the bacteria. The biofilm extracellular polymeric substances might have a role in the wettability changes observed for the systems, as some bacteria in other works have been found to produce biosurfactants within the biofilm.[101]

Biosurfactants are an interesting group of compounds for anti-agglomerant application, due to their environmental friendliness, but the high cost of purified biosurfactants does not compete with the thermodynamic inhibitors applied today.

Being a sulfate reducing bacteria, *Desulfotignum toluenicum* should not be applied live in petroleum production. For lab scale research, incubation should be planned with a longer time scale than 10 months.

5.2 Suggestions for further work

As a direct consequence of the results in this work, it would be interesting to leave the crude oil for a longer incubation period than 10 months, and compare with a sterile sample. In her PhD thesis, Dr. Kristin Erstad worked with fractionation of the crude oil phase, and found one of the fractions to be very efficient at low concentrations, especially when fractionating a crude oil degraded using *Desulfotignum toluenicum* compared to

an aerobically degraded crude oil. Erstad suggested to increase the incubation time for the *D. toluenicum* bacteria, and continue a structure elucidation of compounds in this efficient fraction in order to identify possible model compounds with anti-agglomerating properties.[2] The results on the crude oil phase from this work supports this suggestion.

In the case of the aqueous phase, a longer incubation time is also advisable before any conclusions can be drawn. This would require monitoring of hydrogen sulfide production and flushing it out when it reaches dangerous levels, and refilling substrate and nutrients in order to attain more growth. It is not advisable to make an extraction procedure for compositional analysis for the aqueous phase before any effect of the medium against a crude oil is established.

In the case of biodegradation, I would suggest trying to cultivate nitrate reducing bacteria on crude oil to see the effects, as these have established applicability in MEOR. Trying to optimize bacterial growth with different substrates and test to see whether any inexpensive bacterial cultures have anti-agglomerating properties could be a way to lower the costs, instead of using pure biosurfactants.

Appendix A

383a. Desulfobacterium medium (DSMZ)

Table A.1: Ingredients for medium 383a from DSMZ, Solutions A and B.[49]

Solution A:	
Na_2SO_4	3.00 g
KH_2PO_4	0.20 g
NH_4Cl	0.30 g
NaCl	15.00 g
$MgCl_2$ x 6 H_2O	3.00 g
KCl	0.50 g
$CaCl_2$ x 2 H_2O	0.15 g
Yeast extract	10.00 mg
Resazurin	1.00 mg
Distilled water	920.00 mL
Solution B:	
Trace element solution:	1.00 mL
HCl (25%; 7.7 M)	10.00 mL
$FeCl_2$ x 4 H_2O	1.50 g
$ZnCl_2$	70.00 mg
$MnCl_2$ x 4 H_2O	100.00 mg
H_3BO_3	6.00 mg
$CoCl_2$ x 6 H_2O	190.00 mg
$CuCl_2$ x 2 H_2O	2.00 mg
$NiCl_2$ x 6 H_2O	24.00 mg
Na_2MoO_4 x 2 H_2O	36.00 mg
Distilled water	990.00 mL

First dissolve $FeCl_2$ in the HCl, then dilute in water, add and dissolve the other salts. Finally make up to 1000.0 ml

Table A.2: More ingredients for medium 383a from DSMZ, solutions C-G.[49]

Solution C:	
$NaHCO_3$	2.50 g
Distilled water	50.00 mL
Solution D:	
Recommended substrate: Sodium pyruvate	0.6 g
Solution E:	
Vitamin solution:	20 mL
Biotin	2.00 mg
Folic acid	2.00 mg
Pyridoxine-HCl	10.00 mg
Thiamine-HCl x 2 H_2O	5.00 mg
Riboflavin	5.00 mg
Nicotinic acid	5.00 mg
D-Ca-pantothenate	5.00 mg
Vitamin B12	0.15 mg
p-Aminobenzoic acid	5.00 mg
Lipoic acid	5.00 mg
Distilled water	1000.00 mL
Solution F:	
Na_2SeO_3 x 5 H2O-sol.	
(3 mg in 1 l 0.01 M NaOH)	1.00 mL
Solution G:	
Na_2S x 9 H_2O	0.40 g
Distilled water	10.00 mL

Solution A is prepared and autoclaved anaerobically under 80% N_2 + 20% CO_2. Solution C is filter-sterilized and gassed for 20 min with N_2/CO_2. Solutions B, D, E and F are filter-sterilized and gassed with N_2. Solution G is autoclaved under N_2. Solutions B to G are added to the sterile, cooled solution A in the sequence as indicated. Final pH of the medium should be 7.0. Addition of 10 - 20 mg sodium dithionite per liter (e.g. from 5% (w/v) solution freshly prepared under N_2 and filter-sterilized) may stimulate growth of all strains at the beginning. For transfers use 5 - 10% inoculum. Incubate all strains in the dark.

Appendix B

Whole Oil Chromatograms

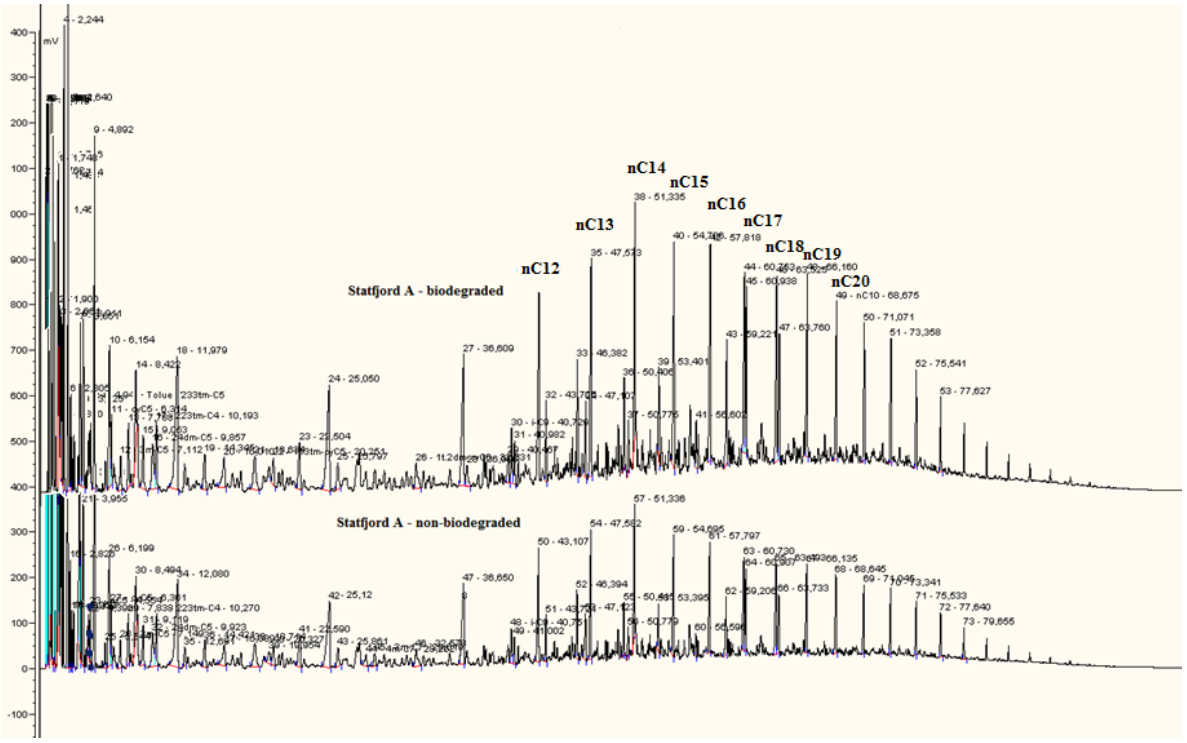

FIGURE B.1: Whole oil chromatogram of Statfjord A oil: Upper: biodegraded, Lower: non-biodegraded. Note that some peaks from the first 5 minutes are overlapping in order to get a better comparison of the nC10-nC26 peaks.

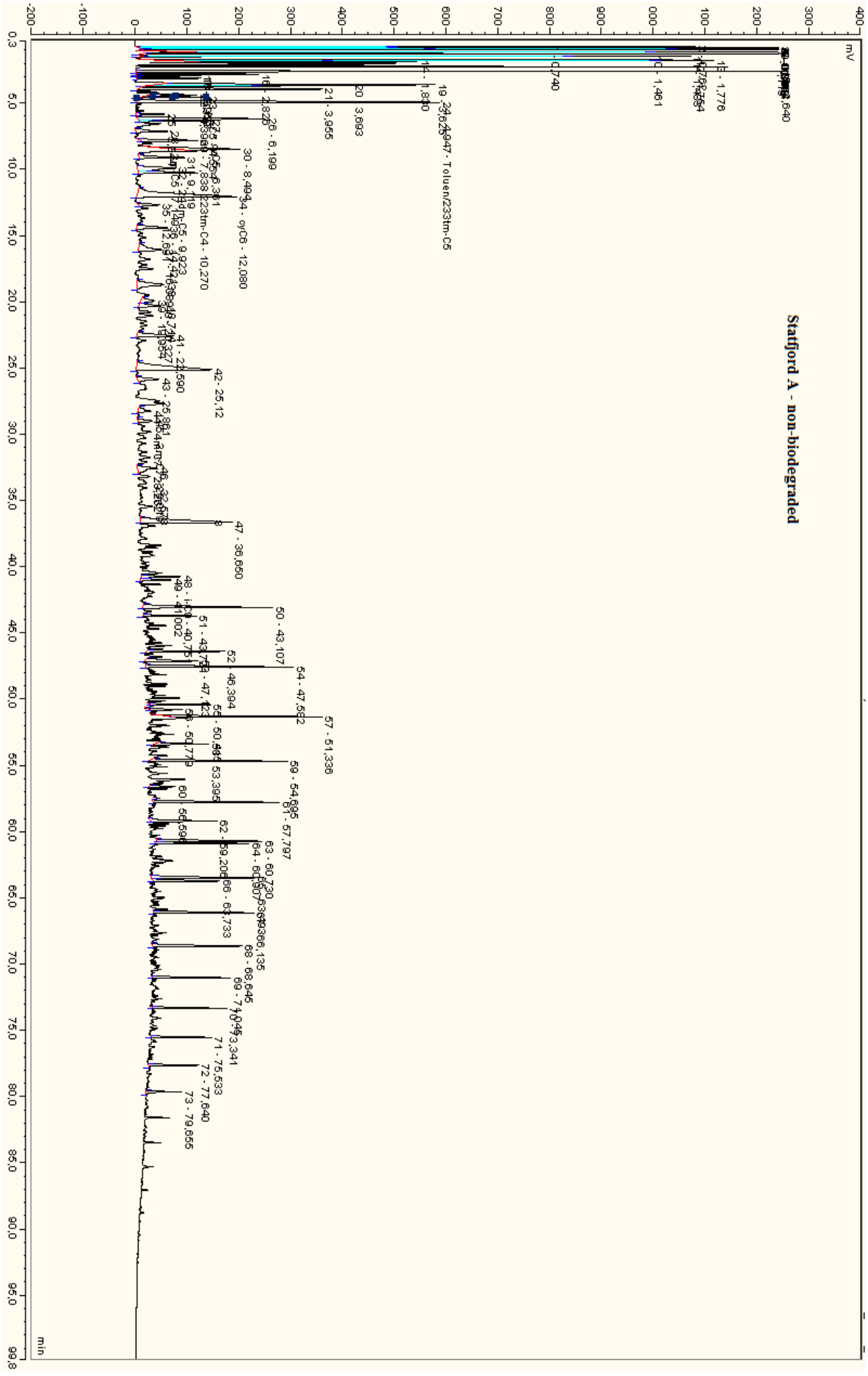

FIGURE B.2: Whole oil chromatogram of non-biodegraded Statfjord A oil.

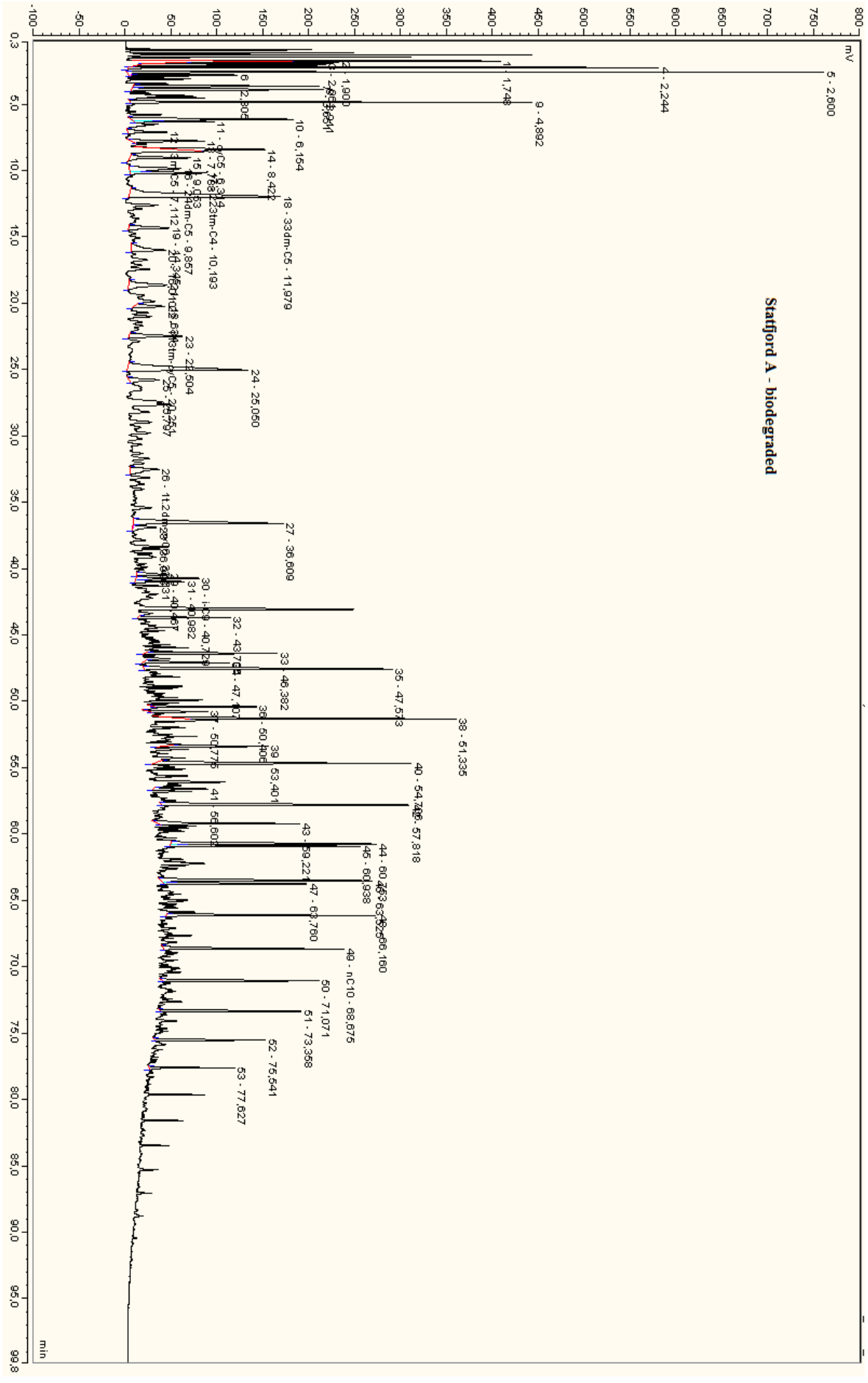

FIGURE B.3: Whole oil chromatogram of biodegraded Statfjord A oil.

Appendix C

Fourier Transform Infrared Spectrum of filtered medium

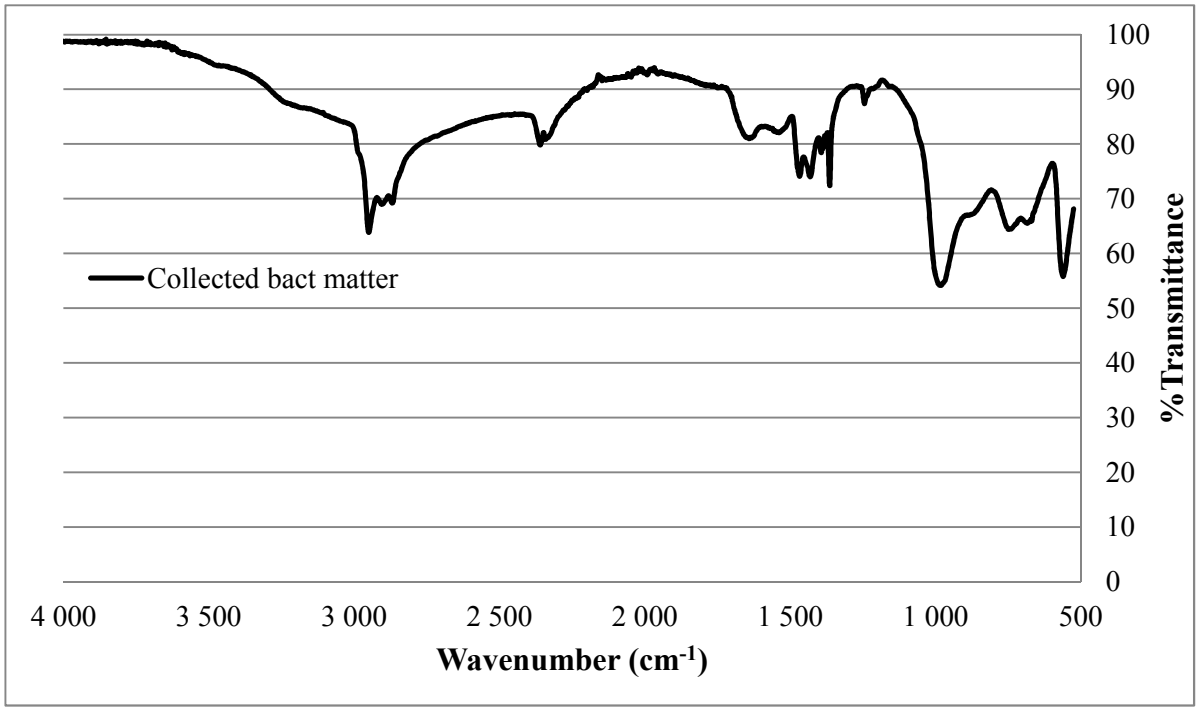

FIGURE C.1: FT-IR spectrum of collected material from filter after filtration of medium containing bacteria cultivated on toluene substrate. The signal at 2943 cm^{-1} confirms the presence of C-H bonds in the sample.[42]

Appendix D

Densities of liquids used in experiments

Table D.1: Densities of liquids used in the different systems, experimentally quantified.

Liquid	**Density (g/mL)**		**Number of parallells**
Marcol 52	0.8316	± 0.00001	2
Marcol 52-NA	0.8325	± 0.00001	2
Marcol 52-NAC	0.8317	± 0.00000	2
Brine	1.0228	± 0.00001	2
Brine-LM	1.0229	± 0.00023	2
Brine-OG	1.0229	± 0.00004	2
Blank medium	1.0153	±0.00000	2
Medium including bacteria cultivated on toluene as a substrate	1.0152	±0.00003	2
Medium including bacteria cultivated on crude oil as a substrate	1.0154	±0.00000	2

Bibliography

[1] E Dendy Sloan, Carolyn Ann Koh, and Amadeu Sum. *Natural gas hydrates in flow assurance*. Gulf Professional Publishing, 2010.

[2] Kristin Erstad. *The influence of crude oil acids on natural inhibition of hydrate plugs*. University of Bergen, 2009.

[3] Anna Elisabet Borgund. *Crude oil components with affinity for gas hydrates in petroleum production*. University of Bergen, 2007.

[4] Guro Aspenes. *The influence of pipeline wettability and crude oil composition on deposition of gas hydrates during petroleum production*. University of Bergen, 2009.

[5] Hege Ommedal and Terje Torsvik. *Desulfotignum toluenicum* sp. nov., a novel toluene-degrading, sulphate-reducing bacterium isolated from an oil-reservoir model column. *International journal of systematic and evolutionary microbiology*, 57(12):2865–2869, 2007.

[6] Gunhild Bødtker, Ina V Hvidsten, Tanja Barth, and Terje Torsvik. Hydrocarbon degradation by dietzia sp. a14101 isolated from an oil reservoir model column. *Antonie Van Leeuwenhoek*, 96(4):459–469, 2009.

[7] Kristin Erstad, Ina V Hvidsten, Kjell Magne Askvik, and Tanja Barth. Changes in crude oil composition during laboratory biodegradation: Acids and oil–water, oil–hydrate interfacial properties. *Energy & Fuels*, 23(8):4068–4076, 2009.

[8] Jane Williams. Status of multiphase flow measurement research. In *SPE Annual Technical Conference and Exhibition*, 1994.

[9] SINTEF and IFE. Flyt, flerfasetransport på sokkelen i 25 år. `http://www.sintef.no/upload/Konsern/Media/flerfase1984-2009brosjyre_lo.pdf`, December 2009. Accessed: May 29^{th} 2013.

[10] RVA Oliemans. Multiphase science and technology for oil/gas production and transport. In *University of Tulsa Centennial Petroleum Engineering Symposium*, 1994.

[11] Gioia Falcone, Catalin Teodoriu, Kurt Reinicke, and Oladele Bello. Multiphase flow modelling based on experimental testing: A comprehensive overview of research facilities worldwide and the need for future developments. In *SPE Annual Technical Conference and Exhibition*, 2007.

[12] E Dendy Sloan Jr and Carolyn Koh. *Clathrate hydrates of natural gases*. Second edition, 2007.

[13] Chang-ling Liu, Yu-guang Ye, and Qing-guo Meng. Determination of Hydration Number of Methane Hydrates Using Micro-Laser Raman Spectroscopy. *Spectroscopy And Spectral Analysis*, 30(4):963–966, 2010.

[14] Richard Birchwood, Jianchun Dai, Dianna Shelander, Ray Boswell, Timothy Collett, Ann Cook, Scott Dallimore, Kasumi Fujii, Yutaka Imasato, Masafumi Fukuhara, et al. Developments in gas hydrates. *Oilfield review*, 22(1), 2010.

[15] E. Dendy Sloan. Clathrate Hydrates: The Other Common Solid Water Phase. *Industrial & Engineering Chemistry Research*, 39(9):3123–3129, 2000.

[16] S. Høiland, K.M. Askvik, P. Fotland, E. Alagic, T. Barth, and F. Fadnes. Wettability of Freon hydrates in crude oil/brine emulsions. *Journal of Colloid and Interface Science*, 287(1):217 – 225, 2005.

[17] F. H. Fadnes. Natural hydrate inhibiting components in crude oils. *Fluid Phase Equilibria*, 117(1 - 2):186 – 192, 1996.

[18] Sylvi Høiland, Anna E Borgund, Philippe Glénat, Per Fotland, Kjell Askvik, Xiaoyun Li, and STATOIL ASA. The wetting index: A quantitative measure of indigenous hydrate plugging tendency; flow test validations. In *Proceed. of the 7th Inter. Conference on Gas Hydrates. Edinburgh, UK*, 2011.

[19] Sylvi Høiland, Anna Elisabeth Borgund, Tanja Barth, Per Fotland, and Kjell Magne Askvik. Wettability of freon hydrates in crude oil/brine emulsions: the effects of chemical additives. In *Proceedings of the Fifth International Conference on Gas Hydrates*, volume 4, pages 1151–1161, 2005.

[20] Malcolm A Kelland. History of the development of low dosage hydrate inhibitors. *Energy & Fuels*, 20(3):825–847, 2006.

[21] EM Leporcher, JL Peytavy, Y Mollier, J Sjöblom, and C Labes-Carrier. Multiphase transportation: hydrate plugging prevention through crude oil natural surfactants. In *SPE Annual Technical Conference and Exhibition*, 1998.

[22] Johan Sjöblom, Bodhild Øvrevoll, GunnHeidi Jentoft, Caterina Lesaint, Thierry Palermo, Anne Sinquin, Patrick Gateau, Loïc Barré, Siva Subramanian, John Boxall, et al. Investigation of the hydrate plugging and non-plugging properties of oils. *Journal of Dispersion Science and Technology*, 31(8):1100–1119, 2010.

[23] Linn Bergfløtdt, Lars Henrik Gjertsen, Johan Sjöblom, Harald Kallevik, and Gisle Øye. Chemical influence on the formation, agglomeration, and natural transportability of gas hydrates. a multivariate component analysis. *Journal of dispersion science and technology*, 25(3):355–365, 2004.

[24] Ayhan Demirbas. Methane hydrates as potential energy resource: Part 1-Importance, resource and recovery facilities. *Energy Conversion and Management*, 51(7):1547–1561, 2010.

[25] James G. Speight. *The chemistry and technology of petroleum*. Fourth edition, 2007.

[26] Tanja Barth, Sylvi Høiland, Per Fotland, Kjell Magne Askvik, Bent Skaare Pedersen, and Anna Elisabet Borgund. Acidic compounds in biodegraded petroleum. *Organic geochemistry*, 35(11):1513–1525, 2004.

[27] Thomas Young and George Peacock. *Miscellaneous works*. Murray, London, 1855.

[28] John C Berg. *An introduction to interfaces and colloids*. World Scientific Publishing Company, 2010.

[29] BP Binks and SO Lumsdon. Influence of particle wettability on the type and stability of surfactant-free emulsions. *Langmuir*, 16(23):8622–8631, 2000.

[30] BP Binks and SO Lumsdon. Catastrophic phase inversion of water-in-oil emulsions stabilized by hydrophobic silica. *Langmuir*, 16(6):2539–2547, 2000.

[31] Thomas A Wittstruck, Jr Brey, ES Wallace, AM Buswell, and WH Rodebush. Solid hydrates of some halomethanes. *Journal of Chemical and Engineering Data*, 6(3):343–346, 1961.

[32] Ajay Singh and Owen P Ward. *Biodegradation and bioremediation*, volume 2. Springer, 2004.

[33] Bo Barker Jørgensen. Mineralization of organic matter in the sea bed – the role of sulphate reduction. *Nature*, 296:643–645, 1982.

[34] Gerda Harms, Karsten Zengler, Ralf Rabus, Frank Aeckersberg, Dror Minz, Ramon Rosselló-Mora, and Friedrich Widdel. Anaerobic oxidation of o-xylene, m-xylene, and homologous alkylbenzenes by new types of sulfate-reducing bacteria. *Applied and environmental microbiology*, 65(3):999–1004, 1999.

[35] Johann Heider, Alfred M Spormann, Harry R Beller, and Friedrich Widdel. Anaerobic bacterial metabolism of hydrocarbons. *FEMS Microbiology Reviews*, 22(5): 459–473, 1998.

[36] Jitendra D Desai and Ibrahim M Banat. Microbial production of surfactants and their commercial potential. *Microbiology and molecular Biology reviews*, 61(1): 47–64, 1997.

[37] Siegmund Lang. Biological amphiphiles (microbial biosurfactants). *Current Opinion in Colloid & Interface Science*, 7(1-2):12 – 20, 2002.

[38] E Kowalewski, I Rueslåtten, KH Steen, G Bødtker, and O Torsæter. Microbial improved oil recovery – bacterial induced wettability and interfacial tension effects on oil production. *Journal of Petroleum science and Engineering*, 52(1):275–286, 2006.

[39] Emerson Y Arashiro and Nicole R Demarquette. Use of the pendant drop method to measure interfacial tension between molten polymers. *Materials Research*, 2(1): 23–32, 1999.

[40] G. Aspenes, S. Høiland, T. Barth, and K.M. Askvik. The influence of petroleum acids and solid surface energy on pipeline wettability in relation to hydrate deposition. *Journal of Colloid and Interface Science*, 333(2):533 – 539, 2009.

[41] G.A. Schramm and Gebrueder Haake (Firm). *A Practical Approach to Rheology and Rheometry*. Haake Rheometer. Haake, 1994.

[42] Donald L. Pavia et.al. *Introduction to Spectroscopy: Fourth International Student Edition*. Fourth edition, 2009.

[43] James M. Miller. *Chromatography Concepts & Contrasts*. Second edition, 2005.

[44] HM Weiss, A Wilhelms, N Mills, J Scotchmer, PB Hall, K Lind, and T Brekke. NIGOGA-The Norwegian Industry Guide to Organic Geochemical Analyses. *Edition four, Published by Norsk Hydro, Statoil, Geolab Nor, SINTEF Petroleum Research and the Norwegian Petroleum Directorate*, 2000.

[45] Linda Kristin Moen. Effekter av reaksjonsmiljø på dannelse og nedbrytning av organiske syrer. *Hovedfagsoppgave i organisk kjemi*, 1996.

[46] W Meredith, S.-J Kelland, and D.M Jones. Influence of biodegradation on crude oil acidity and carboxylic acid composition. *Organic Geochemistry*, 31(11):1059 – 1073, 2000.

[47] Mediaas Heidi, Knut Grande, Britt Hustad, Rasch Anita, Håkon Ruesåtten, and Jens Vindstad. The acid-IER method-a method for selective isolation of carboxylic acids from crude oils and other organic solvents. In *International Symposium on Oilfield Scale*, 2003.

[48] Anna E. Borgund, Kristin Erstad, and Tanja Barth. Fractionation of Crude Oil Acids by HPLC and Characterization of Their Properties and Effects on Gas Hydrate Surfaces. *Energy & Fuels*, 21(5):2816–2826, 2007. doi: 10.1021/ef070100r.

[49] Deutsche Sammlung von Microorganismen und Zellkulturen. 383a desulfovibro sax medium, microorganisms DSMZ. `http://www.dsmz.de/microorganisms/medium/pdf/DSMZ_Medium383a.pdf`, February 2007. Accessed: May 26th 2013.

[50] Joel D. Cline. Spectrophotometric determination of hydrogen sulphide in natural waters. *Limnology and Oceanography*, 14(3):454–458, 1969.

[51] J. Dalton York and Abbas Firoozabadi. Comparing Effectiveness of Rhamnolipid Biosurfactant with a Quaternary Ammonium Salt Surfactant for Hydrate Anti-Agglomeration. *The Journal of Physical Chemistry B*, 112(3):845–851, 2008.

[52] W.J. De Grip and P.H.M. Bovee-Geurts. Synthesis and properties of alkylglucosides with mild detergent action: improved synthesis and purification of β-1-octyl-, -nonyl-, and -decyl-glucose. Synthesis of β-1-undecylglucose and β-1-dodecylmaltose. *Chemistry and Physics of Lipids*, 23(4):321 – 335, 1979.

[53] Avanti Polar Lipids Inc. Technical data sheet, n-octyl-β-D-glucopyranoside. `http://www.avantilipids.com/download.php?file=TechSheets/850511.pdf`, January 2013. Accessed: April 29th 2013.

[54] Avanti Polar Lipids Inc. Technical data sheet, n-dodecyl-β-D-maltopyranoside. `http://www.avantilipids.com/download.php?file=TechSheets/850520.pdf`, January 2013. Accessed: April 29th 2013.

[55] P Stoodley, K Sauer, DG Davies, and JW Costerton. Biofilms as complex differentiated communities. *Annual Reviews in Microbiology*, 56(1):187–209, 2002.

[56] Luanne Hall-Stoodley, J William Costerton, and Paul Stoodley. Bacterial biofilms: from the natural environment to infectious diseases. *Nature Reviews Microbiology*, 2(2):95–108, 2004.

[57] Frances D Hostettler and Keith A Kvenvolden. Alkylcyclohexanes in environmental geochemistry. *Environmental Forensics*, 3(3-4):293–301, 2002.

[58] Johanna Galindo-Alvarez, Veronique Sadtler, Lionel Choplin, and Jean-Louis Salager. Viscous oil emulsification by catastrophic phase inversion: influence of oil viscosity and process conditions. *Industrial & Engineering Chemistry Research*, 50(9):5575–5583, 2011.

[59] P Fotland and KM Askvik. Some aspects of hydrate formation and wetting. *Journal of colloid and interface science*, 321(1):130–141, 2008.

[60] Bernard P Binks. Particles as surfactants – similarities and differences. *Current Opinion in Colloid & Interface Science*, 7(1):21–41, 2002.

[61] BP Binks and SO Lumsdon. Transitional phase inversion of solid-stabilized emulsions using particle mixtures. *Langmuir*, 16(8):3748–3756, 2000.

[62] Kristin Erstad, Sylvi Høiland, Per Fotland, and Tanja Barth. Influence of Petroleum Acids on Gas Hydrate Wettability. *Energy & Fuels*, 23(4):2213–2219, 2009.

[63] Heidi Mediaas, Nick Wolf, Thomas Baugh, Knut Grande, and Jens Vinstad. The discovery of high molecular weight naphthenic acids (arn acid) responsible for calcium naphthenate deposits. In *SPE International Symposium on Oilfield Scale*, 2005.

[64] Øystein Brandal, Ann-Mari D Hanneseth, Pål V Hemmingsen, Johan Sjöblom, Sunghwan Kim, Ryan P Rodgers, and Alan G Marshall. Isolation and characterization of naphthenic acids from a metal naphthenate deposit: Molecular properties at oil-water and air-water interfaces. *Journal of dispersion science and technology*, 27(3):295–305, 2006.

[65] Murtala A Mohammed and Ken S Sorbie. Naphthenic acid extraction and characterization from naphthenate field deposits and crude oils using esms and apci-ms. *Colloids and Surfaces A: Physicochemical and Engineering Aspects*, 349(1):1–18, 2009.

[66] Benjamin Brocart, Maurice Bourrel, Christian Hurtevent, Jean-Luc Volle, and Bernard Escoffier. ARN-type naphthenic acids in crudes: Analytical detection and physical properties. *Journal of dispersion science and technology*, 28(3):331–337, 2007.

[67] Heléne Magnusson, Ann-Mari Dahl Hanneseth, and Johan Sjöblom. Characterization of C80 naphthenic acid and its calcium naphthenate. *Journal of Dispersion Science and Technology*, 29(3):464–473, 2008.

[68] Erland L Nordgård, Ann-Mari Dahl Hanneseth, and Johan Sjöblom. Inhibition of calcium naphthenate. experimental methods to study the effect of commercially available naphthenate inhibitors. *Journal of Dispersion Science and Technology*, 31(5):668–675, 2010.

[69] Kristin Erstad, Sylvi Høiland, Tanja Barth, and Per Fotland. Isolation and molecular identification of hydrate surface active components in petroleum acid fractions. In *6th International Conference on Gas Hydrates, Vancouver, British Columbia, Canada*, 2008.

[70] AE Borgund, K Erstad, and T Barth. Normal phase high performance liquid chromatography for fractionation of organic acid mixtures extracted from crude oils. *Journal of Chromatography A*, 1149(2):189–196, 2007.

[71] Donald F Smith, Tanner M Schaub, Sunghwan Kim, Ryan P Rodgers, Parviz Rahimi, Alem Teclemariam, and Alan G Marshall. Characterization of acidic species in athabasca bitumen and bitumen heavy vacuum gas oil by negative-ion ESI FT- ICR MS with and without acid- ion exchange resin prefractionation. *Energy & Fuels*, 22(4):2372–2378, 2008.

[72] Sigma-Aldrich. Technical information, 70340 naphthenic acid. `http://www.sigmaaldrich.com/catalog/product/aldrich/70340`, February 2012. Accessed: May 21st 2013.

[73] Joyce S Clemente and Phillip M Fedorak. A review of the occurrence, analyses, toxicity, and biodegradation of naphthenic acids. *Chemosphere*, 60(5):585–600, 2005.

[74] G Aspenes, S Høiland, T Barth, and KM Askvik. The influence of petroleum acids and solid surface energy on pipeline wettability in relation to hydrate deposition. *Journal of colloid and interface science*, 333(2):533–539, 2009.

[75] Anna E. Borgund, Sylvi Høiland, Tanja Barth, Per Fotland, and Kjell M. Askvik. Molecular analysis of petroleum derived compounds that adsorb onto gas hydrate surfaces. *Applied Geochemistry*, 24(5):777 – 786, 2009.

[76] Anna E Borgund, Sylvi Høiland, Tanja Barth, Per Fotland, Ramesh A Kini, and Roar Larsen. Critical descriptors for hydrate properties of oils: Compositional features. In *6th International Conference on Gas Hydrates, Vancouver, British Columbia, Canada*, 2008.

[77] Zachary M Aman, Laura E Dieker, Guro Aspenes, Amadeu K Sum, E Dendy Sloan, and Carolyn A Koh. Influence of model oil with surfactants and amphiphilic

polymers on cyclopentane hydrate adhesion forces. *Energy & Fuels*, 24(10):5441–5445, 2010.

[78] Alec Groysman, Alon Goldis, Natali Savchenko, Naphtali Brodsky, and Joseph Pener. Study of corrosiveness of acidic crude oil and its fractions. 2005.

[79] Anne Sinquin, David Arla, Christian Prioux, Jean Louis Peytavy, Philippe Glenat, and Christophe Dicharry. Gas hydrate formation and transport in an acidic crude oil: Influence of salt and ph. *Energy & Fuels*, 22(2):721–728, 2007.

[80] Hossein Moradpour, Antonin Chapoy, and Bahman Tohidi. Controlling hydrate slurry transportability by optimizing anti-agglomerant usage in high water cut systems. *OTC Brasil*, 2011.

[81] S. Høiland, T. Barth, A.M. Blokhus, and A. Skauge. The effect of crude oil acid fractions on wettability as studied by interfacial tension and contact angles. *Journal of Petroleum Science and Engineering*, 30(2):91 – 103, 2001.

[82] Jacob N Israelachvili. *Intermolecular and surface forces: revised third edition*, page 203. Academic press, 2011.

[83] Guro Aspenes, Sylvi Høiland, Anna E. Borgund, and Tanja Barth. Wettability of Petroleum Pipelines: Influence of Crude Oil and Pipeline Material in Relation to Hydrate Deposition. *Energy & Fuels*, 24(1):483–491, 2010.

[84] K. Verschueren. *Handbook of Environmental Data on Organic Chemicals, Four Volume Set*. Wiley, 2008.

[85] Ralf Rabus, Ralph Nordhaus, Wolfgang Ludwig, and Friedrich Widdel. Complete oxidation of toluene under strictly anoxic conditions by a new sulfate-reducing bacterium. *Applied and Environmental Microbiology*, 59(5):1444–1451, 1993.

[86] Alfred M Spormann and Friedrich Widdel. Metabolism of alkylbenzenes, alkanes, and other hydrocarbons in anaerobic bacteria. *Biodegradation*, 11(2-3):85–105, 2000.

[87] George O'Toole, Heidi B Kaplan, and Roberto Kolter. Biofilm formation as microbial development. *Annual Reviews in Microbiology*, 54(1):49–79, 2000.

[88] Rodney M Donlan and J William Costerton. Biofilms: survival mechanisms of clinically relevant microorganisms. *Clinical microbiology reviews*, 15(2):167–193, 2002.

[89] JW Costerton, Philip S Stewart, and EP Greenberg. Bacterial biofilms: a common cause of persistent infections. *Science*, 284(5418):1318–1322, 1999.

[90] Merle E Olson, Howard Ceri, Douglas W Morck, Andre G Buret, and Ronald R Read. Biofilm bacteria: formation and comparative susceptibility to antibiotics. *Canadian Journal of Veterinary Research*, 66(2):86, 2002.

[91] Jin Xu, Cheng Sun, Maocheng Yan, Fuhui Wang, et al. Effects of sulfate-reducing bacteria on corrosion of carbon steel q235 in the crevice by eis. *Int. J. Electrochem. Sci*, 7:11297–11312, 2012.

[92] B Little and R Ray. A perspective on corrosion inhibition by biofilms. *Corrosion*, 58(5):424–428, 2002.

[93] Ramkrishna Sen. Biotechnology in petroleum recovery: The microbial EOR. *Progress in Energy and Combustion Science*, 34(6):714 – 724, 2008.

[94] Fu-shao Li, Mao-zhong An, and Dong-xia Duan. Corrosion inhibition of stainless steel by a sulfate-reducing bacteria biofilm in seawater. *International Journal of Minerals, Metallurgy, and Materials*, 19(8):717–725, 2012.

[95] Rudolf K Thauer, Kurt Jungermann, and Karl Decker. Energy conservation in chemotrophic anaerobic bacteria. *Bacteriological reviews*, 41(1):100, 1977.

[96] S.W. Cui. *Food Carbohydrates: Chemistry, Physical Properties, and Applications*, pages 161–218. CRC PressINC, 2005.

[97] Bernard Lorber, John B Bishop, and Lawrence J DeLucas. Purification of octyl β-d-glucopyranoside and re-estimation of its micellar size. *Biochimica et Biophysica Acta (BBA)-Biomembranes*, 1023(2):254–265, 1990.

[98] Sigma-Aldrich. Product information sheet, n-dodecyl-β-D-maltopyranoside. `http://www.sigmaaldrich.com/etc/medialib/docs/Sigma/Product_Information_Sheet/d4641pis.Par.0001.File.tmp/d4641pis.pdf`, January 2013. Accessed: Mayl 26^{th} 2013.

[99] Guo-Ping Sheng, Han-Qing Yu, and Xiao-Yan Li. Extracellular polymeric substances (EPS) of microbial aggregates in biological wastewater treatment systems: A review. *Biotechnology Advances*, 28(6):882 – 894, 2010.

[100] C. M. Pradier, C. Rubio, C. Poleunis, P. Bertrand, P. Marcus, and C. Compre. Surface Characterization of Three Marine Bacterial Strains by Fourier Transform IR, X-ray Photoelectron Spectroscopy, and Time-of-Flight Secondary-Ion Mass Spectrometry, Correlation with Adhesion on Stainless Steel Surfaces. *The Journal of Physical Chemistry B*, 109(19):9540–9549, 2005.

[101] Mary E Davey, Nicky C Caiazza, and George A O'Toole. Rhamnolipid surfactant production affects biofilm architecture in pseudomonas aeruginosa pao1. *Journal of bacteriology*, 185(3):1027–1036, 2003.

[102] Sigma-Aldrich. 03750 Fluka, Ethylene glycol. `http://www.sigmaaldrich.com/catalog/product/fluka/03750?lang=en`, January 2013. Accessed: May 28^{th} 2013.

[103] Z Huo, E Freer, M Lamar, B Sannigrahi, D.M Knauss, and E.D Sloan Jr. Hydrate plug prevention by anti-agglomeration. *Chemical Engineering Science*, 56(17):4979 – 4991, 2001.

[104] Sigma-Aldrich. S6635 Sigma, Span-20. `http://www.sigmaaldrich.com/catalog/product/sigma/s6635?lang=en`, January 2013. Accessed: May 28^{th} 2013.

[105] Philippe Glenat, Patrick Bourg, and Marie-Laure Bousque TOTAL S.A. France. Producing inside P&T gas hydrates zone with low dose hydrate inhibitors (LDHIs). In *23rd International Oil Field Chemistry Symposium, Geilo, Norway*, 2012.